5-2015

THERMAL ABLATION ALTERS THE TUMOR MICROENVIRONMENT ACTIVATING A ROBUST IMMUNE RESPONSE.

Matthew T. Campbell M.D.

THERMAL ABLATION ALTERS THE TUMOR MICROENVIRONMENT ACTIVATING A ROBUST IMMUNE RESPONSE.

by

Matthew T Campbell, M.D.

Approved

Padmanee Sharma, M.D., Ph.D.

Gary Gallick, Ph.D.

Nizar Tannir, M.D.

Arlene Siefker-Radtke, M.D.

Michael Davies, M.D. ,Ph.D.

APPROVED

Dean The University of Texas

Graduate School of Biomedical Sciences at Houston

THERMAL ABLATION ALTERS THE TUMOR MICROENVIRONMENT ACTIVATING A ROBUST IMMUNE RESPONSE.

A

THESIS

Presented to the Faculty of

The University of Texas

Health Science Center at Houston

and

The University of Texas

MD Anderson Cancer Center

Graduate School of Biomedical Sciences

In Partial Fulfillment

of the Requirements

for the Degree of

MASTER OF SCIENCE

by

Matthew T Campbell, M.D.

Houston, Texas

May, 2015

Acknowledgements

I would like to thank Dr. Pam Sharma for her excellent mentorship during the last 30 months. I would like to thank Dr. Surena Matin for allowing me to collaborate with him on this project and on protocol 2013-0539. I would like to thank Dr. Nizar Tannir, Dr. Arlene Siefker-Radtke, Dr. Gary Gallick, and Dr. Michael Davies for your mentorship and for agreeing to serve on my master's GSBS committee. I would like to thank Dr. Jianjun Gao and Dr. Sumit Subudhi for their extreme kindness and patience helping me with my various immunotherapy related projects. I would like to thank Becky Slack MS and Li Zhang, PhD for statistical support. I would like to thank members of the Sharma lab including Derek Ng Tang, Jing Jing Sun, and Hong Chen for their help in teaching me techniques and helping me perform and analyze studies during my master's project. I would like to thank Karen Millerchip for her help with cytokine studies. I would also like to thank Dr. Robert Wolff for allowing me to participate in the GSBS Master's program. I would like to thank my wife, Steff, and my wonderful daughters Adele and Molly for their patience during my training.

THERMAL ABLATION ALTERS THE TUMOR MICROENVIRONMENT ACTIVATING A ROBUST IMMUNE RESPONSE.

Matthew T Campbell, M.D.

Advisor Professor: Padmanee Sharma, M.D Ph.D

Ablation techniques including radiofrequency ablation (RFA) and cryoablation have been shown to influence the immune system in animal models. Rare abscopal events, a distant metastatic response to a local procedure, have been observed in humans following both RFA and cryoablation. These rare observations have led to interest in further defining the impact of ablation procedures on the immune signature in the tumor microenvironment and in the systemic circulation.

Retrospectively 9 patients with nephrectomy alone (control) were compared to 16 patients treated with ablation. Gene microarray analysis and immunohistochemistry (IHC) for presence of immune cell subtypes were performed on the tissue samples. Prospectively, blood was collected from patients 13 patients who underwent renal ablation for renal cell carcinoma for stage T1a (less than 4cm) at baseline and at day 1, day 28, and 6 months following the procedure. The blood was assessed by flow cytommetry and plasma cytokine levels at each time point following the procedure. GraphPad Prism version 6 was used to perform statistical analysis. The student's t-test, Kruskal Wallis test, Friedman's test, and Dunn's multiple comparisons test were used when appropriate.

IHC identified a significant difference ($p=0.04$) in programmed cell death 1 (PD-1) levels in the tumor invasive margin when comparing control to ablated tumors, while other tumor stains showed no significant differences between the two groups. Gene microarray analysis comparing

control patients to three ablation specimens after RFA found significant differential gene expression in pathways and processes involving the immune system. Flow cytommetry markers consistent with previously characterized T regulatory populations of immune cell were found to trend upward at 24 hours following ablation compared to baseline levels. Cytokine analysis revealed elevated levels of IL-6 that increased at day 1 and returned toward baseline by day 28.

RFA and cryoablation cause local tissue destruction and an inflammatory immune response that can be detected by gene microarray. Significant changes in tissue IHC, plasma cytokine levels, and immune cell populations in peripheral blood flow cytommetry analysis were not detected.

Table of Contents

List of Illustrations

List of Tables

Abbreviations

APCs - Antigen presenting cells

ANOVA – analysis of variance

BUM model - beta-uniform mixture model

CD – cluster of differentiation

CT – center of tumor

CTLA-4 Cytotoxic T lymphocyte associated protein 4

D0 – Day 0 or baseline blood draw

D1 – Day 1 blood draw

D28 – Day 28 blood draw

DC- Dendritic cells

FoxP3 – Forkhead box P3

HCC - Hepatocellular carcinoma

HMGB1 - High mobility group 1

HSP- heat shock proteins

ICOS – inducible T cell costimulator

IFN-γ - interferon gamma

IHC- Immunohistochemistry

IL- interleukin

IM –invasive margin

IPA – Ingenuity Pathway Analysis

iTreg – induced T regulatory cell

lin^- - lineage negative

MDSC – myeloid derived suppressor cells

mRCC - Metastatic renal cell carcinoma

MRMT-1 metastasizing rat's mammary tumor

MUC1 – mucin 1, cell surface associated

N stage – lymph node stage

NK – Natural Killer cells

nTreg – natural T regulatory cell

PD-1 - Programmed Cell death 1

PD-L1 - Programmed Cell death ligand 1

RFA - radiofrequency ablation

RCC - Renal cell carcinoma

RPMI - Roswell Park Memorial Institute

RT-PCR - reverse transcription polymerase chain reaction

SD – standard deviation

SND1 – Staphylococcus Nuclear and Tudor Domain Containing 1

T stage – tumor stage

TCM – T central memory

TEM – T effector Memory

TIL – tumor infiltrating lymphocytes

TNF-α - tumor necrosis factor alpha

Treg – T regulatory cells

TREM1 – Triggering receptor expressed on myeloid cells 1

I. Background:

Thermal ablation refers to interventional procedures that use extreme temperature to cause local tissue damage. The two most common procedures employing extreme temperature consist of radiofrequency ablation (RFA) and cryoablation. Both procedures introduce a metal probe into a tumor using direct visual or imaging guidance with either ultrasound or computated tomography (CT) guidance. Using two temperature extremes, burning tissue in RFA and freezing tissue in cryoablation, small tumors in a number of important anatomical locations can be effectively destroyed. In terms of local treatment strategies, cryo-ablation is an attractive treatment modality for the following reasons: 1) It has been shown to be safe and effective in treating kidney, liver, bone, lung, adrenal and soft tissue masses; 2) It is palliative with the freezing procedure causing a local analgesic effect; 3) It has been shown to be potentially cost-effective in oligometastatic disease [1]. Cryosurgery has been interesting to immunologists and oncologists for decades due to a rare Abscopal type of effect witnessed in several case reported prostate and breast cancer patients [2 3]. Cryo-ablation induces membrane disruption, solution effects, organelle disruption, ice crystallization, and microvascular thrombosis [4]. Depending on the proximity to the cryo-probe, cells appear to be influenced by the different insults in varying degrees. In sum, certain cells appear to experience a necrotic cell death, while others undergo apoptosis. The mechanism of cell death appears to be important in optimally stimulating an immune response. In an in vitro system evaluating the maturation of immature dendritic cells, adding living fibroblasts and apoptotic fibroblasts yielded no maturation, while adding necrotic fibroblasts resulted in significant maturation [5]. Using bone marrow-derived murine macrophages stimulated by either tumor cells undergoing UV induced apoptosis or cryotherapy induced necrosis, Reiter et al found macrophages exposed to necrotic cells exhibited significant antitumor

effect while those exposed to apoptotic cells were immunosuppressed [6]. Work by Sauter et al. found immature dendritic cells (DCs) are capable of phagocytosis of both apoptotic and necrotic tumors cells allowing for cross presentation to $CD8^+$ T cells. Only necrotic tumor cells and a supernatant generated from necrotic tumor cells were capable of maturing DCs allowing for activation of resting $CD4^+$ and $CD8^+$ T cells thus mounting a specific anti-tumor response. Apoptotic cells and a supernatant generated from apoptotic cells were not capable of inducing this maturation [7].

Whether the creation of therapeutic apoptosis or necrosis in tumor cells is immunosuppressive or immune-stimulatory has led to much debate. The danger theory proposed by Polly Matzinger broke from the traditional model that the immune system's main role is to recognize self vs non-self. In her model, Matzinger proposed the immune system is designed to recognize cell injury as danger and to react to these insults [8]. Necrosis leads to the denaturing of proteins and break down of the cell wall integrity leading to the release of important inflammatory molecules including High mobility group 1 (HMGB1), uric acid, and heat shock proteins (HSP) including hsp70, hsp90, calreticulin, and gp96 [9,10] [11]. Scaffidi et al, found that HMGB1 was important for inducing inflammation and enhanced DC maturation, while apoptosis primary or secondary did not release HMGB1 [10]. Basu et al. found the release of HSP induced macrophages to secrete cytokines and induced maturation of DC interacting through the NF-κB [9]. Shi et al. identified uric acid as an important molecule in dendritic cell maturation [11]. Scheffer et al. tested apoptotic and necrotic tumor cells injected into a murine model followed by live tumor cell injection and found apoptotic cells induced significant protection and prolonged survival, while necrotic cell vaccine provided little protection [12]. Conversely, Kotera et al. found pulsing dendritic cells with apoptotic cells produced by ultraviolet B exposure or necrotic

cells produced via freeze/thaw cycles produced equivalent dendritic cell activation and similar anti-tumor effect [13]. Gamrekelashvili et al. used ganciclovir to induced tumor cell apoptosis and a vascular targeting drug, ZD6126, to procedure necrotic tumor cells. In these experiments, the group found when transferring lymphocytes from the spleen and tumor draining lymph nodes to other tumor bearing mice, mice receiving cells from the ganciclovir treated mice were afforded protection while no protection was provided to the mice receiving cells from mice treated with ZD6126. The authors showed this protection was conferred by the CD8+ T cells [14]. Feng et al. found a significant difference in the immunostimulatory nature of non-stressed and heat-stressed apoptotic leukemic cells, with heat-stressed cells capable of inducing maturation of dendritic cells [15]. As a result of these studies, the context and rapidity of induction of necrotic and apoptotic cells appears to be important in the generation of an immune-reactive or immunosuppressive response.

Kolicher is credited by Strauss as introducing electrocoagulation (surgical diathermy) to inoperable cancer in 1910 [16]. In the same publication, Strauss reported his experience treating rectal carcinoma with surgical diathermy he wrote:

> "Clinically the results are remarkable. After the first or second application of diathermy the patient gains weight and the hemoglobin and red cell content and red cell count of the blood are increased to normal levels. Even a patient who has lost a great deal of weight or is cachectic loses all the appearances that are characteristic of a person with advanced carcinoma."[16]

In this work, Strauss hypothesized the reticulo-endothelial system was involved in the dramatic responses seen in patients treated with this approach. Using pigs, McGahan et al. studied the local effects of radiofrequency ablation (RFA) via ultrasound and under both gross and microscopic dissection at autopsy [17]. At the site of the RFA probe a central char was observed.

This char was surrounded by an area of cells that undergo necrosis, the third outer area contained areas of hemorrhage and congestion. The injury evolved over the period of weeks with eventually the area being walled off with granulation tissue and chronic inflammatory cells leading to scar.

Using a VX2 hepatoma model in rabbits, Wissniowski et al. found animals treated with RFA compared to observation had a significant infiltration of T cells within the tumors and evidence of persistent specific circulating T cells [18]. den Brok et al. using a murine model injecting B16-OVA melanoma cells into the flank that RFA alone protected 20% of animals repeated B16-OVA cellular rechallenge in the contralateral flank, but did not protect against challenge with a thymoma cell line. This protection was transferrable to other animals when splenocytes were transferred and was significantly reduced when plasma was used, indicating that the cellular portion of the immune arm provided the effect. Also, RFA combined with CTLA4 blockade was more effective than RFA alone in protecting animals against tumor rechallenge and greatly enhanced survival [19]. Radiofrequency ablation in a murine urothelial carcinoma model generated systemic T cell responses with increased infiltration of dendritic cells within the tumors [20].

In humans, RFA in metastatic liver tumors compared to RFA in localized hepatocellular carcinoma (HCC) tumors produced evidence of trafficking T cells from the systemic circulation to the tumor site with a period of decreased T cells in the peripheral circulation. The T cells in the tumors were found have a strong proliferative response and produced the Th1-associated cytokine, IFN-γ, to tumor associated antigen MUC1 [21]. In an additional study of 12 patients, 6 with HCC, 6 with metastatic colorectal cancer to the liver, RFA to the liver lesion produced T cells in the peripheral circulation that were specific and produced IFN-γ were significantly

elevated at both 4 and 8 week time points after the procedure [22]. In a study of 20 patients with localized HCC unfit for liver transplantation or surgical resection, RFA produced increased frequency of circulating IFN-γ producing specific T cells. However, despite the presence of these cells, patients were not protected against relapse from HCC [23]. Zerbini's group later showed in a group of 20 patients the necrotic tissue collected immediately following RFA for HCC are capable of inducing maturation of antigen presenting cells (APCs) capable of producing specific T cells for HCC [24].

Animal modeling has found cryosurgery under certain conditions to be immunostimulatory and others immunosuppressive [4,25]. Both Sabel and Sidana reviewed the animal modeling systems that have explored cryoimmunology and provide summaries of these experiments. The initial studies evaluating the immune response to cryoablation involved using a rabbit model subjected to cryoablation of the male sex organs resulting in a the production of tissue specific auto-antibody response[26,27]. Myers et al. used multiple mouse types with both fibrosarcoma and mammary cell tumor types and found cryosurgery was more protective against rechallenge with the same tumor type than to amputation or control, but was unable to protect against rechallenge with a different tumor type [28]. Using a rat model, Blackwood et al. found that animals who received cryoablation of both myosarcoma and carcinosarcoma cell line-derived tumors were protected against tumor rechallenge and intraperitoneal implantation [29]. Neel et al. compared mice with virally induced mammary adenocarcinoma or chemically induced sarcoma treated with surgery, cryoablation, or ligation and found mice treated with cryoablation had longer time until tumor recurrence and improved survival after tumor rechallenge [30]. Bagley et al. compared mice with chemically induced limb sarcoma treated with cryosurgery, observation, amputation and harvested splenic lymphocytes. The splenic

lymphocytes from the cryosurgically treated animals had specific cytotoxicity against the chemically induced sarcoma cell lines, but less so against other cancer cell lines [31]. In a rat model using metastasizing rat's mammary tumor (MRMT-1), cryosurgery was compared to surgical excision and using the Winn neutralization assay was found to initially be less immunosuppressive than surgery alone. Based on these findings, the authors concluded the underlying immunosuppressive nature of cryosurgery was related to the development of a suppressor cell response [32]. Using the same rate model, Misio et al. found animals treated with cryosurgery had evidence of tumor regression and protection against the development of lung and lymph node metastasis, which peaked at 10 weeks following the procedure. In contrast, animals treated with surgical excision had continued progressive risk of developing lung and lymph node metastasis that increased with time [33].

In a study of 20 patients with high risk localized prostate cancer treated with cryoablation, patients' serum cytokine levels and immune cyto-lytic activity was assessed at baseline, after 4 weeks and after 8 weeks [34]. The serum cytokines of interest included classic Th1 cytokines interferon gamma (IFN-γ) and tumor necrosis factor alpha (TNF-α) and classic Th2 cytokines interleukin 4 (IL-4) and interleukin 10 (IL-10) with the authors evaluating the Th1/Th2 ratio of IFN-γ/IL-4. The authors found the Th1/Th2 ratio was increased at 4 weeks, but diminished at 8 weeks, suggesting the response was favorable, but not sustained. The T cells were also found to be cyto-lytic to a prostate cell line and not to a renal cell carcinoma cell line supporting specificity of response.

In renal cell carcinoma (RCC), the ratio of Th1 to Th2 cytokines produced by T cells has been found to inversely correlate with tumor grade and stage [35]. Murine modeling has found diminished Th1 cytokine production and responsible T cell subset presence during tumor

progression [36]. Alternatively, tipping the balance to more Th1 cytokine production as compared to Th2 can lead to tumor regression [37].

In an in vivo melanoma mouse model, the authors sought to further understand mechanisms of influencing the immune system in animals treated with cryosurgery, radiofrequency ablation and tumor vaccination. Both RFA and cryosurgery appeared to produce an in situ depot of tumor antigen and debris. The authors used an indium labeled tracer, which was injected into the tumor. Animals were then treated with a dendritic cell vaccine, radiofrequency ablation, cryoablation, or surgical resection. The authors found within tumor draining lymph nodes of animals treated with cryosurgery an increase in immature dendritic cells which took up tumor antigen as well as mature dendritic cells. The cryosurgery group was more resistant to tumor rechallenge and had the longest survival compared to all other animal groups included on study. The authors also found the addition of anti-CTLA4 to cryosurgery or radiofrequency ablation resulted in a significant survival advantage after tumor re-challenge compared to animals treated with anti-CTLA4 alone, RFA alone, or cryosurgery [19].

Within our current group at MD Anderson Cancer Center, work published by Dr. Matin showed the immunogenicity of cryosurgery in an orthotopic renal cell carcinoma mouse model. In this model, cryosurgery of a renal cell carcinoma harboring kidney led to significant infiltration of inflammatory cells including neutrophils, macrophages, and T cells compared to kidneys harboring renal cell carcinoma.[18] Dr. Allison and his previous group at Memorial Sloan Kettering investigated pairing cryosurgery with ipilimumab in a TRAMP prostate cancer mouse model. In this model, mice received a thigh injection with TRAMP C2 cells, one month before undergoing cryo-surgery or a sham procedure on the resulting mass. The mice were then rechallenged the following day with an additional TRAMP C2 cell injection in the opposite

thigh. The mice were then either treated with ipilimumab or placebo. Finally a subset of mice received an anti-CD8 T cell antibody prior to cryosurgery and then at specific intervals during the study. The mice treated with the combination of cryosurgery and ipilimumab had a synergistic response with a significant delay in tumor re-growth and the longest overall survival within the study groups. T cells found in mice from the cryosurgery plus ipilimumab group were specific against the TRAMP C2 cells. These T cells were also active with high levels of IFN-gamma detected in both the secondary tumors and spleens of the mice studied. In contrast, mice treated with cryosurgery alone, ipilimumab alone, or cryosurgery combined with ipilimumab and anti-CD8 T cell antibody had a shortened time until tumor recurrence and a shorter survival compared to the ipilimumab plus cryosurgery group. The authors concluded cryosurgery and CTLA-4 blockade in the TRAMP prostate cancer mouse model produced increased ratio of effector CD8 T cells compared to T regulatory cells, and provided a synergistic response in mice with observed systemic, specific immunity.[19]

Currently, two classes of immune check point inhibitors have achieved FDA approval. The anti-CTLA-4 targeting antibody, ipilimumab was the first drug to show significant survival advantage in patients with metastatic melanoma leading to its FDA approval in this setting [38] . The second class targeting the PD-1/PDL-1 interface, with antibodies developed and tested in clinical trials leading to FDA approval in advanced melanoma and metastatic squamous cell carcinoma of the lung, with active testing in many additional tumor subtypes [39 40 41 42 43 44]. All of these agents showed exciting activity with subsets of patients experiencing durable responses.

In the setting of mRCC, fewer patients have been enrolled on studies involving the immune check point inhibitors compared patients with advanced melanoma. In the smaller sample sizes, both the agents targeting CTLA-4 and PD1/PDL-1 appear of similar to reduced

efficacy in mRCC as found in melanoma. Granted, phase I trials assess safety and dose as the primary endpoints, but in each trial efficacy was a secondary endpoint. In the phase I trial evaluating ipilimumab, there was a response rate of 9.8%(6 of 61 pts) for all patients treated, though this increased to 12.5% (5 of 40pts) in the subset treated with maximum dosing 10mg/kg [45]. In the phase I anti-PD-1 study, patients with mRCC had a 27% response rate (9 of 33pts) [42]. Finally, in the anti-PD-L1 study, patients with mRCC had a response rate of 11.7% (2 of 17pts) [46]. Our group has significant experience with the use of the immune check point inhibitors in clinical trials. Dr. Sharma served as a co-led author on preoperative CTLA-4 blockade [47 48]. We currently have within the GU department a phase II trial evaluating ipilimumab plus androgen deprivation in prostate cancer, a phase I clinical trial evaluating nivolumab in combination with sunitinib, pazopanib, or ipilimumab in patients with mRCC, and are participating in the phase III trial PDL-1 vs. everolimus in patients with mRCC.

In the United States, in 2015, roughly 60,000 individuals will be diagnosed with a renal or renal pelvis neoplasm and 15,000 will die from these malignancies [49]. Renal cell carcinoma (RCC) represents the vast majority of these cases with the clear cell subtype being the most common histology accounting for 80% of RCC cases. Surgical management for localized RCC remains the treatment of choice though 30% of patients with localized disease are destined to recur. Metastatic RCC (mRCC) is considered largely incurable. When patients with mRCC have long term disease free survival they typically have oligometastatic disease and are cured with aggressive surgery or when they have a complete response to an immunotherapy, which currently represents approximately 5%-10% of patients. Immunotherapy was initially explored in mRCC in the form of cytokine therapy with high dose interleukin-2 (HD-IL-2) and interferon-alpha (IFN-α) as all standard combination chemotherapy approaches and radiation treatments

were proven ineffective in the metastatic setting [50] [51] [52]. With HD-IL-2, 5-7% of patients with mRCC will have a complete response and even with prolonged follow up for well over a decade without relapse. Complete responses are restricted to clear cell histology and are most common in patients who have had a previous nephrectomy (removal of primary tumor) and in patients with lung only metastasis.

Though 7 agents have received United States Food and Drug Administration approval for the treatment of metastatic renal cell carcinoma over the last decade, none of these agents (all targeting either the vascular endothelial growth factor axis or mammalian target of rapamycin pathway) offer cure. Continuing to expand the pool of patients responsive to immunotherapy is paramount to increasing the potential cure fraction for patients with mRCC. Cryoablation and radiofrequency ablation are procedures readily available across the clinical spectrum. At MD Anderson Cancer Center, a clinical trial investigating the use of a monoclonal CTLA-4 targeting antibody, tremelimumab, with or without cryoablation is planned. In an effort to study the impact of cryoablation alone we sought to perform both retrospective and prospective analysis of patients who received thermal ablation at UT MD Anderson Cancer Center.

Based on this evidence, the central hypothesis of my project is thermal ablation procedures cause a significant local inflammatory response leading to an immunogenic gene signature that will be confirmed with detectable changes in immune cells identified in tissue and in the peripheral circulation. In order to test this hypothesis the following aims were studied:

1. To determine in a retrospective cohort of patients treated with thermal ablation followed by nephrectomy if an inflammatory, immunogenic signature is detected compared to patients treated with nephrectomy alone.

2. To determine in a retrospective cohort of patients if there is a correlation between the gene signature produced with thermal ablation followed by nephrectomy with changes detected in immunohistochemistry for specific immune cell subsets compared to patients treated with nephrectomy alone.
3. To determine in a prospective cohort of patients if thermal ablation produces detectable changes in peripheral blood immune cell subsets and cytokine levels that can be detected over one day, four weeks, and a 6 month timeframe.

II. Material and Methods

At UT MD Anderson Cancer 17 patients who underwent an ablative procedure from 2004 to 2012 and later underwent a nephrectomy were retrospectively analyzed on protocol PA-09-0383. The nephrectomy samples were compared to 9 patients who received nephrectomy alone using immunohistochemical studies and gene microarray analysis. On a separate arm of PA-09-0383, 13 patients who underwent an ablative procedure to the kidney were prospectively analyzed using blood based studies.

Immunohistochemistry

After nephrectomy, the specimen was formalin fixed and paraffin embedded. Appropriate blocks of tissue were selected by Dr. Priya Rao of the genitourinary pathology department. Dr. Jorge Blando of the immunotherapy platform sliced the tissue into 5 μm sections. Immunohistochemistry stains for CD3, CD4, CD8, CD20, CD45RO, CD57, CD68, FoxP3, Granzyme B, PD-1, and PD-L1 were performed as per protocol on the immunotherapy platform at UT MD Anderson Cancer Center. The selection of these antibodies allowed for enumeration of specific T cell subsets CD3, CD4, CD8, CD45RO, regulatory T cell subset

FoxP3, cytotoxic cells Granzyme B, and the immune checkpoint axis PD-1 and PD-L1. CD3, CD4, CD8, CD20, CD45RO, CD57, CD68, FoxP3, Granzyme B are validated antibodies. PD-1 and PD-L1 staining was confirmed by two pathologists Dr. Jorge Blando and Dr. Ignacio Wastuba. If a discrepancy in scoring of staining existed, both pathologists reviewed the slides together to come to consensus. Briefly, sections of 5 μm thickness were selected placed on charged slides heated overnight and then were deparaffinized using xylene and graded alcohols. Slides were then placed in a DAKO HipH buffer solution and heated to 97°C for 15 minutes. The slides were then incubated overnight with the primary antibody at 5°C. The following morning the Powervision kit (Vision Biosystems) was used as the secondary antibody. Exposure to diaminobenzidene served as the chromogene and counterstaining was performed using hematoxylin. All tissue specimens were then evaluated using hematoxylin-eosin (H&E) staining. A Leica system using Aperio software was used to tabulate the total number of stained cells/mm^3 per 5 high power fields (HPF) at 20x magnification. The PD-L1 h-score was calculated by taking the PDL-1 epithelial stained cells/PDL-1 tumoral stained cells. Control patients received nephrectomy alone, ablation or treatment refer to patients who received an ablation procedure followed later by nephrectomy. Distant refers to patients who underwent a non-renal ablation followed later by nephrectomy; local refers to patients who received ablation to the kidney followed by nephrectomy, which was either partial or radical.

Peripheral Blood Collection and Processing

Blood was collected as per Dr. Padmanee Sharma's laboratory protocol. Blood was drawn into BD Venous Blood collection heparinized green top tubes. Tubes were spun down at 400 times gravity for 20 seconds and placed into polypropylene conicals. The conicals were then spun at 410 times gravity for 10 minutes. The plasma layer was then collected and spun at 885

times gravity for 10 minutes. Aliquots of plasma were collected and placed into cryogenic vails and NUNC tubes. Plasma was then diluted in a 1:1 ratio with Roswell Park Memorial Institute (RPMI) medium (Cellgro). Ficolling blood was performed using Leucosep tubes. In brief 15mL of lymphocyte separation medium (LSM) (Cellgro) was added to the Leucosept tube and centrifuged for 1 minute at 400 times gravity. After centrifuging was completed, 35mL of plasma was added to Leucosept tube and centrifuged at 1000 times gravity for 12 minutes. The plasma layer was then removed to the level of 1cm above the lymphocyte layer. The lymphocyte layer was then collected into 50mL polypropylene conical tube. The volume was then brought to 50mL with RPMI medium. The tube was then spun at 400 times gravity for 15 minutes. The supernatant was decanted and the pellet was gently resuspended. To remove any residual red blood cells, 30mL of ammonium chloride lysis buffer was added to the resuspended pellet. The tube was then spun at 450 times gravity for 6 minutes. The pellet was then harvested. All resuspended pellets were combined into a 50mL polypropylene conical tube and brought to 50mL volume with RPMI. A 20μL aliquot was collected in a 12 x 75mm test tube and added to 20 μL of 0.4% Trypan Blue (BioWhittaker). The cell suspension concentration was determined with a hemacytometer. Peripheral blood mononuclear cells (PBMCs) were isolated from plasma.

Flow Cytommetry

The following antibodies were used for flow cytommetry CD3 FITC, CD4 AmCyan, CD8 APC, CD19 FITC, (BD PharMingen), CD45RO Pacific blue (Biolegend) ICOS PECy7 (eBioscience), FoxP3 PE (eBioscience), CD25 APC (EBioscience), LAP APC (R&D FAB), CD127 eflour 450 (eBioscience), CD33 eflour 450 (eBioscience), CD14 PECy7 (eBioscience), CD16 APCCy (BD PharMingen, CD56 Pacific blue (Biolegend), CD11b APC (EBioscience). Intracellular staining for FoxP3 was performed using manufacturer guidelines. The antibodies were selected to

enumerate the presence of T cells, T cell subsets including potential regulatory and effector subsets, macrophage, myeloid derived suppressor cells, and dendritic cells. Samples were analyzed using the FACSCanto II (Becton Dickinson) and data were then analyzed using BD FACSDiva software. Gates were selected based on isotype controls as previously published [53] [54] [47]. All samples were tested in triplicate.

Cytokine Analysis

Patient plasma was used to perform cytokine analysis using the Meso scale discovery Th1/Th2 kit. [55] Samples were prepared and tested in triplicate as per manufacturer's guidelines. Cytokines tested included interferon gamma (IFN-γ), interleukin-2 (IL-2), interleukin-4 (IL-4), interleukin-5 (IL-5), interleukin-6 (IL-6), interleukin-10 (IL-10), interleukin-12p70 (IL-12p70), interleukin-13 (IL-13), tumor necrosis factor alpha (TNF-α). These cytokines were selected to quantify a variety of known Th1 and Th2 related cytokines. Appropriate standards were used. The kits were analyzed on MDS QuickPlex SQ 120 per manufacturer's guidelines. All samples were tested in triplicate.

Gene Microarray Analysis

Total RNA was extracted from renal cell carcinoma (RCC) tissue using miRNeasy Kit (Qiagen). The gene expression was assessed by Affymetrix's GeneChip Human 2.0 ST Array. Data was analyzed using the Ingenuity Platform Analysis as previously described [56].

Statistical Analysis

Data were collected with Microsoft Excel. All analysis was conducted using GraphPad Prism version 6 and SAS 9.4 software. Due to the small sample sizes, non-parametric analysis

was conducted. For immunohistochemistry, the student's t test, Kruskal Wallis, and Dunn's multiple comparison's test were used to analyze the data. The gene microarray analysis was conducted using the Ingenuity pathway analysis. When comparing the normal renal tissue to renal cell carcinoma tissue, a fold cutoff of ±2 and p value cut off of 0.05 was employed allowing for a false positive call rate of 25%. When comparing nephrectomy only to patients who underwent ablation prior to nephrectomy, a fold cutoff of ±1.5 and p value cut off of 0.05 was used again allowing for a false positive call rate of 25%. The beta-uniform mixture model (BUM model) was used to generate a histogram of the p values generated for the differentially expressed genes assuming a normal distribution. For the flow cytommetry analysis and cytokine analysis the Friedman test was used to test for differences among groups when samples were matched over various time points, the Kruskal Wallis was used when samples were not matched to determine significant between groups, and the Dunn's multiple comparisons test was used between to test for differences between multiple groups. A one sided p value of 0.05 was used to reject the null hypothesis.

III. Results

Clinical Characteristics

Clinical characteristics for patients on the retrospective portion of the study are shown in Table 1. Clinical characteristics for patients on the prospective portion of the study are shown in Table 2.

	Nephrectomy Only N=9	Radiofrequency Ablation N = 11	Cryoablation N = 6
Age (years)	67±11.9	64±10.8 years	66±7.3 years
Race			
Caucasian	4 (44%)	9 (82%)	4 (67%)
Black	2 (22%)	1 (9%)	0
Hispanic	3 (33%)	1 (9%)	2 (33%)
Histology			
Clear Cell	8 (89%)	9 (82%)	6 (100%)
Other	1 (11%)	2 (18%)	0
Clinical T Stage			
T1a	6 (67%)	7 (64%)	3 (50%)
T1b	3 (33%)	2 (18%)	3 (50%)
≥T2	0	0	0
Unknown	0	2 (18%)	0
Pathologic T Stage			
T1a	6 (67%)	8 (73%)	2 (33%)
T1b	3 (33%)	2 (18%)	3 (50%)
T2	0	0	0
T3a	0	1 (9%)	1 (17%)
Metastatic Disease			
No	9 (100%)	8 (73%)	3 (50%)
Yes		3 (27%)	3 (50%)
Time (Ablation to Surgery) years		1.6 ± 1.6	0.9 ± 1.6
< 1 year		4 (36%)	4 (66%)
➢ 1 year		7 (64%)	2 (33%)

Table 1 Clinical Characteristics of Retrospective Patients: Nephrectomy Only (control), radiofrequency ablation followed by nephrectomy, and cryoablation followed by nephrectomy

	Radiofrequency Ablation N = 8	Cryoablation N = 5
Age (years)	64 ± 13	71 ±12.8
Race		
White	7 (87%)	3 (60%)
Hispanic	1 (13%)	2 (40%)
Histology		
Clear cell	6 (75%)	5 (100%)
Other	2 (25%)	0%
Clinical Stage		
T1a	8 (100%)	5 (100%)
Von Hippel Lindau		
Yes	1 (13%)	1 (20%)
No	7 (87%)	4 (80%)

Table 2 Clinical Characteristics: Prospective patients treated with ablation followed by serial blood draws.

Gene Microarray Analysis

The gene microarray analysis was performed through the Ingenuity Pathway Analysis (IPA). The initial unbiased analysis of both tumor tissue versus normal tissue and ablated tissue vs. control tissue was carried out using 10 tumor samples and 8 normal kidney specimens. A total of 719 genes were found to be differentially expressed between the normal and tumor tissue. Using a fold cutoff of ±2 and p value cut off of 0.05 allowing for a false positive call rate of 25%, 195 genes were found to have a significant positive change in expression and 524 were found to have a negative change in expression. Table 3 shows the 20 most up-regulated pathways involved, Table 4 shows the 10 most positive differentially expressed genes and table 5 shows the 10 most negative differentially expressed genes. Ingenuity groupings of genes includes location, pathways involved, processed involved, diseases involved, and interaction. For example a pathway normally involves signaling, processes involve transport/activation, and interaction involves the number of other genes an individual gene influences or is influenced by according to Ingenuity.

Pathways	DEGs	pValue
LPS/IL-1 Mediated Inhibition of RXR Function	23	4.70868E-06
Glycine Betaine Degradation	5	1.25694E-05
Complement System	7	0.00013831
α-tocopherol Degradation	3	0.000177904
Coagulation System	7	0.000204598
Xenobiotic Metabolism Signaling	23	0.000280209
4-hydroxyproline Degradation I	2	0.0012802
β-alanine Degradation I	2	0.0012802
Sucrose Degradation V (Mammalian)	3	0.002235949
PXR/RXR Activation	8	0.002620771
Valine Degradation I	4	0.003336923
FXR/RXR Activation	9	0.003611253
Methionine Salvage II (Mammalian)	2	0.003749206
Atherosclerosis Signaling	11	0.004123248
LXR/RXR Activation	11	0.004123248
Retinoate Biosynthesis I	5	0.005232584
Uracil Degradation II (Reductive)	2	0.007320507
Arginine Degradation I (Arginase Pathway)	2	0.007320507
Thymine Degradation	2	0.007320507
D-glucuronate Degradation I	2	0.007320507

Table 3: Tumor Tissue versus Normal Tissue Top 20 Pathways Upregulated

Symbol: Name	Fold Change	Notes	Molecular Function	Location	Pathways	Processes	Diseases	Interactions
TNFAIP6: tumor necrosis factor, alpha-induced protein 6	10.59	0	Other	Extracellular Space	1	6	4	2
C3: complement component 3	9.325	1	Peptidase	Extracellular Space	5	114	41	13
LOX: lysyl oxidase	5.61	1	Enzyme	Extracellular Space	1	23	14	4
LAMA4: laminin, alpha 4	4.639	1	Enzyme	Extracellular Space	0	13	18	0
FABP4: fatty acid binding protein 4, adipocyte	4.639	1	Transporter	Cytoplasm	1	51	17	5
NNMT: nicotinamide N-methyltransferase	4.513	1	Enzyme	Cytoplasm	0	1	12	1
ST8SIA4: ST8 alpha-N-acetyl-neuraminide alpha-2,8-sialyltransferase 4	4.504	0	Enzyme	Cytoplasm	0	18	0	2
HILPDA: hypoxia inducible lipid droplet-associated	4.466	1	Other	Cytoplasm	0	1	7	1
DNAH11: dynein, axonemal, heavy chain 11	4.048	1	Enzyme	Cytoplasm	0	2	14	0
EBF2: early B-cell factor 2	4.036	1	Other	Nucleus	0	13	10	0

Table 4: 10 Most up-regulated genes comparing renal cell carcinoma tissue to normal tissue

Symbol: Name	Fold Change	Notes	Molecular Function	Location	Pathways	Processes	Diseases	Interactions
EGF: epidermal growth factor	-13.691	1	growth factor	Extracellular Space	30	120	19	31
MT1H: metallothionein 1H	-16.098	1	Other	Unknown	0	36	20	4
ALDOB: aldolase B, fructose-bisphosphate	-16.969	1	Enzyme	Cytoplasm	4	2	8	5
SCNN1G: sodium channel, non-voltage-gated 1, gamma subunit	-20.544	0	ion channel	Plasma Membrane	2	25	9	6
MUC15: mucin 15, cell surface associated	-21.564	0	Other	Extracellular Space	0	0	0	0
MT1G: metallothionein 1G	-22.472	1	Other	Unknown	0	0	9	1
KNG1: kininogen 1	-37.356	1	Other	Extracellular Space	8	85	18	13
UMOD: uromodulin	-46.644	1	Other	Extracellular Space	0	33	25	3
AQP2: aquaporin 2 (collecting duct)	-48.554	0	Transporter	Plasma Membrane	1	9	8	5
SLC12A1: solute carrier family 12 (sodium/potassium/chloride transporters), member 1	-74.282	1	Transporter	Plasma Membrane	1	33	28	3

Table 5: 10 most down regulated genes comparing renal cell carcinoma tissue to normal tissue

For Ingenuity pathway analysis for ablation versus nephrectomy only, a fold change cut off of ±1.5 $p \leq 0.05$ was used to detect differentially expressed genes with again a false positive call rate of 25%. A total of 10 nephrectomy alone patients and 5 nephrectomy following ablation patients were used for this analysis. A total of 495 differentially expressed genes were identified in this analysis. Table 6 shows the top 20 pathways altered by ablation as compared to nephrectomy alone. The Table shows the number of differentially expressed genes and the cumulative significance of the pathway. Of note, 9 pathways are directly involved in immune cell quantity, movement, connectivity, and function. Of particular interest is the connection between innate and adaptive immunity and dendritic cell maturation. Table 7 shows the top 30 biologic processes and is represented in similar fashion as table 6. Every biologic process represented is involved in immune response. Table 8 and Table 9 detail the top 20 up-regulated and top 20 down-regulated genes respectively. Both tables are designed in the same format as Table 5 discussed above. Whether the differences in groups reflects biologic differences, differences in immune cell infiltrate, or differences in the tumor stroma are not known or characterized in our analysis.

Pathways	DEGs	pValue
Atherosclerosis Signaling	15	2.05E-07
Granulocyte Adhesion and Diapedesis	17	9.32E-07
PI3K Signaling in B Lymphocytes	14	2.41E-06
Inhibition of Matrix Metalloproteases	8	3.26E-06
Leukocyte Extravasation Signaling	17	5.95E-06
Phospholipases	9	7.77E-06
Eicosanoid Signaling	8	0.000111
Dendritic Cell Maturation	13	0.00037
Caveolar-mediated Endocytosis Signaling	8	0.000385
Agranulocyte Adhesion and Diapedesis	13	0.000508
Airway Pathology in Chronic Obstructive Pulmonary Disease	3	0.0007
Axonal Guidance Signaling	22	0.000713
Gαq Signaling	11	0.00089
Prostanoid Biosynthesis	3	0.001031
Crosstalk between Dendritic Cells and Natural Killer Cells	8	0.001422
Communication between Innate and Adaptive Immune Cells	8	0.001527
Endothelin-1 Signaling	11	0.002822
Role of Macrophages, Fibroblasts and Endothelial Cells in Rheumatoid Arthritis	16	0.002935
D-myo-inositol (1,4,5)-Trisphosphate Biosynthesis	4	0.003688
Phospholipase C Signaling	13	0.004362

Table 6: Top 20 Pathways Altered by Ablation versus surgery alone

Biological Process	DEGs	pValue
cell movement of leukocytes	75	9.88421E-22
leukocyte migration	80	6.26341E-21
cell movement of myeloid cells	57	4.45404E-19
quantity of leukocytes	78	5.18822E-18
cell movement of granulocytes	44	3.89424E-17
proliferation of lymphocytes	65	1.18815E-16
cell movement	123	1.28232E-16
proliferation of blood cells	71	1.47787E-16
proliferation of immune cells	68	2.20192E-16
infiltration of cells	44	6.12338E-16
cell movement of phagocytes	53	8.08087E-16
infiltration of leukocytes	42	1.58868E-15
shape change of leukocytes	20	1.79493E-15
cell death of immune cells	59	3.57496E-15
migration of cells	111	3.99319E-15
function of leukocytes	53	4.44619E-15
cell movement of neutrophils	36	4.60373E-15
cell death of blood cells	60	6.8719E-15
inflammatory response	60	2.37932E-14
cell movement of mononuclear leukocytes	46	2.80598E-14
activation of leukocytes	57	3.1411E-14
antibody response	26	3.48625E-14
migration of mononuclear leukocytes	39	6.75305E-14
Necrosis	136	1.34569E-13
binding of cells	47	1.36191E-13
quantity of lymphocytes	59	1.54307E-13
cell movement of lymphocytes	40	1.91728E-13
activation of cells	71	3.29801E-13
quantity of T lymphocytes	49	3.55297E-13
proliferation of T lymphocytes	52	4.71932E-13

Table 7: Top 30 biologic processes altered by ablation compared to surgery alone

Symbol: Name	Fold Change	Notes	Molecular Function	Location	Pathways	Processes	Diseases	Interactions
SLC12A1: solute carrier family 12 (sodium/potassium/chloride transporters), member 1	12.311	1	Transporter	Plasma Membrane	1	5	10	1
MMP12: matrix metallopeptidase 12 (macrophage elastase)	9.899	1	Peptidase	Extracellular Space	7	43	22	4
KIAA1199: KIAA1199	8.481	1	Other	Cytoplasm	0	0	10	0
ALDOB: aldolase B, fructose-bisphosphate	8.273	1	Enzyme	Cytoplasm	4	0	6	3
UMOD: uromodulin	7.863	1	Other	Extracellular Space	0	21	13	0
DPT: dermatopontin	6.98	1	Other	Extracellular Space	0	3	9	1
IBSP: integrin-binding sialoprotein	6.282	1	Other	Extracellular Space	0	6	12	3
MT1G: metallothionein 1G	6.104	1	Other	Unknown	0	0	12	1
MMP9: matrix metallopeptidase 9 (gelatinase B, 92kDa gelatinase, 92kDa type IV collagenase)	5.225	1	Peptidase	Extracellular Space	21	113	48	34
LRRC15: leucine rich repeat containing 15	5.201	1	Other	Plasma Membrane	0	1	9	1
COMP: cartilage oligomeric matrix protein	5.073	0	Other	Extracellular Space	0	8	3	0
KNG1: kininogen 1	4.931	1	Other	Extracellular Space	8	72	19	7
AQP2: aquaporin 2 (collecting duct)	4.591	0	Transporter	Plasma Membrane	1	2	1	2
CCL19: chemokine (C-C motif) ligand 19	4.338	1	Cytokine	Extracellular Space	2	127	10	3
CHI3L1: chitinase 3-like 1 (cartilage glycoprotein-39)	3.988	1	Enzyme	Extracellular Space	1	50	21	4
C7: complement component 7	3.847	1	Other	Extracellular Space	2	2	17	2
MS4A1: membrane-spanning 4-domains, subfamily A, member 1	3.708	1	Other	Plasma Membrane	0	37	20	3
LGI2: leucine-rich repeat LGI family, member 2	3.524	1	Other	Extracellular Space	0	0	9	0
PLA2G7: phospholipase A2, group VII (platelet-activating factor acetylhydrolase, plasma)	3.511	1	Enzyme	Extracellular Space	8	30	7	0
RANBP3L: RAN binding protein 3-like	3.502	0	Other	Unknown	0	0	0	0

Table 8: Top 20 most upregulated genes comparing ablation to surgery alone

Symbol: Name	Fold Change	Notes	Molecular Function	Location	Pathways	Processes	Diseases	Interactions
PLA1A: phospholipase A1 member A	-2.259	0	Enzyme	Extracellular Space	1	1	0	2
ARHGEF28: Rho guanine nucleotide exchange factor (GEF) 28	-2.273	1	Other	Cytoplasm	0	7	9	0
HOXA4: homeobox A4	-2.382	1	transcription regulator	Nucleus	0	8	15	0
PDE11A: phosphodiesterase 11A	-2.472	1	Enzyme	Cytoplasm	6	2	12	0
PLA2G16: phospholipase A2, group XVI	-2.488	0	Enzyme	Nucleus	8	7	0	0
VLDLR: very low density lipoprotein receptor	-2.507	0	Transporter	Plasma Membrane	2	6	4	0
EGFR: epidermal growth factor receptor	-2.515	1	Kinase	Plasma Membrane	36	83	23	40
ARHGEF35: Rho guanine nucleotide exchange factor (GEF) 35	-2.64	0	Other	Unknown	0	0	0	0
KIF21A: kinesin family member 21A	-2.718	1	Other	Cytoplasm	0	0	11	0
SPINK13: serine peptidase inhibitor, Kazal type 13 (putative)	-2.768	0	Other	Unknown	0	0	0	0
MT1L: metallothionein 1L (gene/pseudogene)	-2.836	0	Other	Cytoplasm	0	0	5	2
SERPINI1: serpin peptidase inhibitor, clade I (neuroserpin), member 1	-2.866	0	Other	Extracellular Space	0	4	6	1
C19orf33: chromosome 19 open reading frame 33	-2.922	0	Other	Nucleus	0	0	0	0

Table 9: Top 10 most downregulated genes comparing ablation to surgery alone

To help confirm quality control and to enhance our analysis we were assisted by the Bioinformatics Department at UT MD Anderson Cancer Center. In this analysis, one sample in the post ablation group was found to be significantly different than the rest and was excluded from additional analysis. The quality control analysis is shown in Table 10 and Figure 1 revealing a significant outlier. As a result, of the four post treatment samples remaining 3 were from patients who received radiofrequency ablation and 1 had received cryoablation prior to nephrectomy. Using a beta-uniform mixture model or BUM model, the distribution of p values was tabulated and the generated histogram is found in Figure 2. In this model, the assumption is there will be no significant interesting genes and the p-values should fall in a normal distribution curve. If the p-values all segregate close to 0, this indicates a higher likelihood of detecting important findings [57]. Figure 3 displays the most significant core pathways altered. In this table, the –log of the p value is represented on the Y axis, with higher bar graphs indicating greater likelihood of significance. The color of the bar graph indicates the Z-score in relationship to standard value of the canonical signaling pathways. If the bar is orange the pathway is significantly upregulated. If the bar is white the pathway is similar to normal observed signaling levels. If the bar is blue it is significantly down-regulated and if the bar is gray the baseline signaling characteristics are not well defined at this time. Finally the ratio represented refers to the number of genes significantly up-regulated or down-regulated and is divided by the total number of genes in the pathway.

	Sample 1	Samples 2	Samples 3	Sample 4	Sample 5
Sample 1	1	0.9	0.9	0.4	0.9
Sample 2	0.9	1	0.9	0.4	0.9
Sample 3	0.9	0.9	1	0.4	0.9
Sample 4	0.4	0.4	0.4	1	0.4
Sample 5	0.9	0.9	0.9	0.4	1

Table 10: Quality control (QC) assessment shows that one sample of the post treatment group appears to be an outlier and one of the samples in the pretreatment is distinct from other samples.

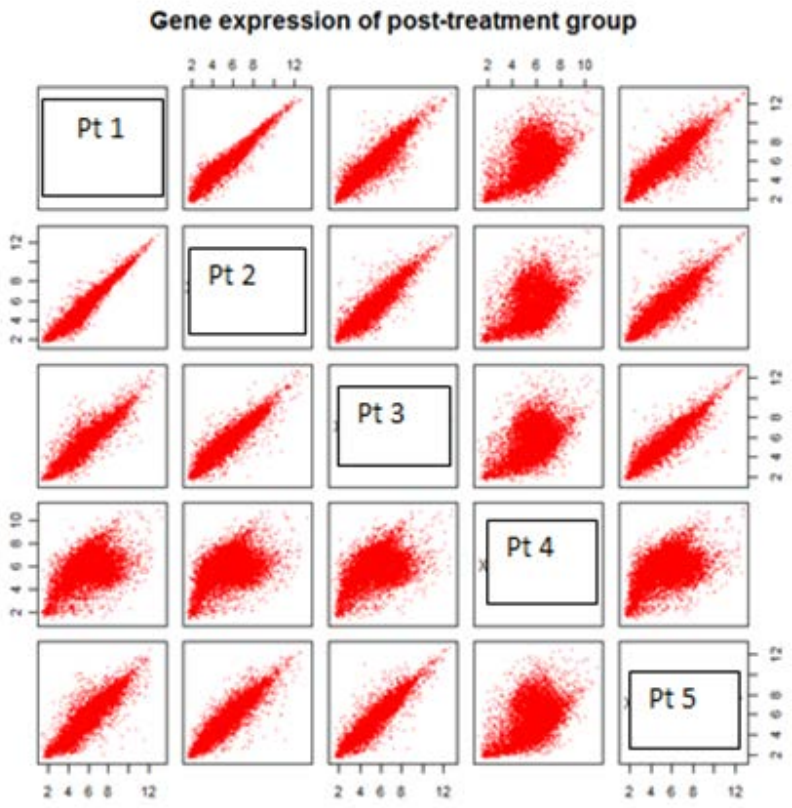

Figure 1: QC assessment shows that one sample of the post treatment group appears to be an outlier and one of the samples in the pretreatment is distinct from other samples.

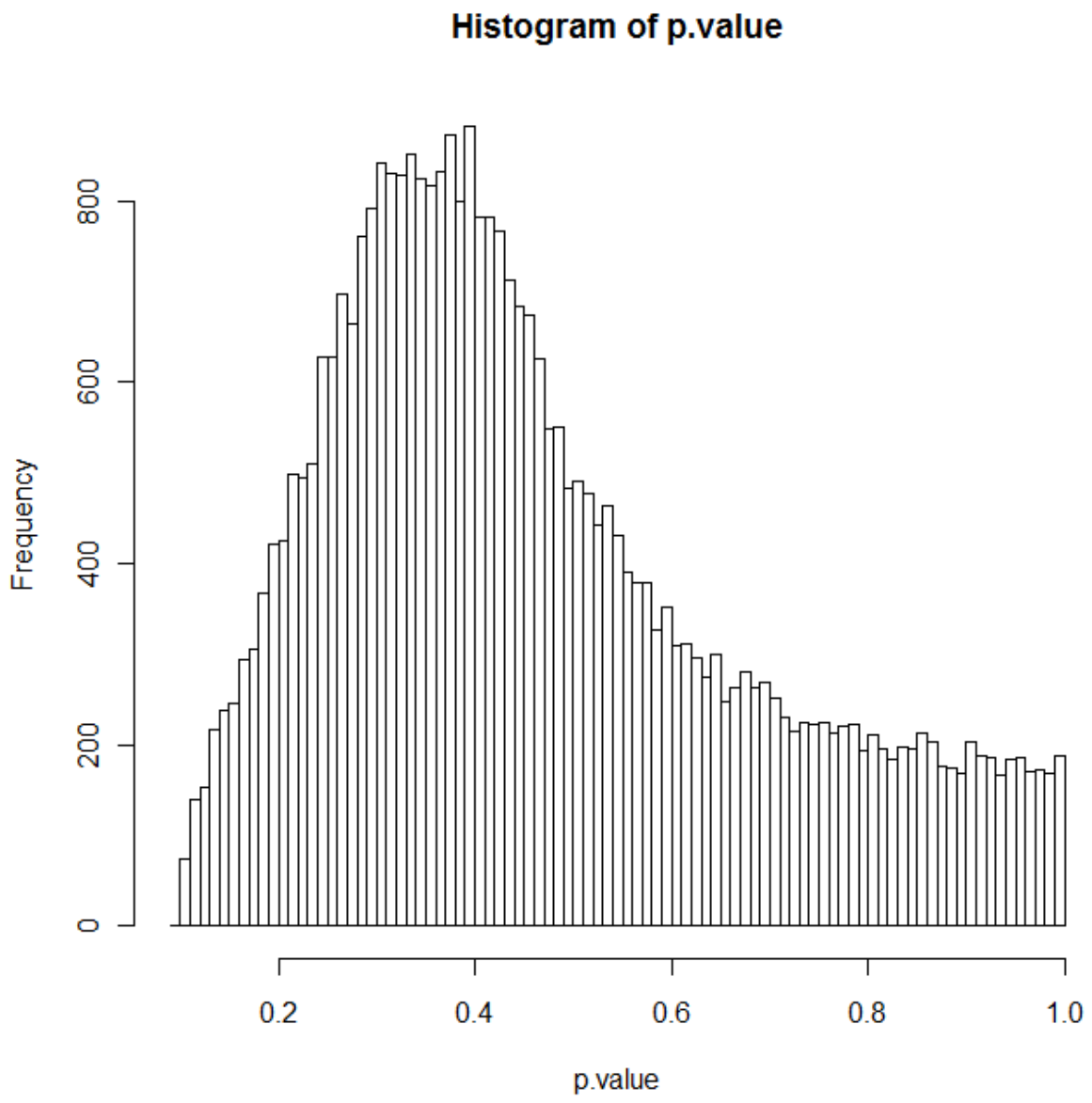

Figure 2: Histogram of p values BUM model: 4 post treatment samples were compared with 9 nephrectomy only samples.

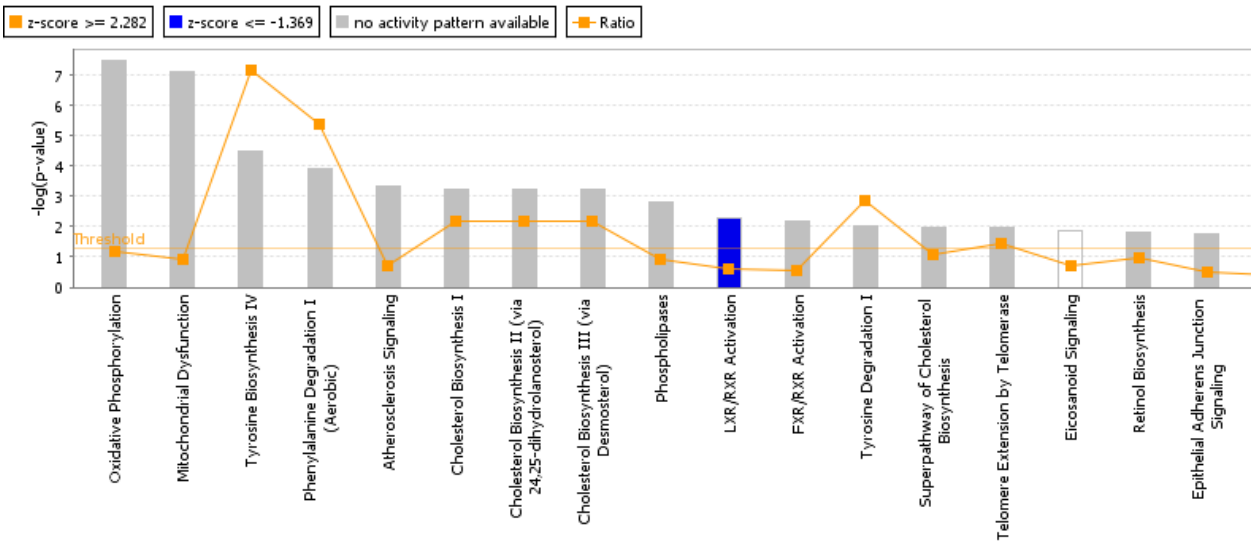

Figure 3: Core pathways altered. IPA core pathway analysis. Settings: p value cutoff: 0.05; Log ratio cutoff 0.4.

In an attempt to gain more uniformity, the Ingenuity pathway analysis was performed excluding the cryoablation sample and included the three samples treated with radiofrequency ablation prior to nephrectomy again using nephrectomy only as the comparator arm. In this analysis, Figure 4 is the histogram from the BUM model and shows significant improvement as compared to the BUM model generated in Figure 2, with the majority of p values approaching 0. Figure 5 shows the core pathways altered and uses the same approach for analysis described above for Figure 3. The top pathway was "Connection between Innate and Adaptive Immune Cells". The majority of the top pathways involve immune cell signaling, maturation, differentiation, trafficking, and inflammation. Table 11 lists the top regulatory upstream molecules and their downstream targets. All molecules included on this list except one (SND1), directly target immune signaling.

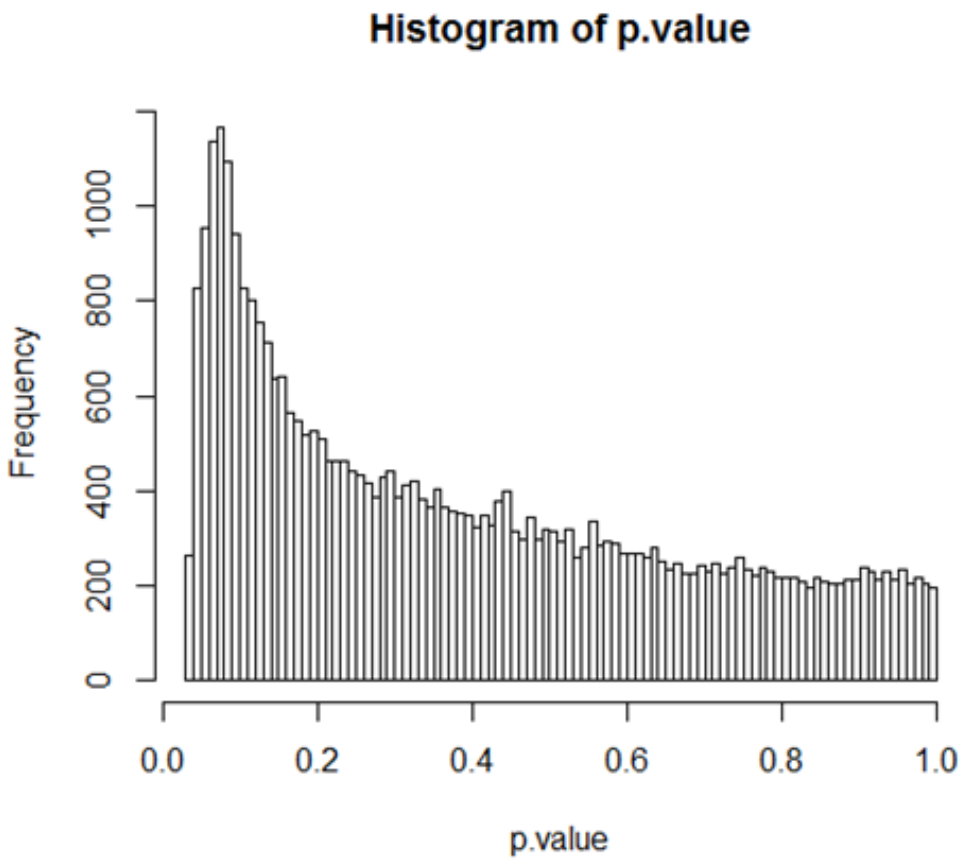

Figure 4: Histogram of p values: 3 post treatment samples were compared with 9 nephrectomy only samples.

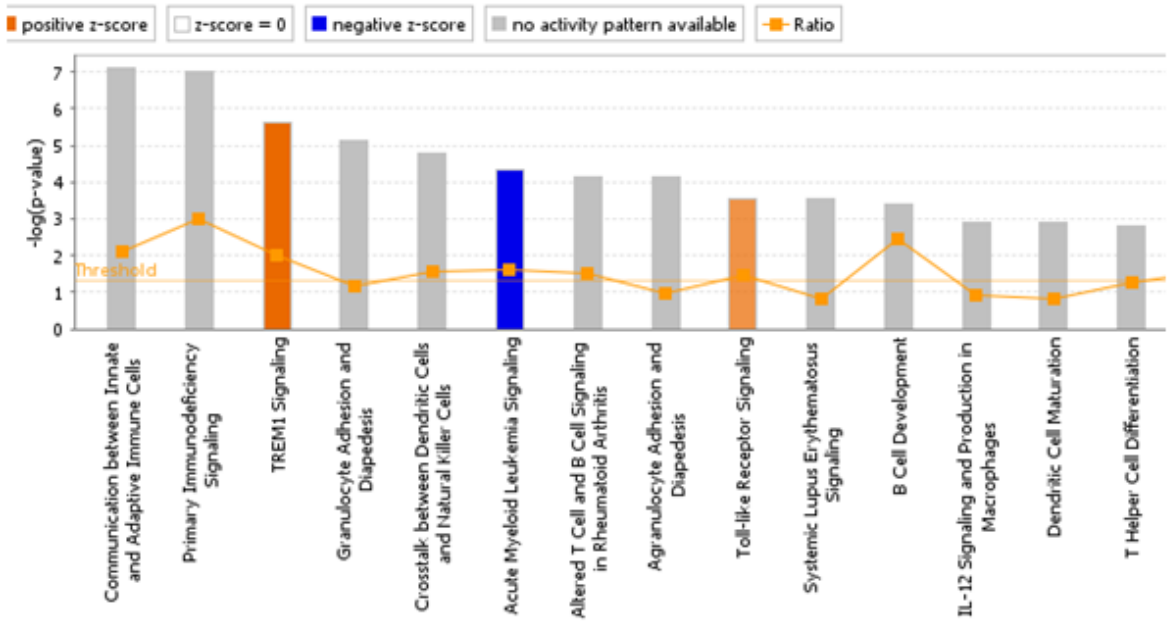

Figure 5: Core pathways altered. IPA core pathway analysis. Settings: p value cutoff: 0.05; Log ratio cutoff 0.4. The most significant pathway altered is "communication between innate and adaptive immune cells" pathway.

Upstrea...	Log Rat...	Activation ...	p...	Target molecules in dataset
TREM1	↑1.173	2.747	1.73E-09	↑CD83, ↑CD86, ↑CXCL5, ↑F3, ↑GEM, ↑GLA, ↑IL1B, ↑INHBA, ↑MAP3K8, ↑MMP1
IL3	↓-0.033	0.873	2.09E-08	↑CD83, ↑CD86, ↑CSF1R, ↑FCGR2B, ↑IL1B, ↑PIM1, ↑SPI1
CCL2	↓-0.323	0.186	5.98E-08	↑FOLR2, ↑INHBA, ↑MMP1, ↑SERPINE1, ↑SLC11A1, ↑TIMP1
CD40	↑0.078	-0.166	1.19E-07	↑BCL2A1, ↑CD83, ↑CD86, ↑FCGR2B, ↑IL1B, ↑SAMSN1, ↑SLAMF1, ↑SLAMF7, ↑TCL1A, ↑TLR2
IL1B	↑0.469	3.458	3.55E-07	↑BCL2A1, ↑CCL13, ↑CCL3L1, ↑CEBPB, ↑CXCL5, ↑IL18, ↑IL1B, ↑LCP1, ↑MMP1, ↓PPARGC1A
TCR		1.941	4.48E-07	↓ABLIM1, ↓APOD, ↑BCL2A1, ↑CD28, ↑CD38, ↑CTLA4, ↑LPIN2, ↑MAP3K8, ↑PDE3B, ↑PIM1
STAT3	↑0.120	2.391	1.47E-06	↑C5AR1, ↑CCDC88A, ↑CD209, ↑CD83, ↑CD86, ↑ICOS, ↑PIM1, ↑PTGS2, ↑SLAMF1, ↑TIMP1
IL4	↑0.017	1.336	2.18E-06	↑CD209, ↑CD83, ↑CD86, ↑FCGR2B, ↑ICOS, ↑IL18, ↑MMP1, ↑PIM1, ↑SLAMF7
P38 MAPK		2.261	4.63E-06	↑CD83, ↑CD86, ↑CEBPB, ↑IL1B, ↑INHBA, ↑MMP1, ↑PTGS2, ↑SERPINE1, ↑TIMP1, ↑TLR2
mir-155	↑0.064	-2.213	4.86E-06	↑CD209, ↑CEBPB, ↑IL1B, ↑SERPINE1, ↑SPI1
CSF2	↑0.128	2.813	5.05E-06	↑CD209, ↑CD38, ↑CSF2RB, ↑FCGR2B, ↑IL1B, ↑PIM1, ↑TLR2, ↑TPM4
SND1	↑0.118		9.53E-06	↓ADIRF, ↑EREG, ↑KYNU, ↑LAPTM5, ↑PTGS2
TLR4	↑0.255	2.169	1.58E-05	↑CD38, ↑CD86, ↑IL18, ↑IL1B, ↑MMP1, ↑PTGS2
TNF	↑0.069	3.574	1.71E-05	↑BCL2A1, ↑CD83, ↑CD86, ↑CXCL16, ↑CXCL5, ↑DUSP10, ↑F3, ↑IL1B, ↑INHBA, ↑KYNU
JUN	↑0.277	1.706	1.93E-05	↑CXCL5, ↑EREG, ↑IL1B, ↑MMP1, ↓PARD6B, ↑PTGS2, ↑PTX3, ↑SERPINE1
FANCC	↓-0.910		2.58E-05	↑IL1B, ↓PCLO, ↑PTGS2, ↑PTPRC, ↑PTX3, ↓TOM1L1
FOXL2	↑0.050	1.546	2.90E-05	↑BCL2A1, ↑CCL3L1, ↑CCL3L3, ↑CH25H, ↓PPARGC1A, ↑PTGS2
TLR7	↑0.452	1.600	4.49E-05	↑CD83, ↑CD86, ↓CHST9, ↑IGK, ↑IL1B, ↑PTX3
BCR (complex)		0.811	4.97E-05	↑BCL2A1, ↑CD86, ↑PIM1, ↑PTGS2, ↑SLAMF7, ↑TCL1A
IL11	↑0.155		5.45E-05	↑IL1B, ↑MMP1, ↑TIMP1
IL13	↓-0.173	-0.508	5.66E-05	↑ADAM28, ↑CD209, ↑CD86, ↑CLEC4A, ↑CXCL5, ↑DUSP10, ↑GAS7, ↑IL1B, ↑MS4A4A, ↑TLR1
CD40LG	↑0.346	2.226	6.04E-05	↑ADAM28, ↑CD83, ↑CD86, ↑FCGR2B, ↑IL1B, ↑PIM1, ↑PTGS2
Jnk		2.429	1.26E-04	↑CD209, ↑CD83, ↑CD86, ↑IL1B, ↑MMP1, ↑PTGS2
LAMA3	↑0.069		1.38E-04	↑IL1B, ↑MMP1
IL17A	↓-0.065	1.605	1.62E-04	↑BCL2A1, ↑CD83, ↑CXCL5, ↑IL1B, ↑PTGS2
IL10	↑0.445	-0.186	2.05E-04	↑BCL2A1, ↑CD83, ↑CD86, ↑FCGR2B, ↑IL1B, ↑TIMP1
RELA	↑0.086	2.340	2.47E-04	↑CEBPB, ↑CXCL5, ↑IGK, ↑IL1B, ↑MMP1, ↑PTGS2, ↑PTX3, ↑TLR2
PLG	↓-0.427		2.48E-04	↑F3, ↑IL1B, ↑PTGS2

Table 11: Upstream pathway regulators; the columns are as follows: Gene name of the upstream regulator, log ratio of the upstream regulator in the dataset, activation z-score, and target molecules.

Immunohistochemistry (IHC)

The tumoral and peritumoral infiltration of cytoplasmic staining $CD4^+$ cells were tabulated for patients who underwent nephrectomy alone (control), patients who underwent any ablation procedure prior to nephrectomy (treatment), patients who underwent a distant ablation to a site other than the renal primary tumor (distant), and patients who underwent an ablation to the kidney and later had a nephrectomy (local). Figure 6, Figure 7, and Figure 8 show examples of IHC staining for CD3, CD4, CD8, CD20, CD57, CD68, FoxP3, Granzyme B, PD-1, PD-L1 tumoral cells, PD-L1 immune cells. Slides were selected to involve normal renal tissue, the invasive margin, and tumoral tissue, Figures 6-8 represent examples of slides used in analysis. In Figure 6, CD3 is a pan marker for T cells capturing both CD4 and CD8 T cell populations. CD4 and CD8 are T cell subset markers and CD20 is a marker for B cell populations. In Figure 7, CD45RO stains for T cell memory subset, CD57 stains for NK cells, and CD68 for macrophages. In Figure 8, FoxP3 is stained to capture a T cell regulatory subset of cells, Granzyme B stains cytotoxic cells, PD-1 stains immune cells expressing this immune check point, and PD-L1 stains both tumoral and immune cells expressing this immune check point ligand.

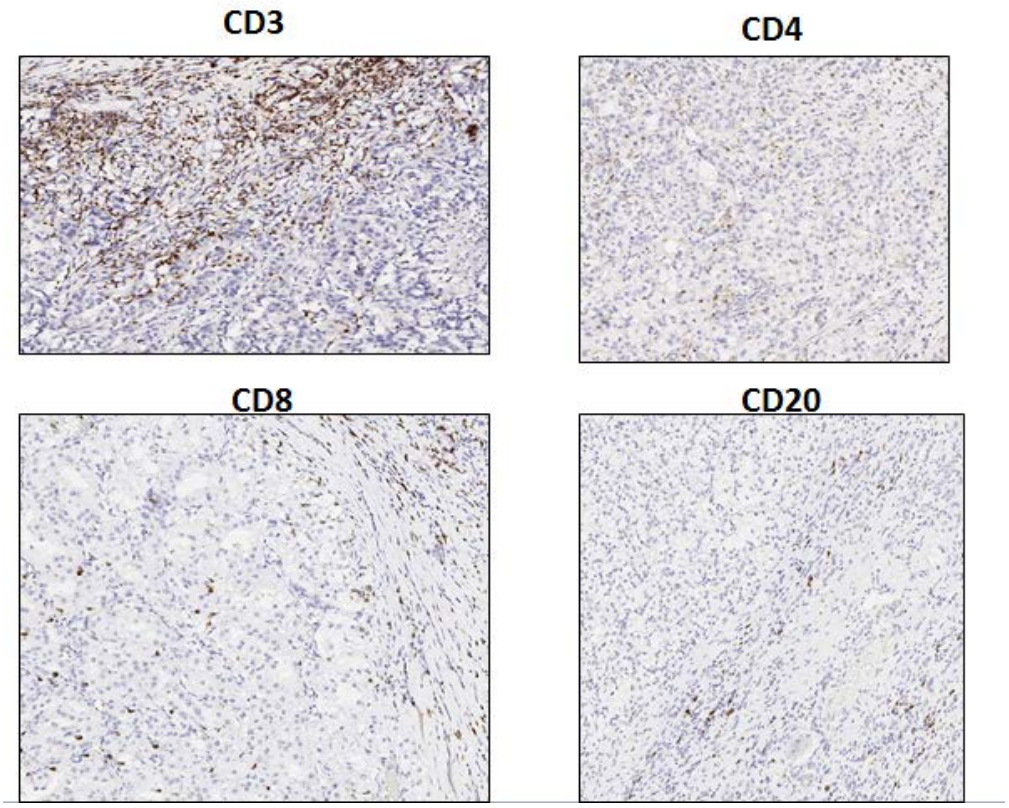

Figure 6: Immunohistochemistry staining: CD3 T cell marker, CD4 subset of T cells, CD8 subset of T cells, CD20 marker of B cells. Each slide contained a section of normal renal architecture (N), the invasive margin (IM), and the center of tumor (CT). Cells were stained and the number of stained cells/mm^3 per 5 high power fields (HPF) at 20x magnification was quantified.

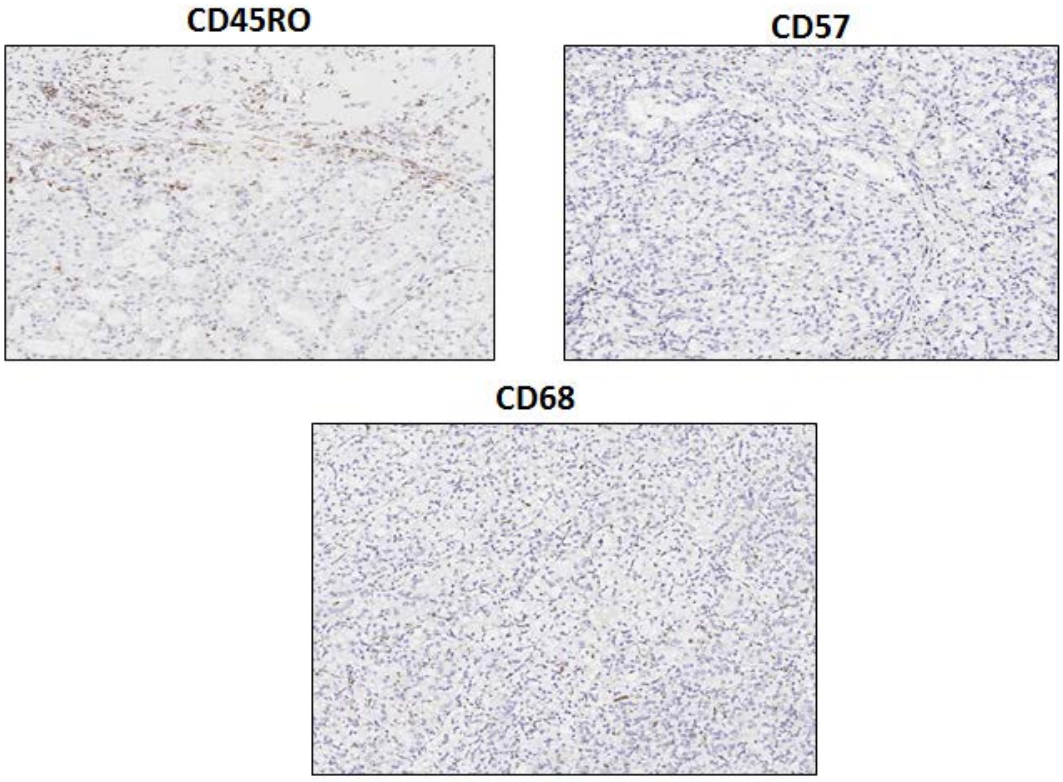

Figure 7: Immunohistochemistry staining: CD45RO a stain for a subset of T cell memory cells, CD57 a stain for natural killer (NK) cells, CD68 a stain for macrophages. Each slide contained a section of normal renal architecture (N), the invasive margin (IM), and the center of tumor (CT). Cells were stained and the number of stained cells/mm^3 per 5 high power fields (HPF) at 20x magnification was quantified.

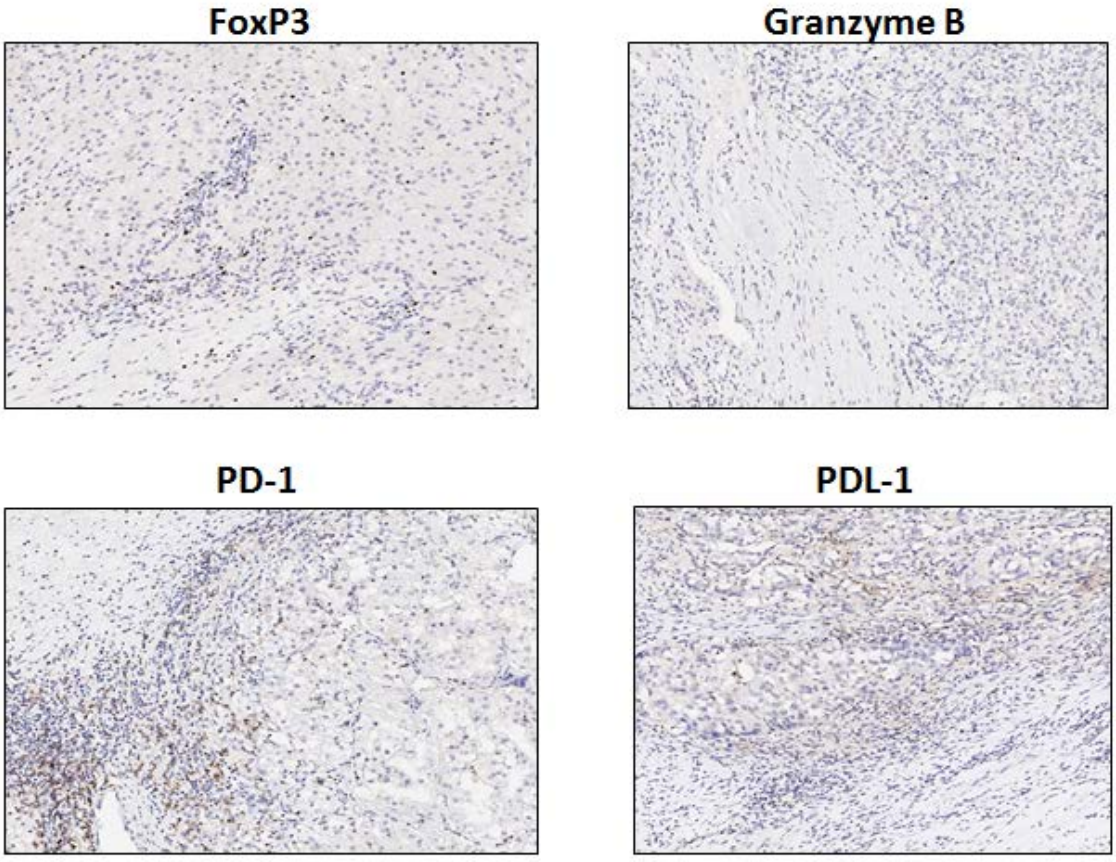

Figure 8: Immunohistochemistry: FoxP3 a stain for regulatory T cells, Granzyme B a stain for active cytotoxic T cells, PD-1 I(programmed death receptor 1), PD-L1 (programmed death receptor ligand 1). Each slide contained a section of normal renal architecture (N), the invasive margin (IM), and the center of tumor (CT). Cells were stained and the number of stained cells/mm^3 per 5 high power fields (HPF) at 20x magnification was quantified.

Figures 9 through 14 represent the analysis of IHC that were initially performed by Dr. Priya Rao. The IHC stains included CD4, CD8, CD45RO, Granzyme B, FoxP3, KP-1 (a stain for macrophages). In Figures 9 through 14, the entire population of patients was analyzed in the top graph and only patients who received nephrectomy within 1 year (control and ablation patients) were evaluated in the bottom graph. No significant differences were detected in $CD4^+$ T cells (Figure 9), $CD8^+$T cells (Figure 10), $CD45RO^+$T cells (Figure 11), Forkhead P3 (FoxP3) (Figure 12) Granzyme B (Figure 13), or KP-1 (CD68) (Figure14) in the entire population or analyzing patients who received nephrectomy within 1 year following ablation.

In 2014, the methods of enumerating staining immune cells were changed to be consistent across all studies using the immunotherapy platform. The changes included having each slide capture a section of normal renal architecture, the invasive margin, and the tumor. In an effort to be consistent with future studies, we selected appropriate tumor blocks, recut tissue, and re-stained slides using the new immunotherapy platform selected stains. Figures 15 thru 17 represent the percent staining of cells in normal tissue (N) referring to renal tissue that is not intimately involved with tumor, the invasive margin (IM), and the center of tumor (CT). Control refers to patients who were treated with nephrectomy alone and ablation refers to patients who received ablation. We selected only patients who received nephrectomy within one year following an ablation procedure for this repeat analysis. Unfortunately, 3 patients' tissue blocks had significant fixation artifacts and were unable to be used. We are attempting to locate at this time whether additional tissue blocks are available. In Figure 15, no differences were detected by student's T test when comparing $CD3^+$T cells, $CD4^+$ T cells, $CD8^+$ T cells, and $CD45RO^+$ T cells between patients treated with nephrectomy alone or ablation later followed by nephrectomy. The portions of the slide labeled as N, IM, and CT, revealed no differences

between the two groups of patients. In Figure 16, $CD20^+$ B cells, $CD68^+$ macrophages, FoxP3 (regulatory T cell stain), and granzyme B (cytotoxic T cell stain) were analyzed and no detectable difference was found between groups. In Figure 17, a difference between PD-1 staining was found between the IM and a trend toward difference in the CT was detected, with more staining being detected in patients treated with ablation compared to nephrectomy alone. Other analysis in Figure 12 included the PD-L1 staining in tumoral and immune cells, and the PD-L1 H score did not find a significant difference between the two groups of patients.

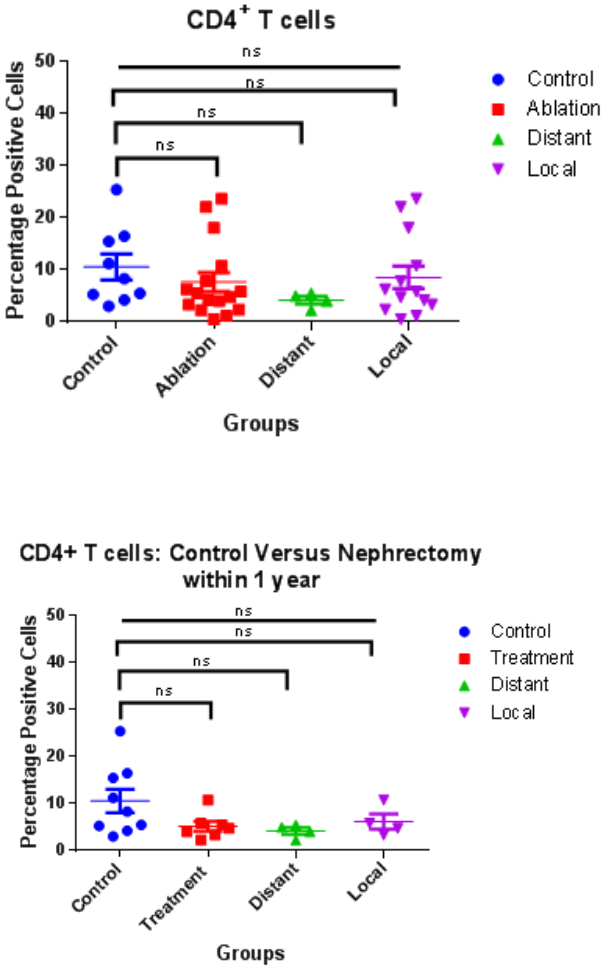

Figure 9: Initial Immunohistochemistry for CD4+ T cells. The top figure includes all patients. Control refers to nephrectomy alone (n=9) , Ablation refers to any patient who underwent an ablation procedure prior to nephrectomy (n=16) , distant refers to ablation to the kidney followed by nephrectomy at a later date (n=3), local refers to ablation of a distant organ followed by later nephrectomy (n=13). The bottom figure includes patients who had ablation followed by nephrectomy within 1 year: control (n=9), treatment (ablation) (n=7), distant (n=3), local (n=4). Kruskal Wallis test is top line, Dunn's multiple comparisons test between each group compared to control. ns = non-significant, * = $p<0.05$.

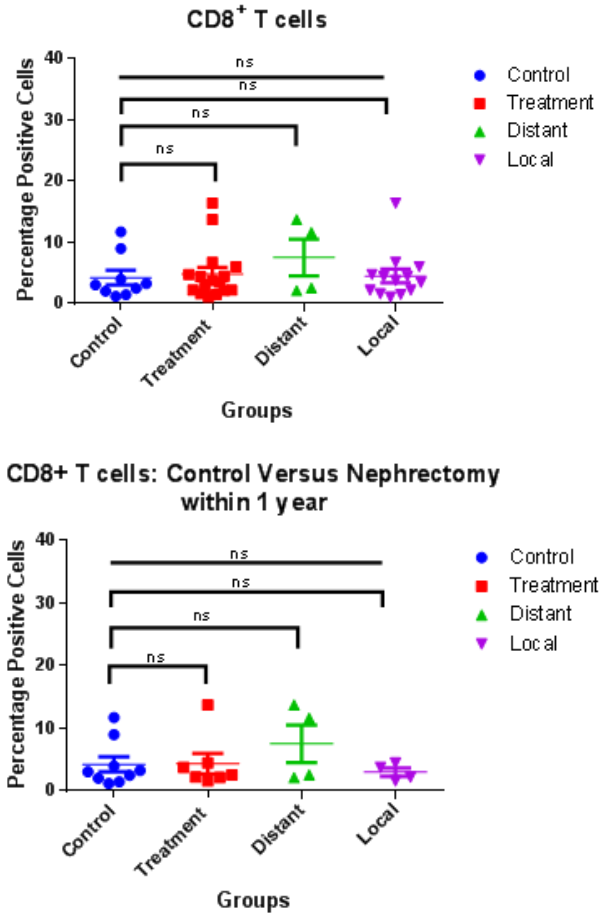

Figure 10: Initial Immunohistochemistry for CD8+ T cells. The top figure includes all patients. Control refers to nephrectomy alone (n=9) , Treatment refers to any patient who underwent an ablation procedure prior to nephrectomy (n=16) , distant refers to ablation to the kidney followed by nephrectomy at a later date (n=3), local refers to ablation of a distant organ followed by later nephrectomy (n=13). The bottom figure includes patients who had ablation followed by nephrectomy within 1 year: control (n=9), treatment (ablation) (n=7), distant (n=3), local (n=4). Kruskal Wallis test is top line, Dunn's multiple comparisons test between each group compared to control. ns = non-significant, * = $p<0.05$.

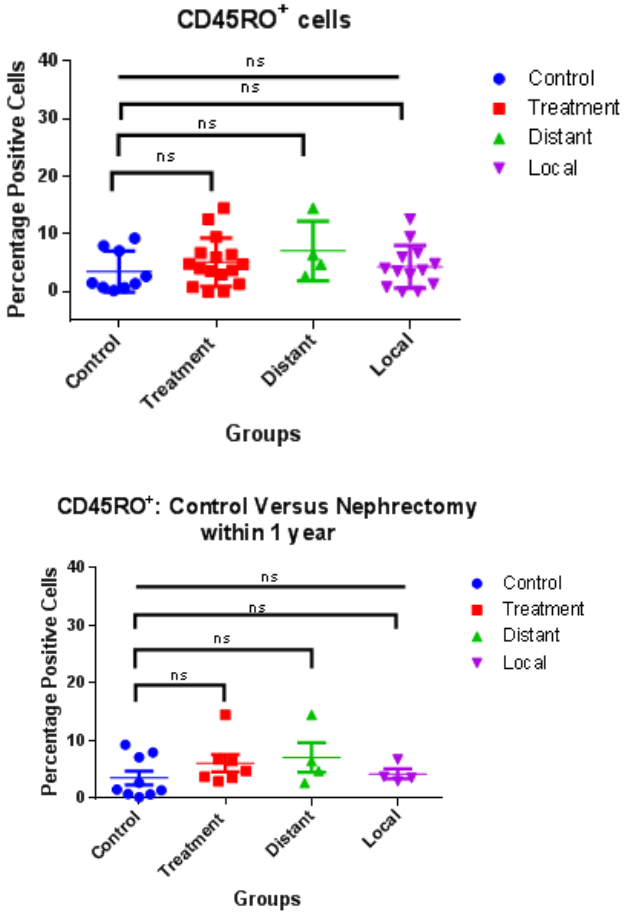

Figure 11: Initial Immunohistochemistry for CD45RO$^+$ T cells. The top figure includes all patients. Control refers to nephrectomy alone (n=9) , Ablation refers to any patient who underwent an ablation procedure prior to nephrectomy (n=16) , distant refers to ablation to the kidney followed by nephrectomy at a later date (n=3), local refers to ablation of a distant organ followed by later nephrectomy (n=13). The bottom figure includes patients who had ablation followed by nephrectomy within 1 year: control (n=9), treatment (ablation) (n=7), distant (n=3), local (n=4). Kruskal Wallis test is top line, Dunn's multiple comparisons test between each group compared to control. ns = non-significant, * = $p<0.05$.

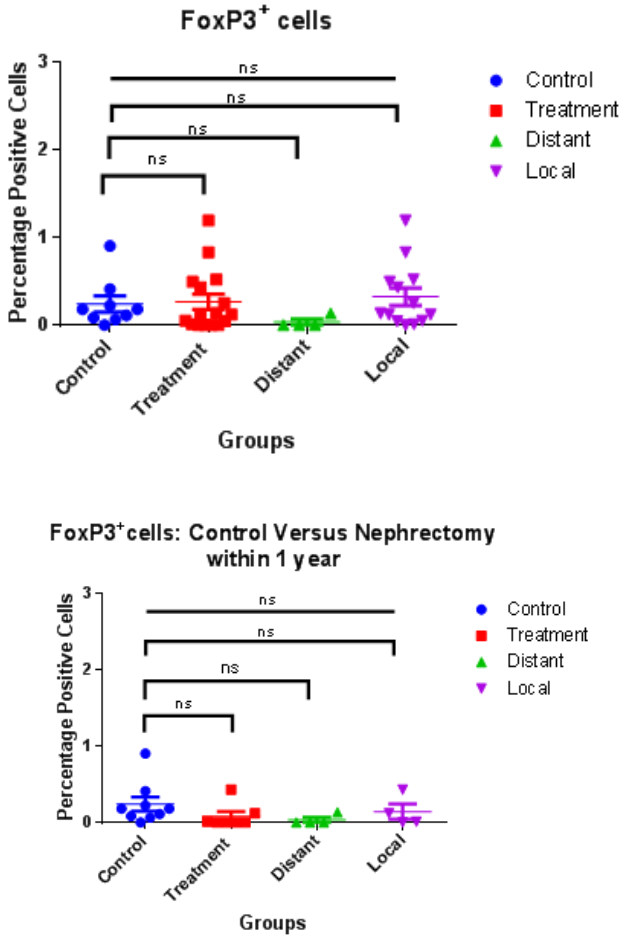

Figure 12: Initial Immunohistochemistry for FoxP3^{+} cells. The top figure includes all patients. Control refers to nephrectomy alone (n=9) , Ablation refers to any patient who underwent an ablation procedure prior to nephrectomy (n=16) , distant refers to ablation to the kidney followed by nephrectomy at a later date (n=3), local refers to ablation of a distant organ followed by later nephrectomy (n=13). The bottom figure includes patients who had ablation followed by nephrectomy within 1 year: control (n=9), treatment (ablation) (n=7), distant (n=3), local (n=4). Kruskal Wallis test is top line, Dunn's multiple comparisons test between each group compared to control. ns = non-significant, * = $p<0.05$.

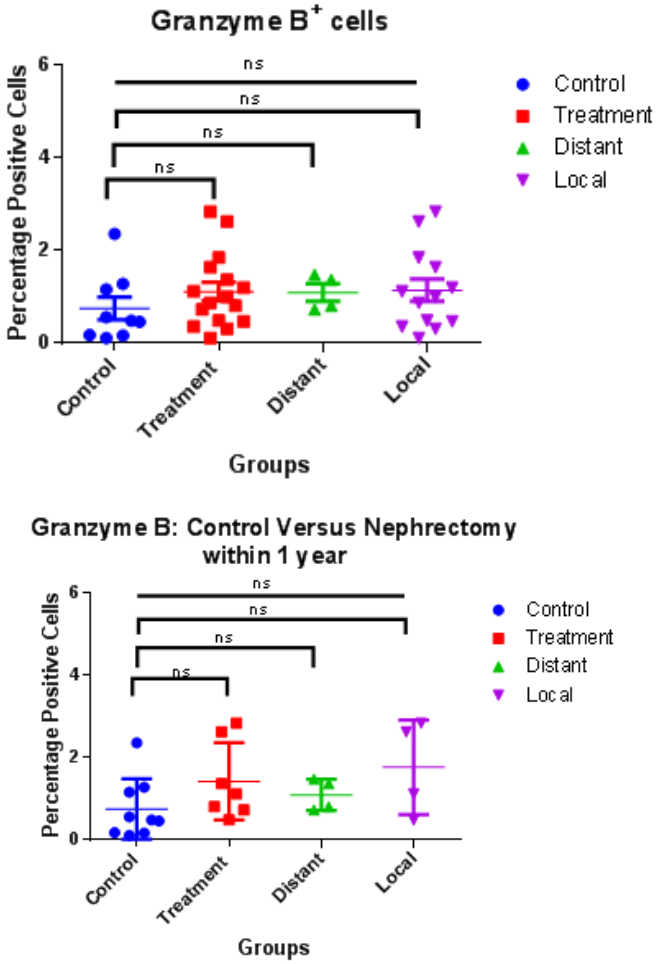

Figure 13: Initial Immunohistochemistry for Granzyme B^+ cells. The top figure includes all patients. Control refers to nephrectomy alone (n=9) , Ablation refers to any patient who underwent an ablation procedure prior to nephrectomy (n=16) , distant refers to ablation to the kidney followed by nephrectomy at a later date (n=3), local refers to ablation of a distant organ followed by later nephrectomy (n=13). The bottom figure includes patients who had ablation followed by nephrectomy within 1 year: control (n=9), treatment (ablation) (n=7), distant (n=3), local (n=4). Kruskal Wallis test is top line, Dunn's multiple comparisons test between each group compared to control. ns = non-significant, * = $p<0.05$.

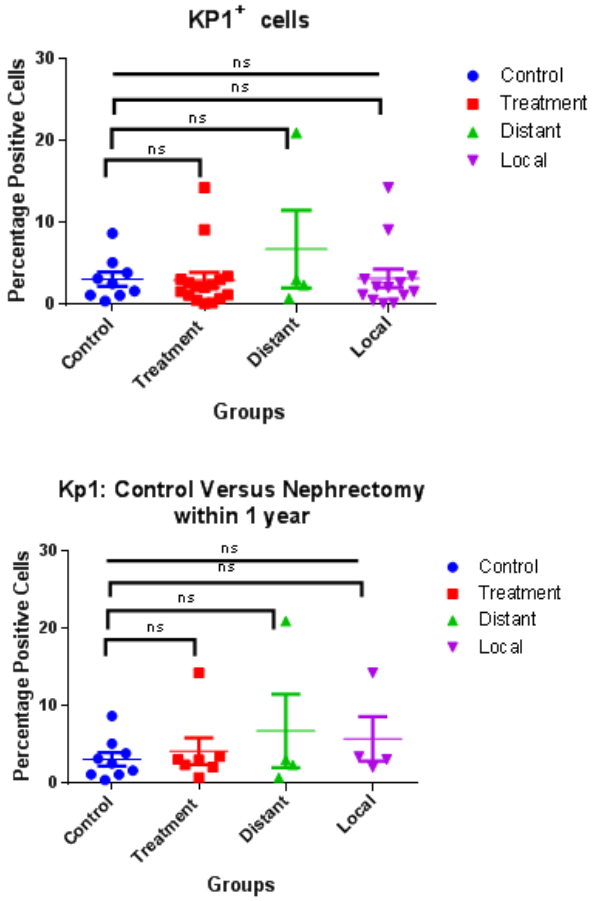

Figure 14: Initial Immunohistochemistry for $KP1^{+}$ cells, which represents a stain for macrophages. The top figure includes all patients. Control refers to nephrectomy alone (n=9) , Ablation refers to any patient who underwent an ablation procedure prior to nephrectomy (n=16), distant refers to ablation to the kidney followed by nephrectomy at a later date (n=3), local refers to ablation of a distant organ followed by later nephrectomy (n=13). The bottom figure includes patients who had ablation followed by nephrectomy within 1 year: control (n=9), treatment (ablation) (n=7), distant (n=3), local (n=4). Kruskal Wallis test is top line, Dunn's multiple comparisons test between each group compared to control. ns = non-significant, * = $p<0.05$.

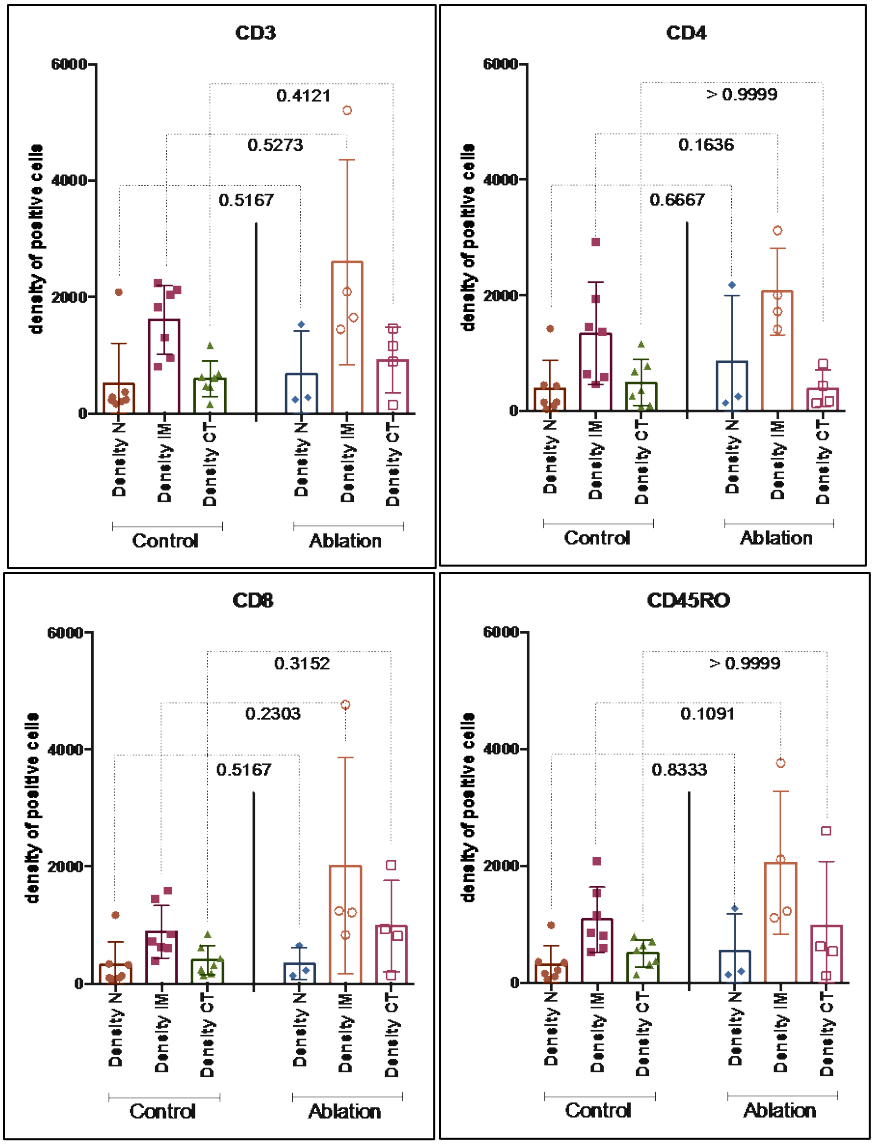

Figure 15: Updated IHC using new immunotherapy platform protocol. Density N refers to normal kidney tissue, Density IM refer to invasive margin, Density CT refers to center of tumor. Controls refers to patients who received nephrectomy alone, ablation refers to group of patients who received ablation procedure prior to nephrectomy. Groups are compared with student t test. CD3 T cell marker, CD4 subset of T cells, CD8 subset of T cells, CD45RO a stain for a subset of T cell memory cells.

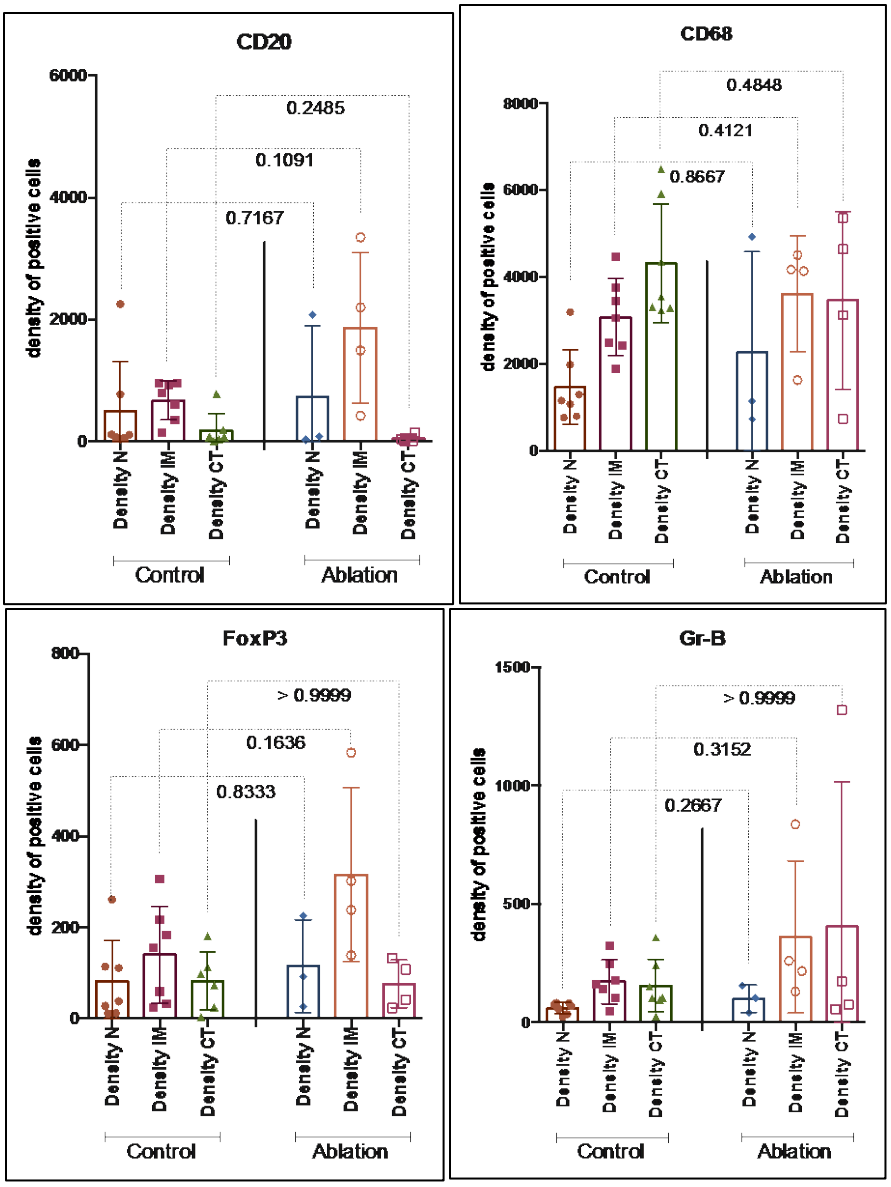

Figure 16: Updated IHC using new immunotherapy platform protocol. Density N refers to normal kidney tissue, Density IM refer to invasive margin, Density CT refers to center of tumor. Controls refers to patients who received nephrectomy alone, ablation refers to group of patients who received ablation procedure prior to nephrectomy. Groups are compared with student t test. CD20 B cell stain, CD68 macrophage stain, FoxP3 stain for regulatory subset, Gr-B granzyme B for cytotoxic cells.

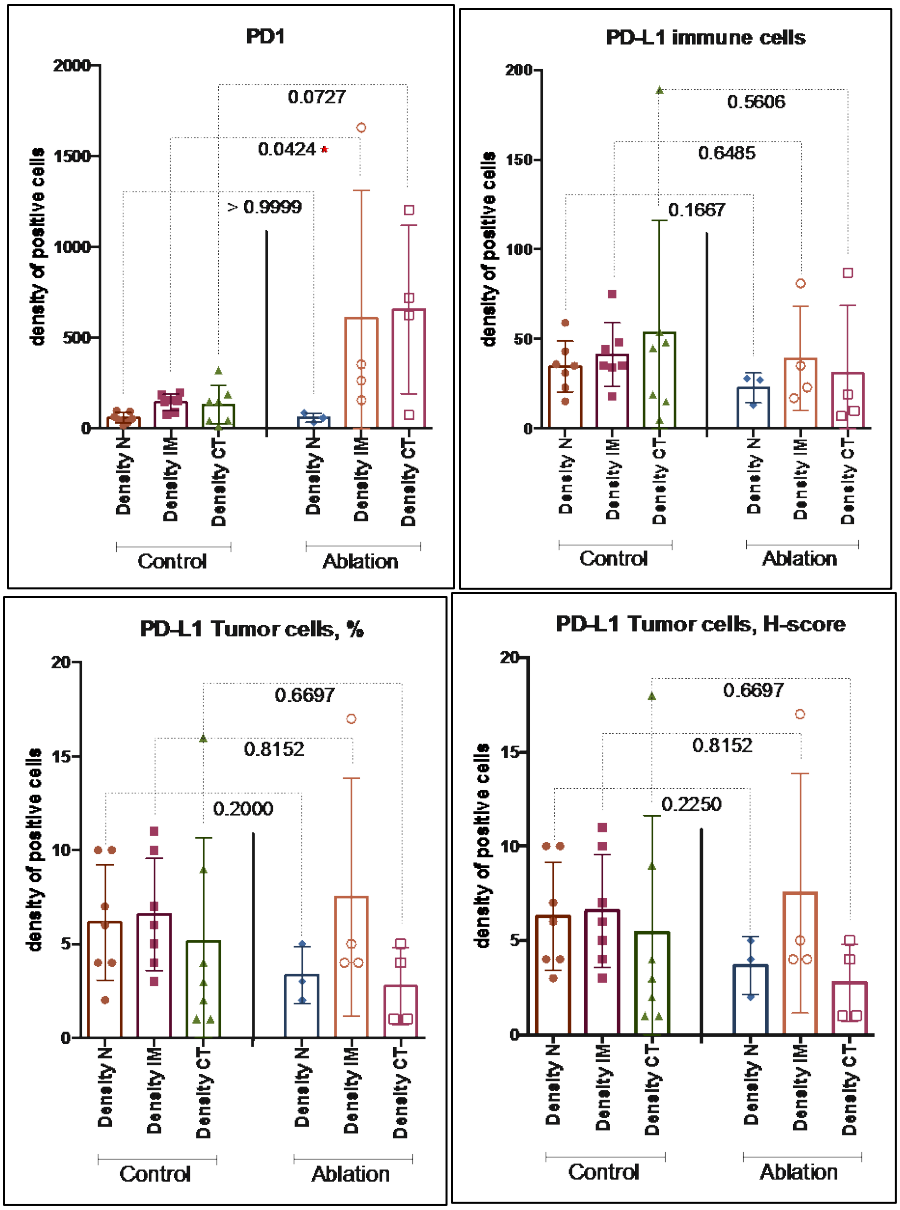

Figure 17: Updated IHC using new immunotherapy platform protocol. Density N refers to normal kidney tissue, Density IM refer to invasive margin, Density CT refers to center of tumor. Controls refers to patients who received nephrectomy alone, ablation refers to group of patients who received ablation procedure prior to nephrectomy. Groups are compared with student t test. PD-1 program death receptor 1, PD-L1 programmed death receptor ligand 1 expressing immune cells, PD-L1 program death receptor ligand 1 expressing tumor cells, and PD-L1 H score.

Flow cytommetry

Figures 18 through 32 represent the flow cytommetry analysis for patients analyzed prospectively after ablation to a primary renal cell carcinoma in the kidney. Day 0 (D0) reflects a baseline blood draw prior to ablation procedure and could occur within a one month period prior to the procedure. Day 1 (D1) reflects the immediate day following procedure while the patient remained hospitalized. Day 28 (D28) is the blood draw obtained 4 weeks following procedure at a scheduled return visit with urology. Day 180 is the blood draw obtained at 6 months following the ablation procedure. Several patients had a blood draw at 4 months and 1 year following the procedure without the 6 month blood draw. These blood draws were excluded from the analysis. In each of the figures, A represents the gating used for flow cytommetry. B represents all patients with baseline (day 0), day 1, day 28, and day 180 blood draws with percentage of positive cells. Kruskal-Wallis (unmatched data) and Dunn's multiple comparisons tests were used to determine statistical significance. C represents patients who had all four scheduled blood draws, and D represents individual patients with 3 blood draws at baseline, day 1, and day 28. For both C and D, Friedman's test (matched data at each time point) and Dunn's multiple comparisons tests were used to determine statistical significance. $CD4^+$T cells (Figure 18), $CD8^+$T cells (Figure 19), $CD19^+$B cells (Figure 20), $CD4^+ICOS^{hi}$ T cells (Figure 21), $CD8^+ICOS^{hi}$ T cells (Figure 22), $CD4^+CD45RO^+$T cells (Figure 28), lin-$CD4^+CD45RO^+CD62L^+CCR7^-$ T cells representing T effector memory (Figure 29), lin-$CD4^+CD45RO^+CD62L^+CCR7^+$ T cells representing T central memory (Figure 30), macrophage (Figure 31), and myeloid derived suppressor cells (Figure 32) did not show significant differences between baseline and later time points. The regulatory immune subsets included $CD4^+FoxP3^+$ T cells (Figure 23), $CD8^+FoxP3^+$ T cells (Figure 24), $CD4^+CD25^+FoxP3^+$ T cells

(Figure 25), $CD4^+CD25^+Lap^+$ T cells (Figure 26), and $CD4^+CD25^+CD127^-$T cells(Figure 27). The $CD4^+FoxP3^+$ T cells did show a statistically significant change between groups and a statistically significant increase between the day 1 blood draw that returned almost to baseline by the day 28 blood draw. Similarly, $CD4^+CD25^+Lap^+$ T cells showed a statistically significant change between groups and a statistically significant increase between the day 1 blood draw that returned almost to baseline by the day 28 blood draw. Both the $CD4^+CD25^+FoxP3^+$ T cells and the $CD4^+CD25^+CD127^-$ T cells had similar trends that approached, but did not reach significance.

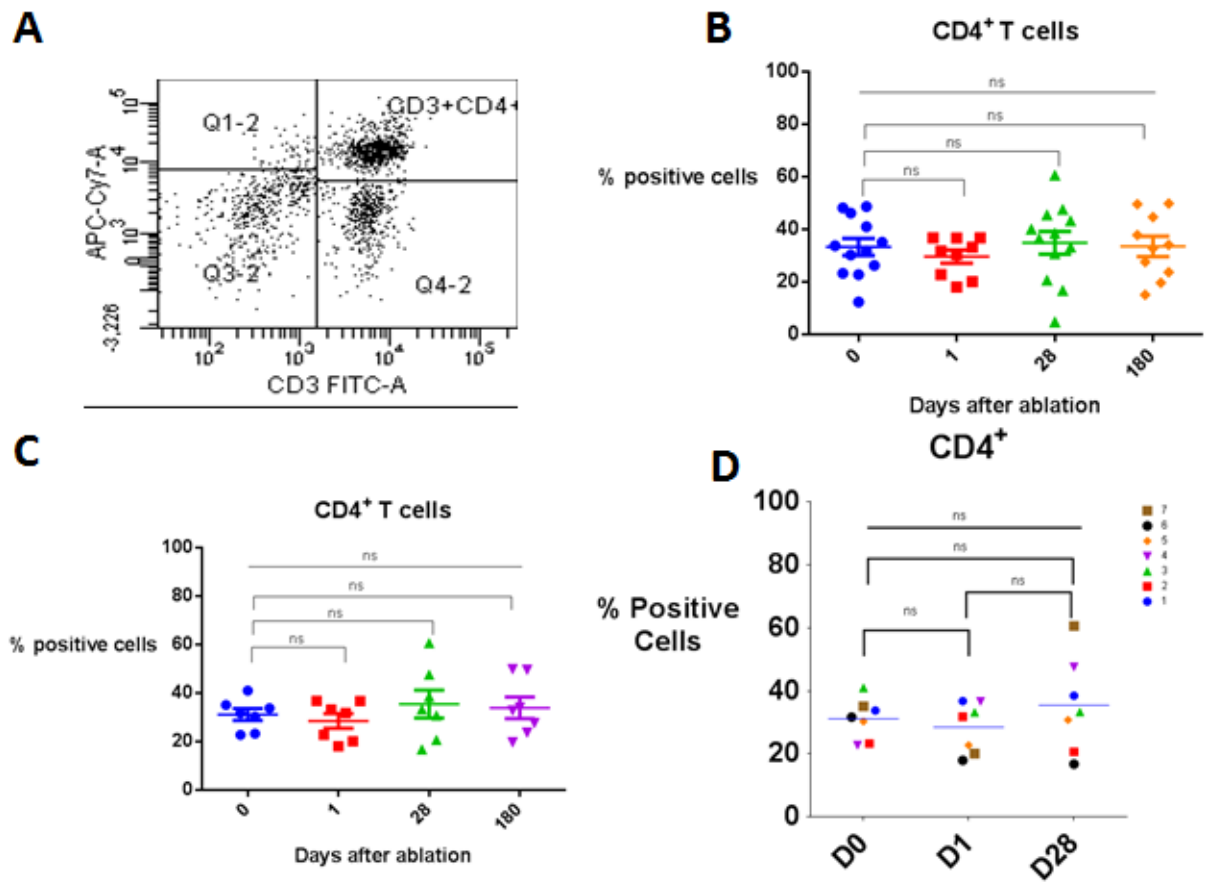

Figure 18 Flow cytommetry analysis $CD4^+$ T cells: A represents the gating used for flow cytommetry, samples tested in triplicate. B represents all patients with baseline (day 0), day 1, day 28, and day 180 blood draws with percentage of positive $CD4^+$ T cells. Kruskall-Wallis and Dunn's multiple comparisons tests were used to determine statistical significance. C represents patients who had blood draws at 4 time points, and D represents individual patients with 3 blood draws at baseline, day 1, and day 28. For both C and D, Friedman's test and Dunn's multiple comparisons tests were used to determine statistical significance. (ns = not significant, * = $p<0.05$)

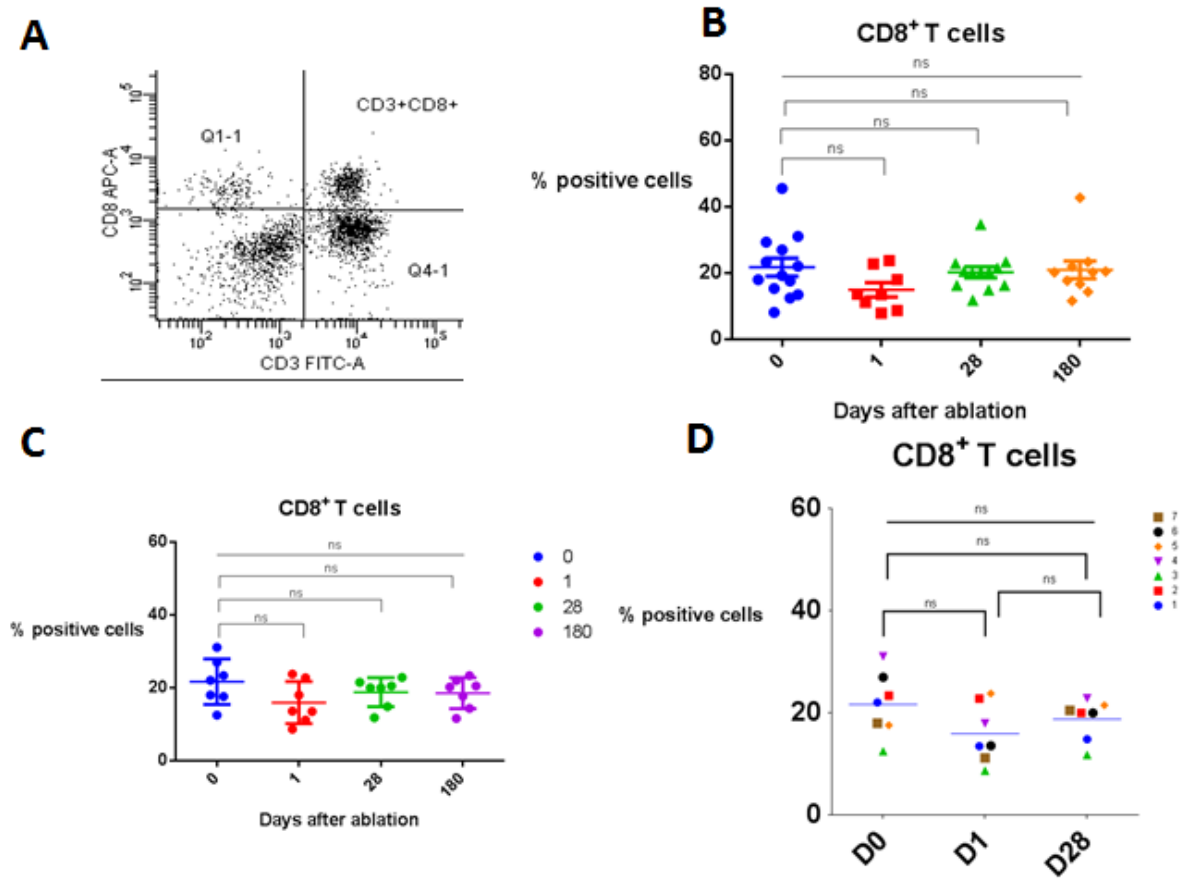

Figure 19 Flow cytommetry analysis $CD8^+$ T cells: A represents the gating used for flow cytommetry, samples tested in triplicate. B represents all patients with baseline (day 0), day 1, day 28, and day 180 blood draws with percentage of positive $CD8^+$ T cells. Kruskall-Wallis and Dunn's multiple comparisons tests were used to determine statistical significance. C represents patients who had blood draws at 4 time points, and D represents individual patients with 3 blood draws at baseline, day 1, and day 28. For both C and D, Friedman's test and Dunn's multiple comparisons tests were used to determine statistical significance. (ns = not significant, * = $p<0.05$)

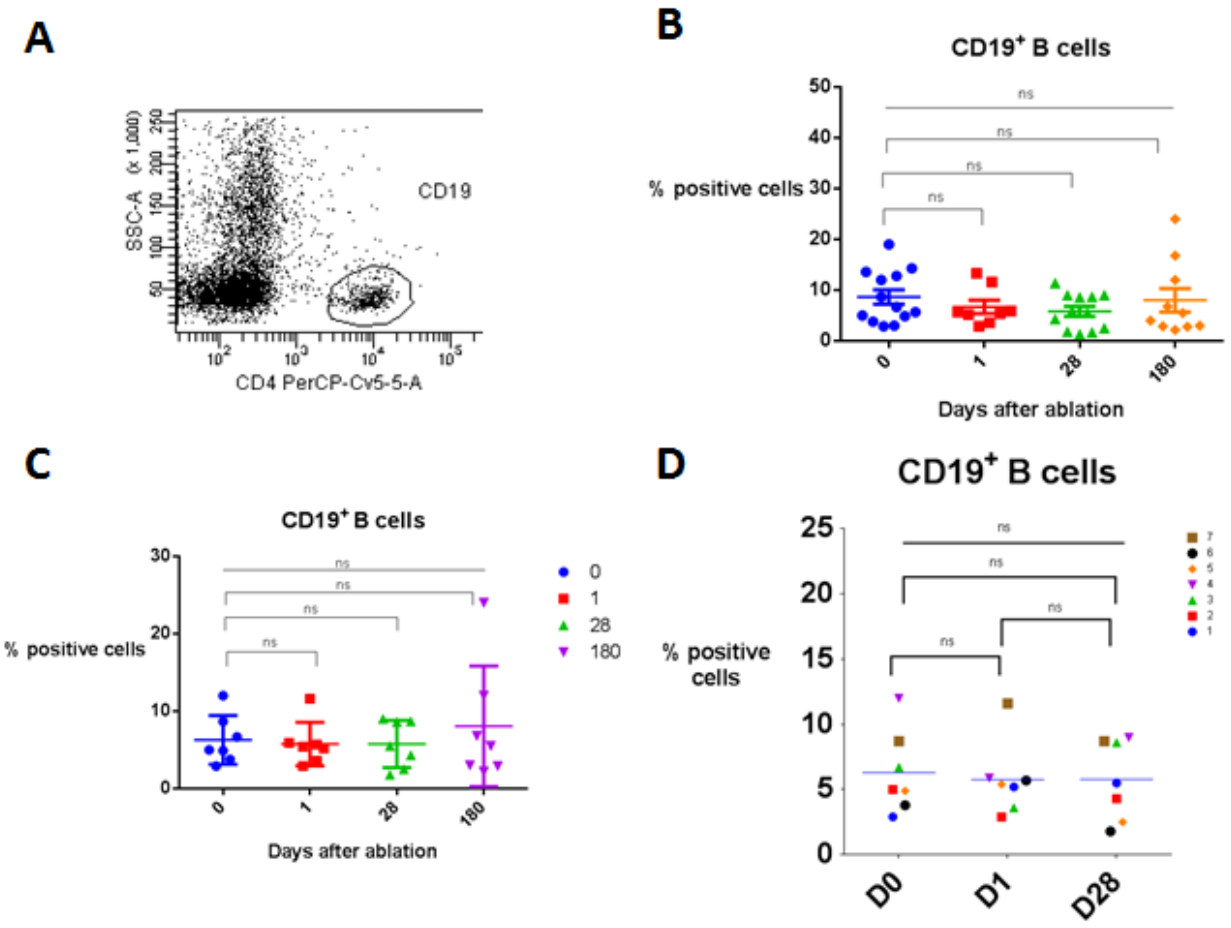

Figure 20 Flow cytommetry analysis $CD19^+$ B cells: A represents the gating used for flow cytommetry, samples tested in triplicate. B represents all patients with baseline (day 0), day 1, day 28, and day 180 blood draws with percentage of positive $CD19^+$ B cells. Kruskall-Wallis and Dunn's multiple comparisons tests were used to determine statistical significance. C represents patients who had blood draws at 4 time points, and D represents individual patients with 3 blood draws at baseline, day 1, and day 28. For both C and D, Friedman's test and Dunn's multiple comparisons tests were used to determine statistical significance. (ns = not significant, * = $p<0.05$)

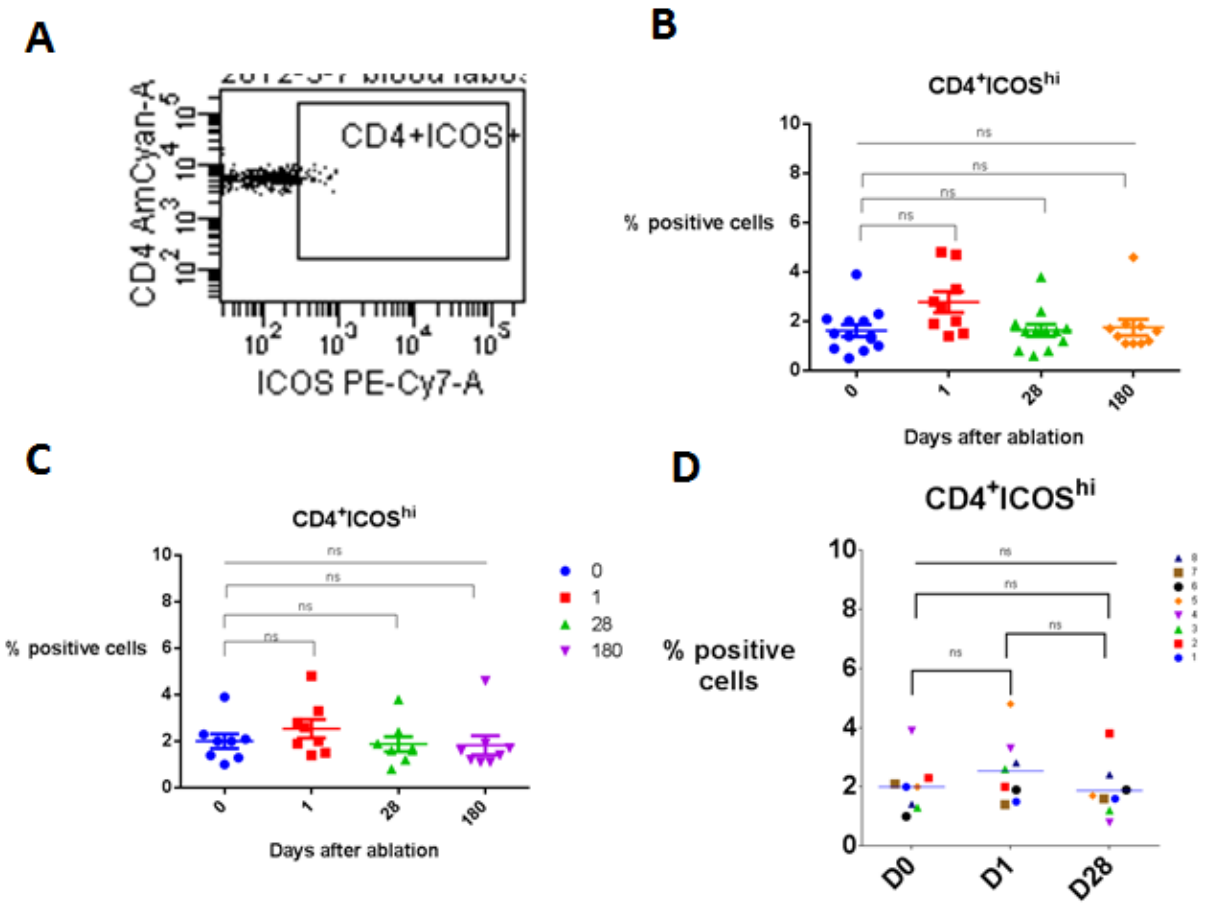

Figure 21 Flow cytommetry analysis $CD4^+$ $ICOS^{hi}$ T cells: A represents the gating used for flow cytommetry, samples tested in triplicate. B represents all patients with baseline (day 0), day 1, day 28, and day 180 blood draws with percentage of positive $CD4^+$ $ICOS^{hi}$ T cells. Kruskall-Wallis and Dunn's multiple comparisons tests were used to determine statistical significance. C represents patients who had blood draws at 4 time points, and D represents individual patients with 3 blood draws at baseline, day 1, and day 28. For both C and D, Friedman's test and Dunn's multiple comparisons tests were used to determine statistical significance. (ns = not significant, * = $p<0.05$)

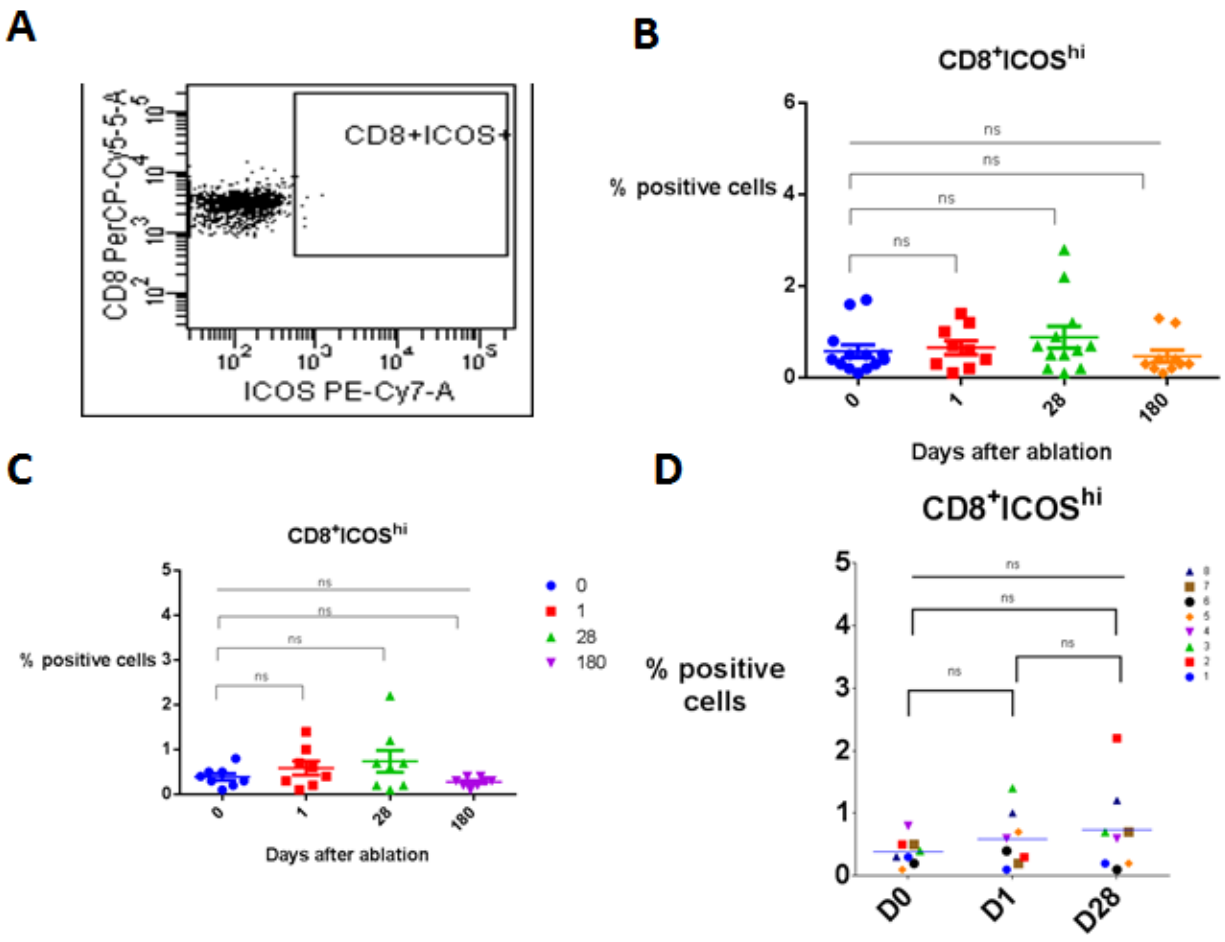

Figure 22 Flow cytommetry analysis CD8^{+} ICOS^{hi} T cells: A represents the gating used for flow cytommetry, samples tested in triplicate. B represents all patients with baseline (day 0), day 1, day 28, and day 180 blood draws with percentage of positive CD8^{+} ICOS^{hi} T cells. Kruskall-Wallis and Dunn's multiple comparisons tests were used to determine statistical significance. C represents patients who had blood draws at 4 time points, and D represents individual patients with 3 blood draws at baseline, day 1, and day 28. For both C and D, Friedman's test and Dunn's multiple comparisons tests were used to determine statistical significance. (ns = not significant, * = $p<0.05$)

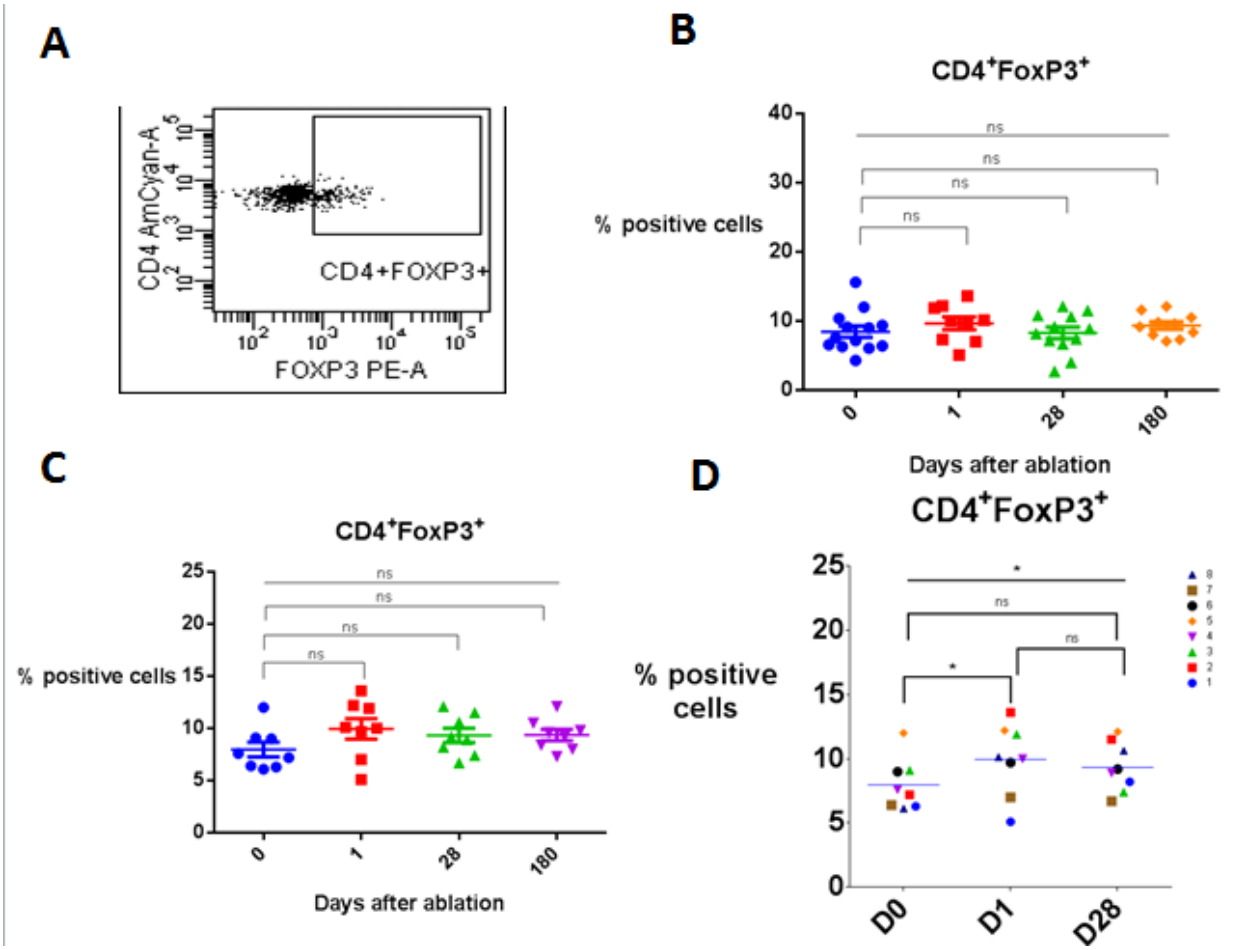

Figure 23: Flow cytommetry analysis $CD4^+$ $FoxP3^+$ T cells: A represents the gating used for flow cytommetry, samples tested in triplicate. B represents all patients with baseline (day 0), day 1, day 28, and day 180 blood draws with percentage of positive $CD4^+$ $FoxP3^+$ T cells. Kruskall-Wallis and Dunn's multiple comparisons tests were used to determine statistical significance. C represents patients who had blood draws at 4 time points, and D represents individual patients with 3 blood draws at baseline, day 1, and day 28. For both C and D, Friedman's test and Dunn's multiple comparisons tests were used to determine statistical significance. (ns = not significant, * = $p<0.05$)

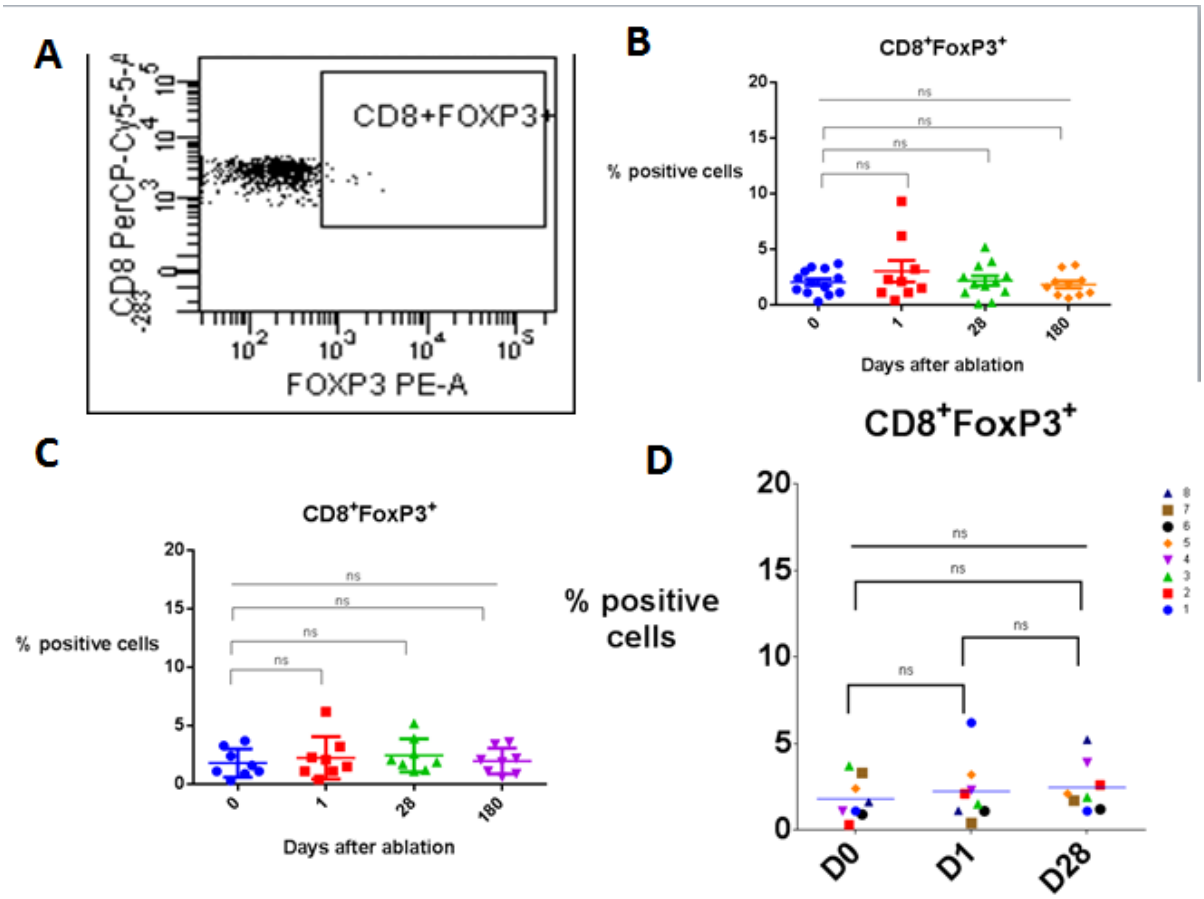

Figure 24 Flow cytommetry analysis $CD8^+$ $FoxP3^+$ T cells Figure: A represents the gating used for flow cytommetry, samples tested in triplicate. B represents all patients with baseline (day 0), day 1, day 28, and day 180 blood draws with percentage of positive $CD8^+$ $FoxP3^+$ T cells. Kruskall-Wallis and Dunn's multiple comparisons tests were used to determine statistical significance. C represents patients who had blood draws at 4 time points, and D represents individual patients with 3 blood draws at baseline, day 1, and day 28. For both C and D, Friedman's test and Dunn's multiple comparisons tests were used to determine statistical significance. (ns = not significant, * = $p<0.05$)

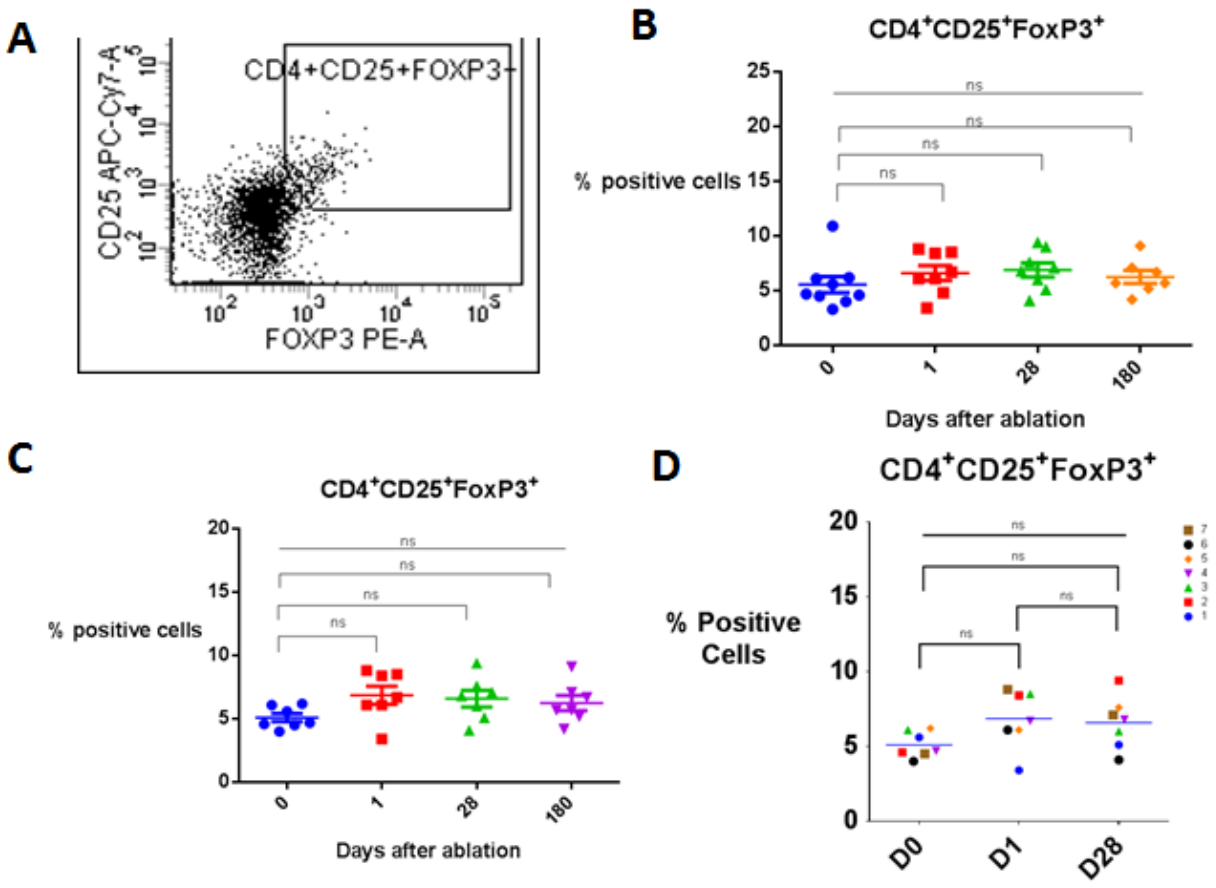

Figure 25 Flow cytommetry analysis $CD4^+$ $CD25^+$ $FoxP3^+$ T cells: A represents the gating used for flow cytommetry, samples tested in triplicate. B represents all patients with baseline (day 0), day 1, day 28, and day 180 blood draws with percentage of positive $CD4^+$ $CD25^+$ $FoxP3^+$ T cells. Kruskall-Wallis and Dunn's multiple comparisons tests were used to determine statistical significance. C represents patients who had blood draws at 4 time points, and D represents individual patients with 3 blood draws at baseline, day 1, and day 28. For both C and D, Friedman's test and Dunn's multiple comparisons tests were used to determine statistical significance. (ns = not significant, * = $p<0.05$)

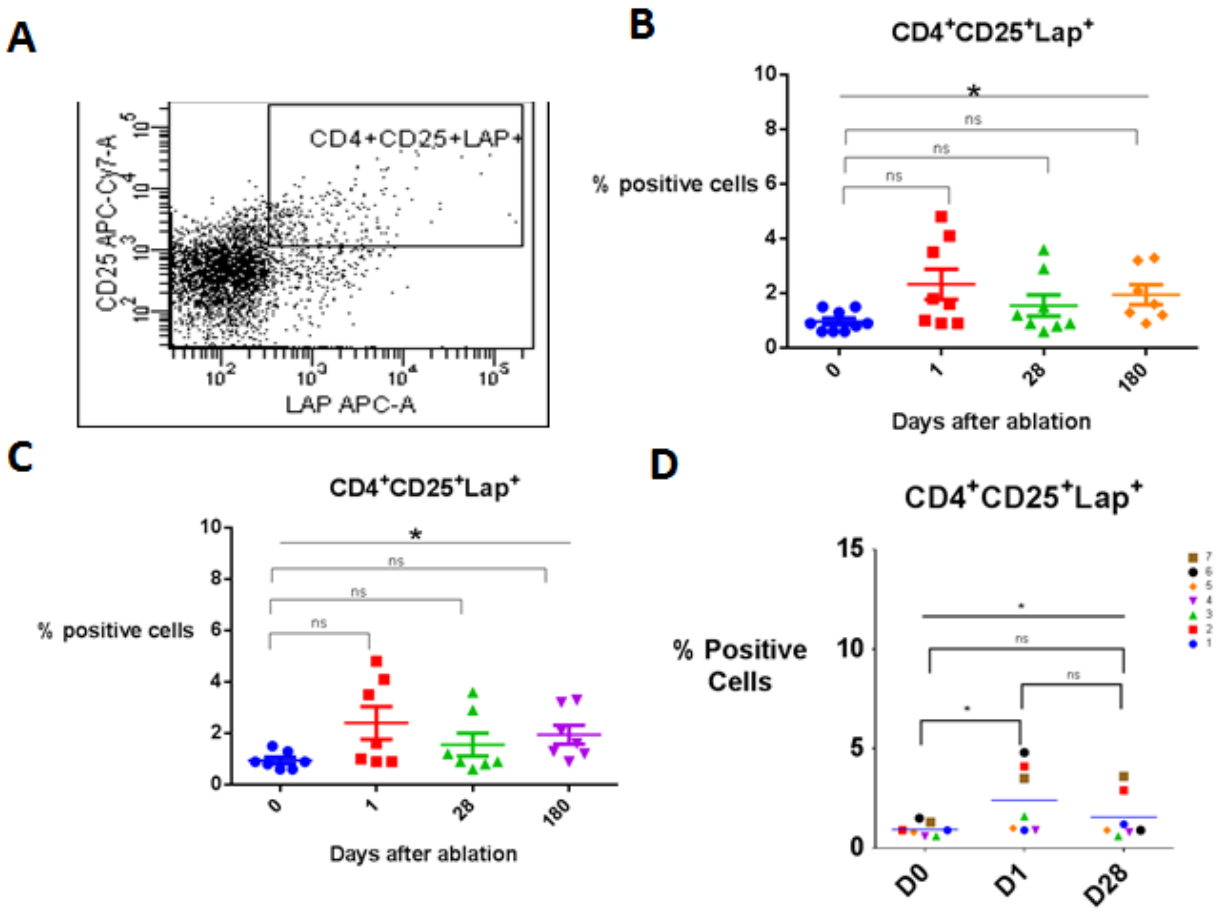

Figure 26 Flow cytommetry analysis $CD4^+$ $CD25^+$ Lap^+ T cells: A represents the gating used for flow cytommetry, samples tested in triplicate. B represents all patients with baseline (day 0), day 1, day 28, and day 180 blood draws with percentage of positive $CD4^+$ $CD25^+$ Lap^+ T cells. Kruskall-Wallis and Dunn's multiple comparisons tests were used to determine statistical significance. C represents patients who had blood draws at 4 time points, and D represents individual patients with 3 blood draws at baseline, day 1, and day 28. For both C and D, Friedman's test and Dunn's multiple comparisons tests were used to determine statistical significance. (ns = not significant, $p<0.05$)

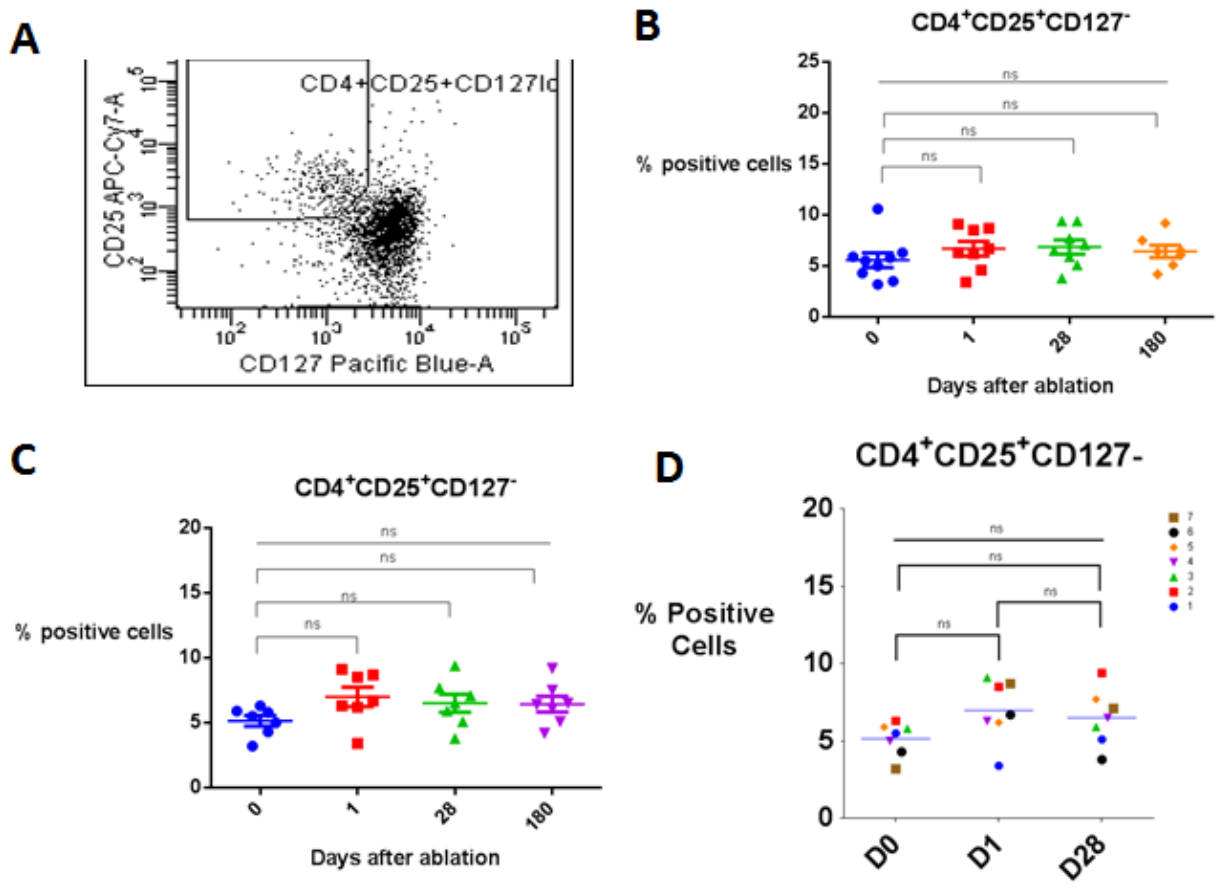

Figure 27 Flow cytommetry analysis $CD4^+$ $CD25^+$ $CD127^-$ T cells: A represents the gating used for flow cytommetry, samples tested in triplicate. B represents all patients with baseline (day 0), day 1, day 28, and day 180 blood draws with percentage of positive $CD4^+$ $CD25^+$ $CD127^-$ T cells. Kruskall-Wallis and Dunn's multiple comparisons tests were used to determine statistical significance. C represents patients who had blood draws at 4 time points, and D represents individual patients with 3 blood draws at baseline, day 1, and day 28. For both C and D, Friedman's test and Dunn's multiple comparisons tests were used to determine statistical significance. (ns = not significant, * = $p<0.05$)

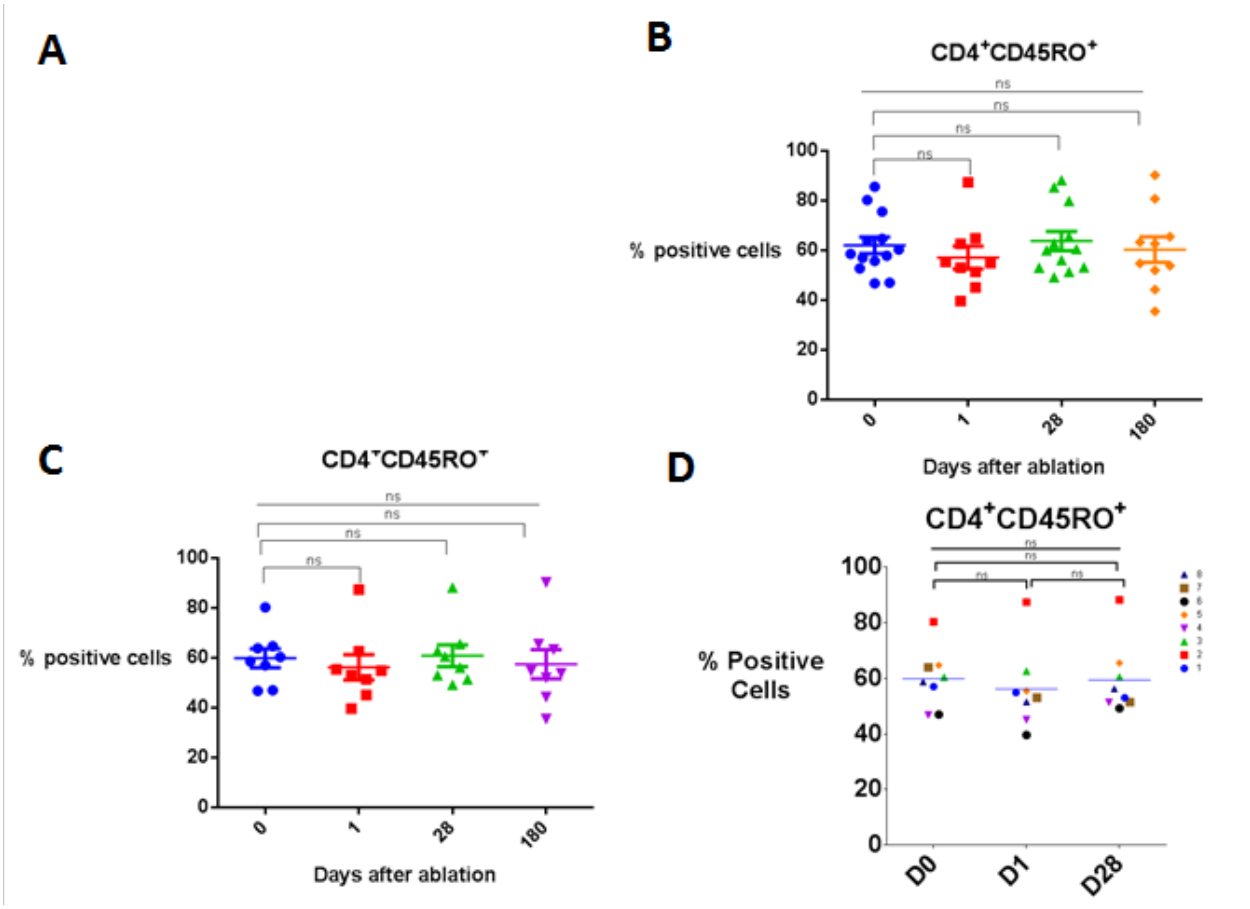

Figure 28 Flow cytommetry analysis $CD4^+$ $CD45RO^+$ Tcells: A represents the gating used for flow cytommetry, samples tested in triplicate. B represents all patients with baseline (day 0), day 1, day 28, and day 180 blood draws with percentage of positive $CD4^+$ $CD45RO^+$ T cells. Kruskall-Wallis and Dunn's multiple comparisons tests were used to determine statistical significance. C represents patients who had blood draws at 4 time points, and D represents individual patients with 3 blood draws at baseline, day 1, and day 28. For both C and D, Friedman's test and Dunn's multiple comparisons tests were used to determine statistical significance. (ns = not significant, * = $p<0.05$)

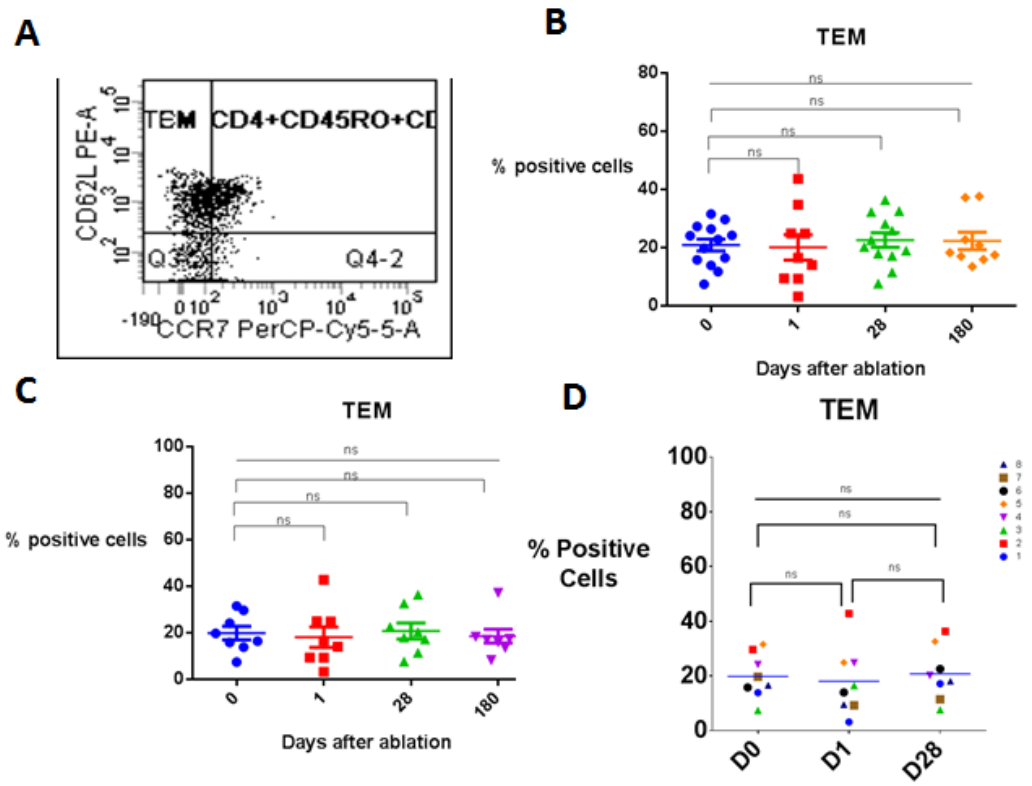

Figure 29 Flow cytommetry analysis TEM (T Effector Memory) lin-$CD4^{+}CD45RO^{+}CD62L^{+}CCR7^{-}$ T cells: A represents the gating used for flow cytommetry, samples tested in triplicate. B represents all patients with baseline (day 0), day 1, day 28, and day 180 blood draws with percentage of positive TEM T cells. Kruskall-Wallis and Dunn's multiple comparisons tests were used to determine statistical significance. C represents patients who had blood draws at 4 time points, and D represents individual patients with 3 blood draws at baseline, day 1, and day 28. For both C and D, Friedman's test and Dunn's multiple comparisons tests were used to determine statistical significance. (ns = not significant, * = $p<0.05$)

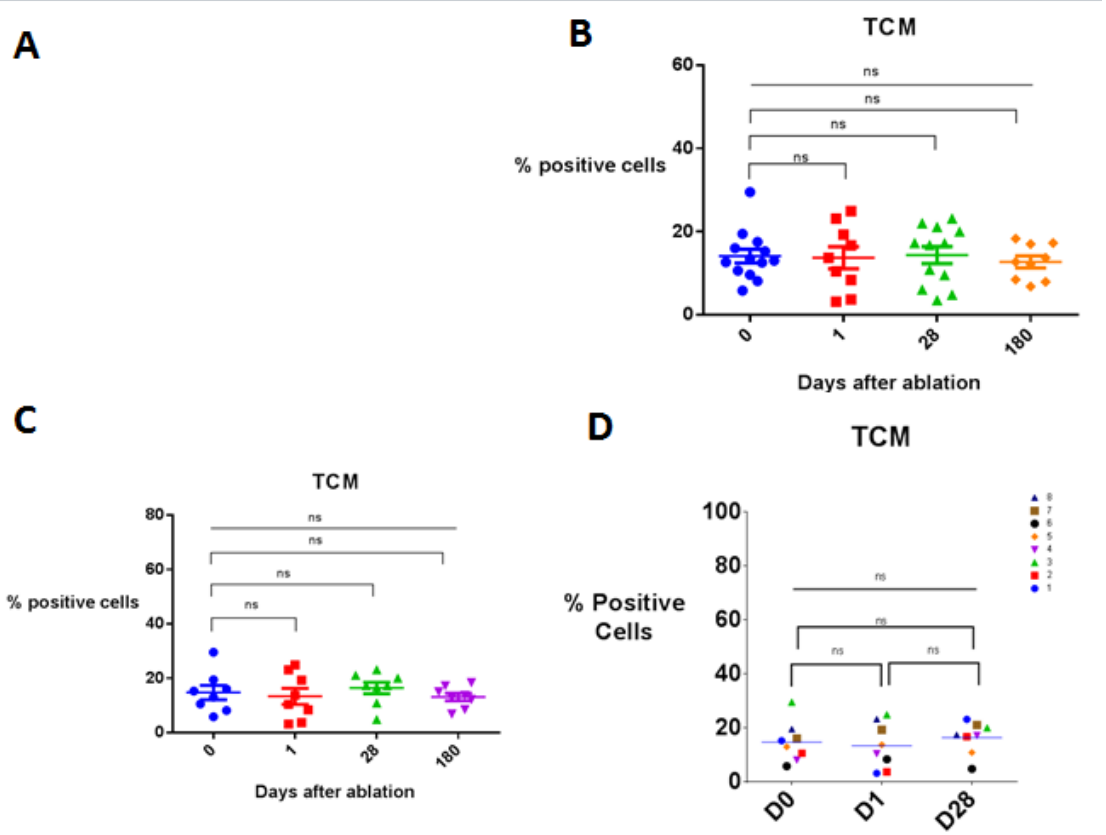

Figure 30 Flow cytommetry analysis TCM (T Central Memory) lin-$CD4^{+}CD45RO^{+}CD62L^{+}CCR7^{+}$T cells: A represents the gating used for flow cytommetry, samples tested in triplicate. B represents all patients with baseline (day 0), day 1, day 28, and day 180 blood draws with percentage of positive TCM cells. Kruskall-Wallis and Dunn's multiple comparisons tests were used to determine statistical significance. C represents patients who had 4 time point blood draws, and D represents individual patients with 3 blood draws at baseline, day 1, and day 28. For both C and D, Friedman's test and Dunn's multiple comparisons tests were used to determine statistical significance. (ns = not significant, * = $p<0.05$)

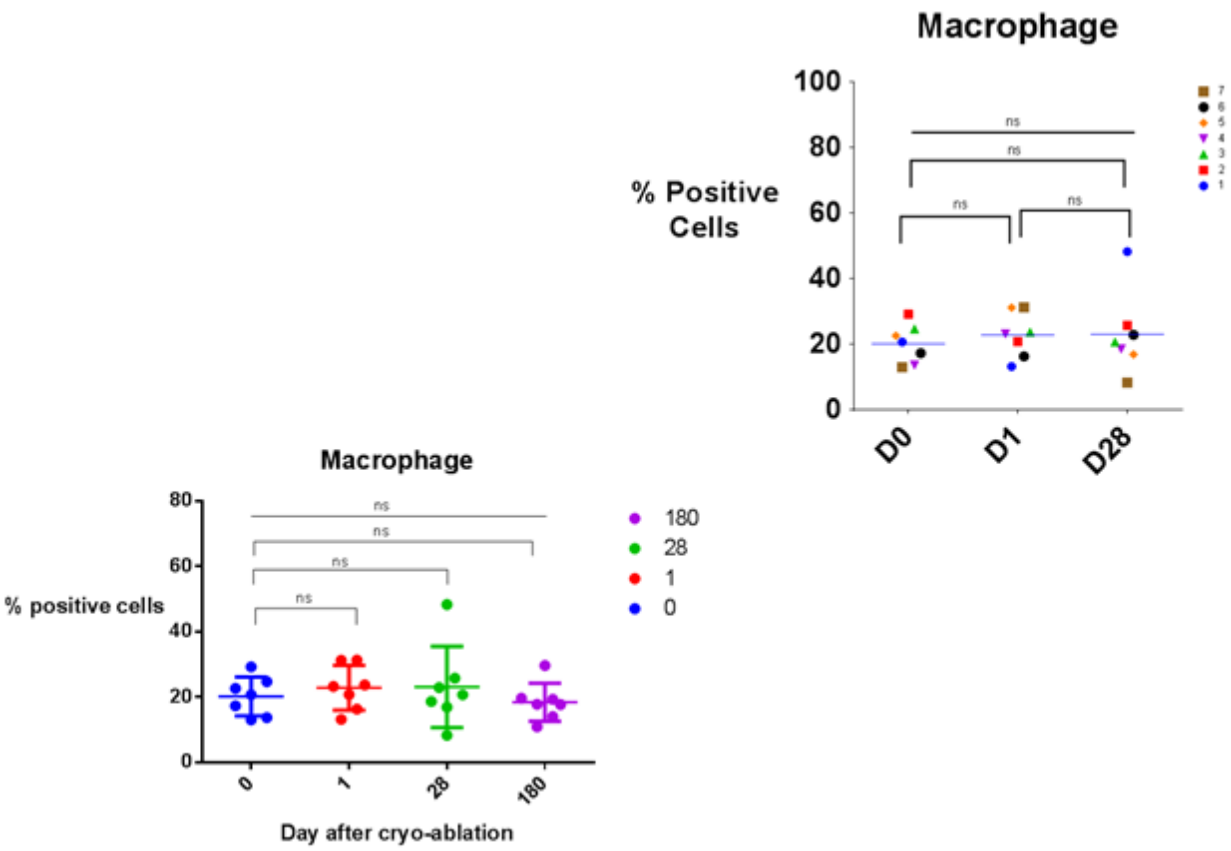

Figure 31 Macrophage: A represents the gating used for flow cytommetry, samples tested in triplicate. B represents all patients with baseline (day 0), day 1, day 28, and day 180 blood draws with percentage of positive CD4+ T cells. Kruskall-Wallis and Dunn's multiple comparisons tests were used to determine statistical significance. C represents patients who had blood draws at 4 time points, and D represents individual patients with 3 blood draws at baseline, day 1, and day 28. For both C and D, Friedman's test and Dunn's multiple comparisons tests were used to determine statistical significance. (ns = not significant, * = $p<0.05$)

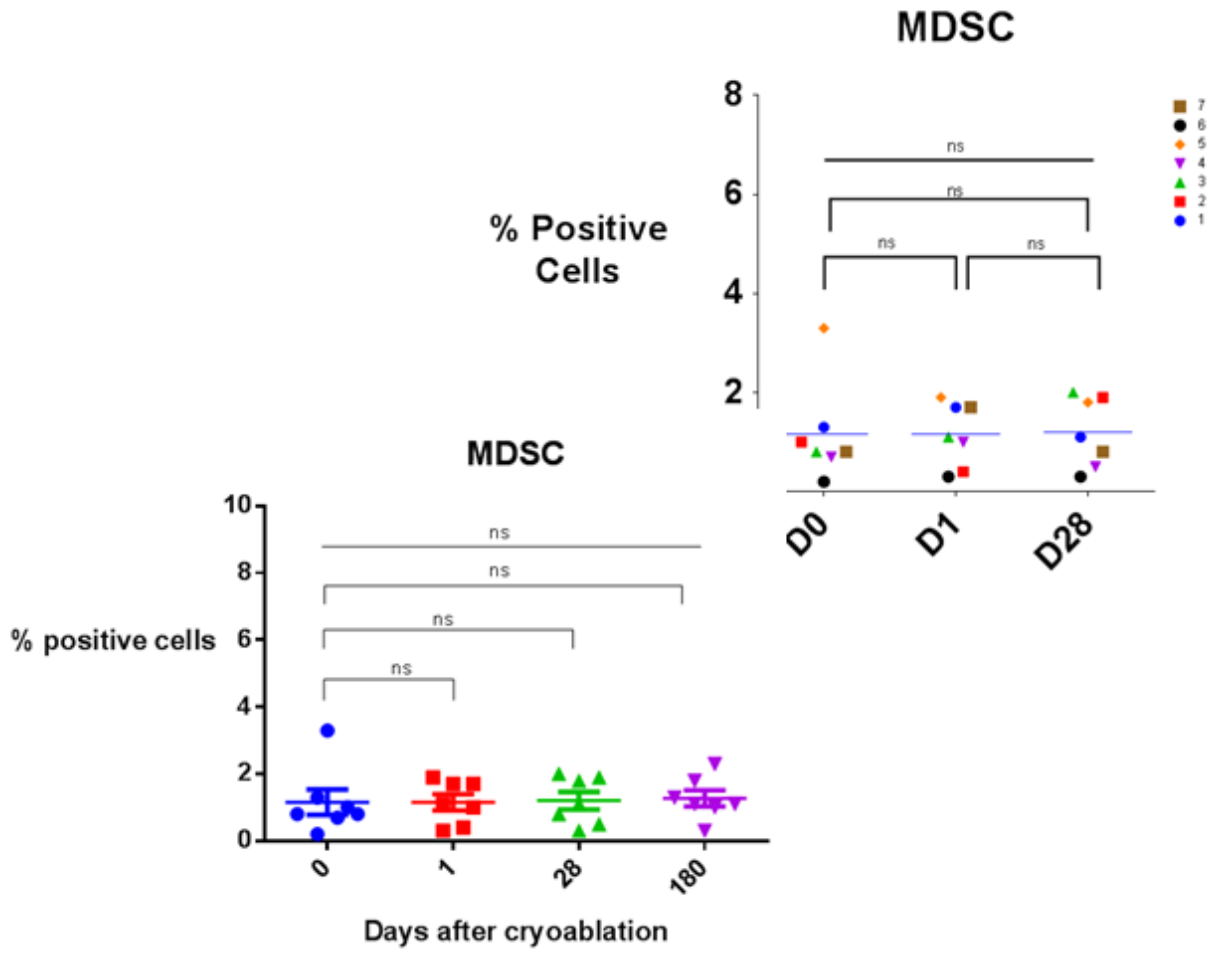

Figure 32 MDSC (Myeloid derived suppressor cells): A represents the gating used for flow cytommetry, samples tested in triplicate. B represents all patients with baseline (day 0), day 1, day 28, and day 180 blood draws with percentage of positive CD4+ T cells. Kruskall-Wallis and Dunn's multiple comparisons tests were used to determine statistical significance. C represents patients who had 4 time point blood draws, and D represents individual patients with 3 blood draws at baseline, day 1, and day 28. For both C and D, Friedman's test and Dunn's multiple comparisons tests were used to determine statistical significance. (ns = not significant, * = $p<0.05$)

Cytokine Studies

The results of serum cytokine studies are represented in Figures 33 through 43. All 10 cytokines were measured prospectively in pg/mL and displayed on the x-axis in Figure 33 with the mean cytokine level at three time points represented by three bar graphs. The first bar represents day 0 or baseline, the second bar represents 24 hours or day 1 following the ablation, the third bar represents day 28 after the ablation. IL-6 was the cytokine that exhibited the highest levels in the serum at each time point and did exhibit statistically significant change from baseline to day 1. Figure 34-43 show 7 patients who had matched baseline, 24 hour, and 28 day blood draws. The most significant change was in IL-6 with a significant increase between baseline and day 1 based on the Dunn's multiple comparison test. The group difference based on the Kruskal Wallis test of IL-6 approached significance with $p=0.052$. IL-10 did show a significant difference between groups using the Friedman test with a trend downward from baseline to day 1 to day 28. IL-12p70 also found a significant difference between day 1 and day 28 and between groups. However, the level of IL-12p70 detected in the serum was very low approaching the level of the first standard and the confidence to report this finding is small.

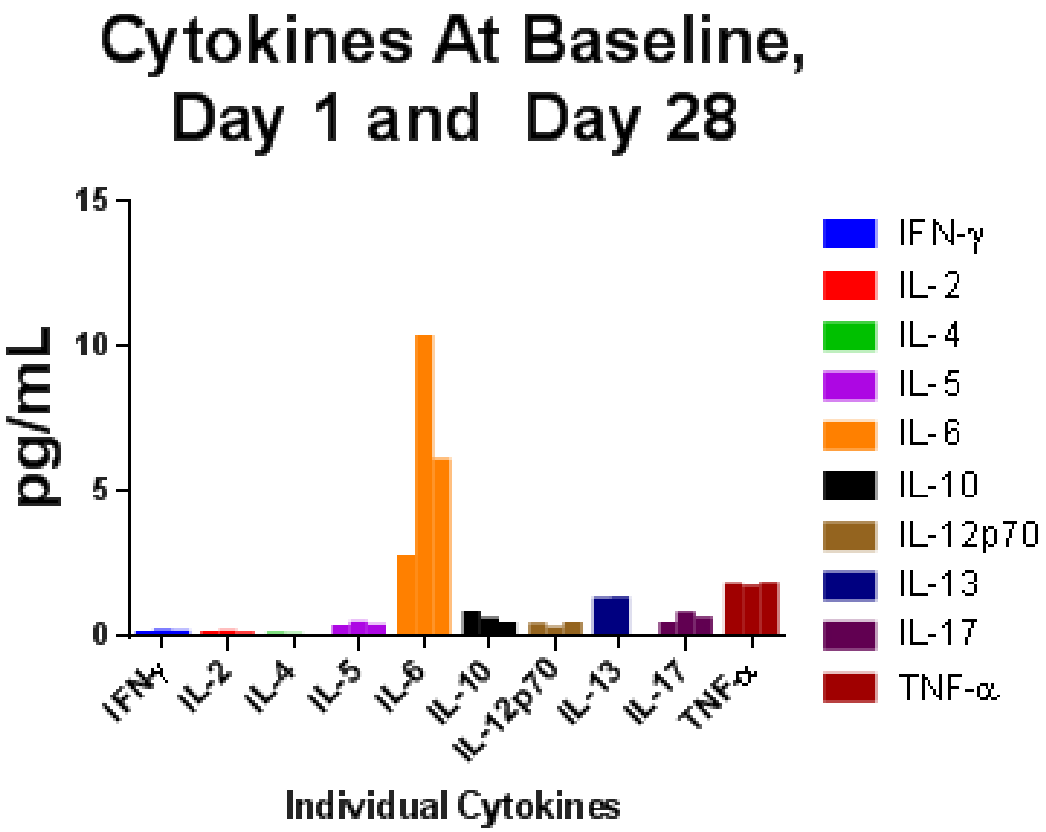

Figure 33: Post ablation levels of cytokines. Each cytokine is represented with 3 bars, the first bar corresponds to the baseline blood draw, bar 2 is day 1 following procedure, bar 3 is day 28 blood draw.

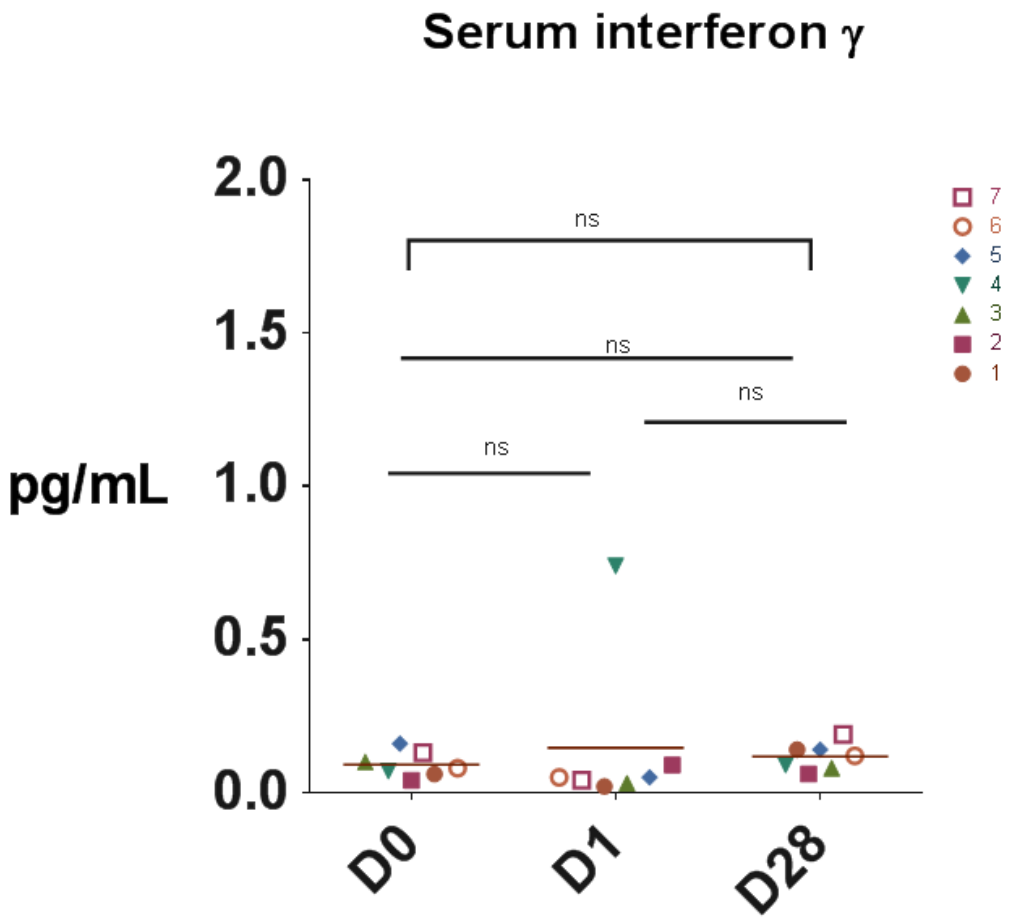

Figure 34: Serum interferon γ level at baseline (D0), day 1 (D1), and day 28 (D28). Each patient is represented with a different colored symbol. As each patient had 3 blood draws, the Friedman's test and Dunn's multiple comparisons tests were used to determine statistical significance. (ns = not significant, * = $p<0.05$)

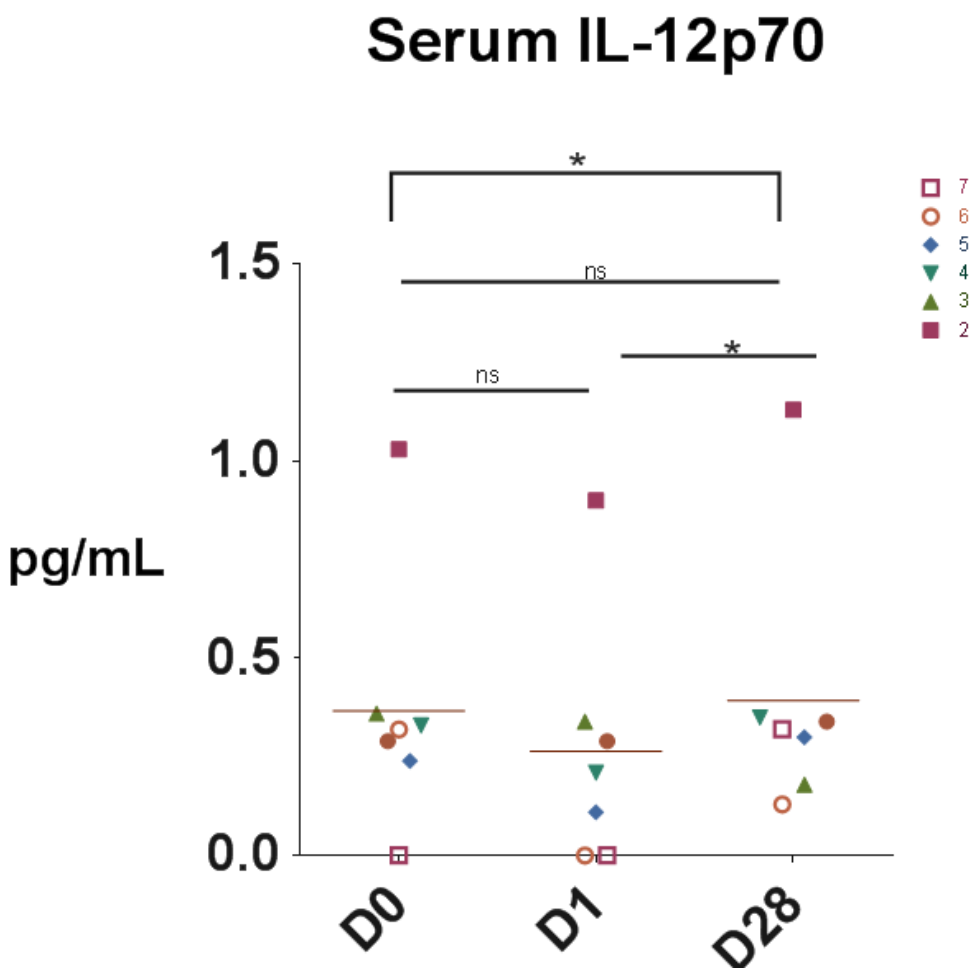

Figure 35: Serum IL-12p70 level at baseline (D0), day 1 (D1), and day 28 (D28). Each patient is represented with a different colored symbol. The Friedman's test and Dunn's multiple comparison tests were used to determine statistical significance. (ns = not significant, * = significant with $p<0.05$)

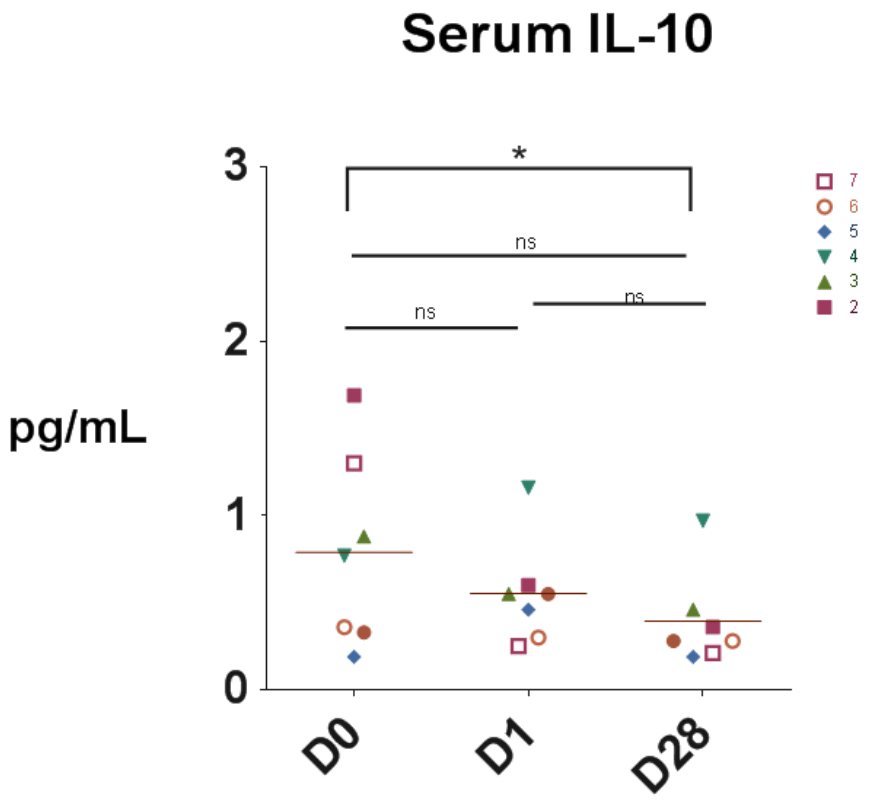

Figure 36: Serum IL-10 level at baseline (D0), day 1 (D1), and day 28 (D28). Each patient is represented with a different colored symbol. As each patient had 3 blood draws, the Friedman's test and Dunn's multiple comparisons tests were used to determine statistical significance. (ns = not significant, * = $p<0.05$)

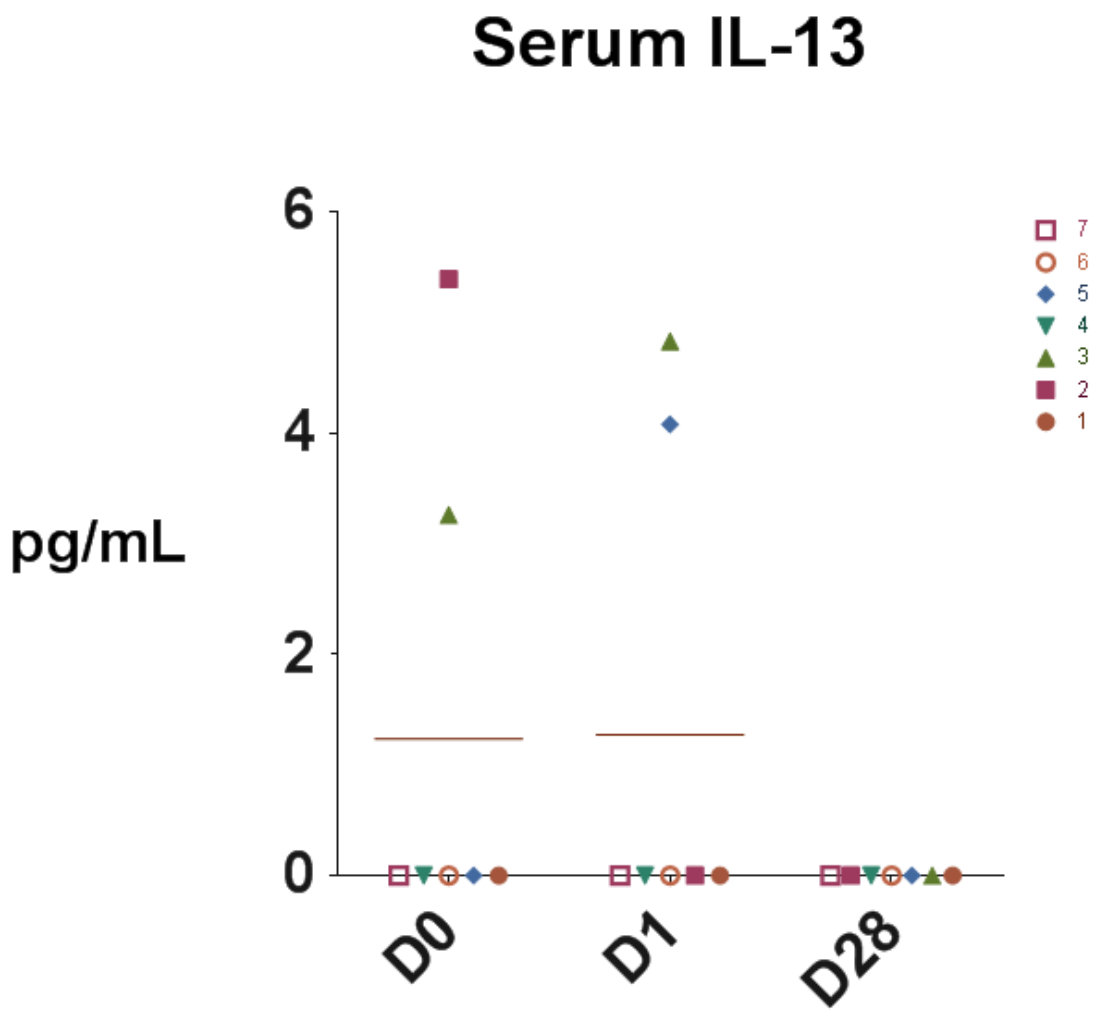

Figure 37: Serum IL-13 level at baseline (D0), day 1 (D1), and day 28 (D28). Each patient is represented with a different colored symbol. As each patient had 3 blood draws, the Friedman's test and Dunn's multiple comparisons tests were used to determine statistical significance.

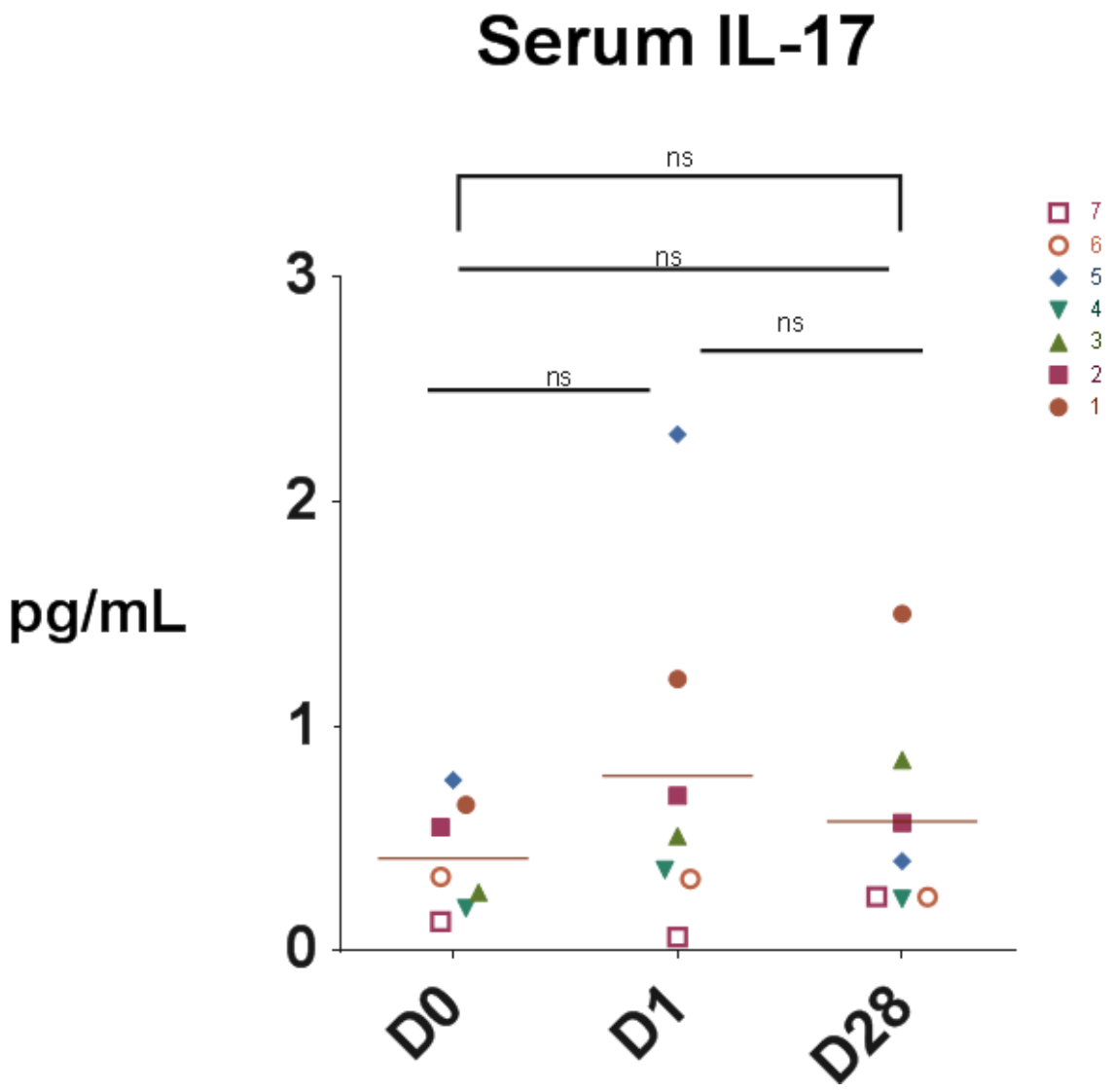

Figure 38: Serum IL-17 level at baseline (D0), day 1 (D1), and day 28 (D28). Each patient is represented with a different colored symbol. As each patient had 3 blood draws, the Friedman's test and Dunn's multiple comparisons tests were used to determine statistical significance. (ns = not significant, * = $p<0.05$)

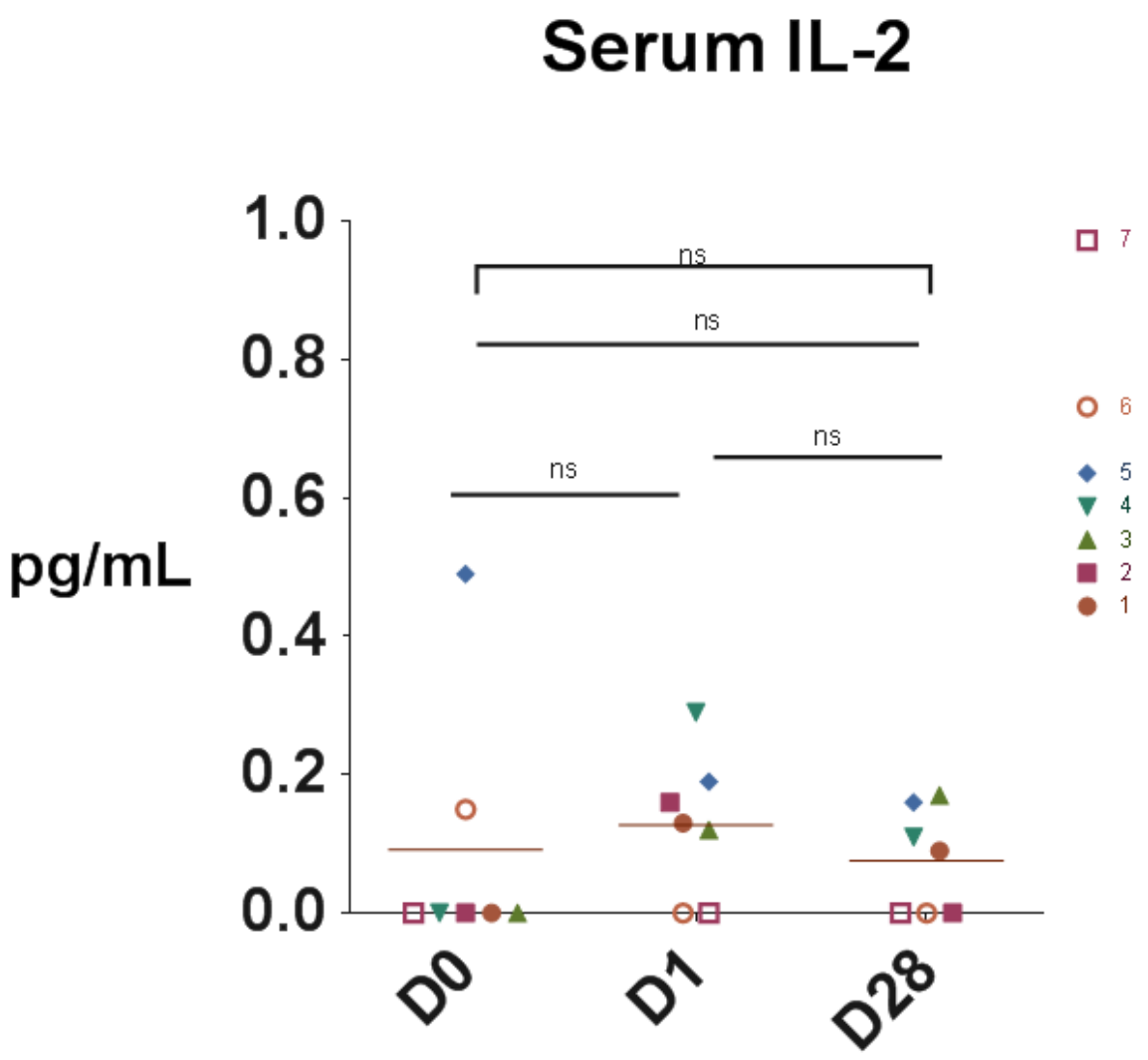

Figure 39: Serum IL-2 level at baseline (D0), day 1 (D1), and day 28 (D28). Each patient is represented with a different colored symbol. As each patient had 3 blood draws, the Friedman's test and Dunn's multiple comparisons tests were used to determine statistical significance. (ns = not significant, * = $p<0.05$)

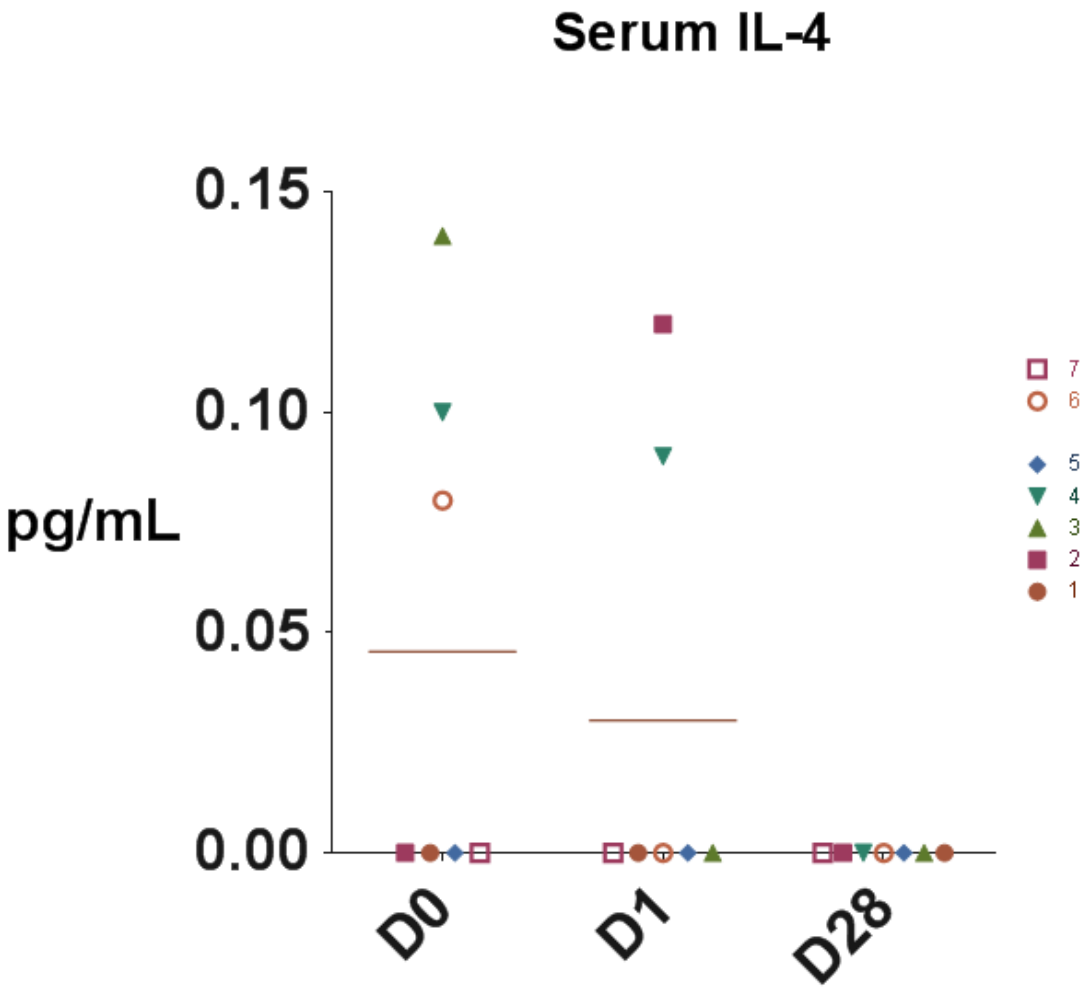

Figure 40: Serum IL-4 level at baseline (D0), day 1 (D1), and day 28 (D28). Each patient is represented with a different colored symbol. As each patient had 3 blood draws, the Friedman's test and Dunn's multiple comparisons tests were used to determine statistical significance. (ns = not significant, * = $p<0.05$)

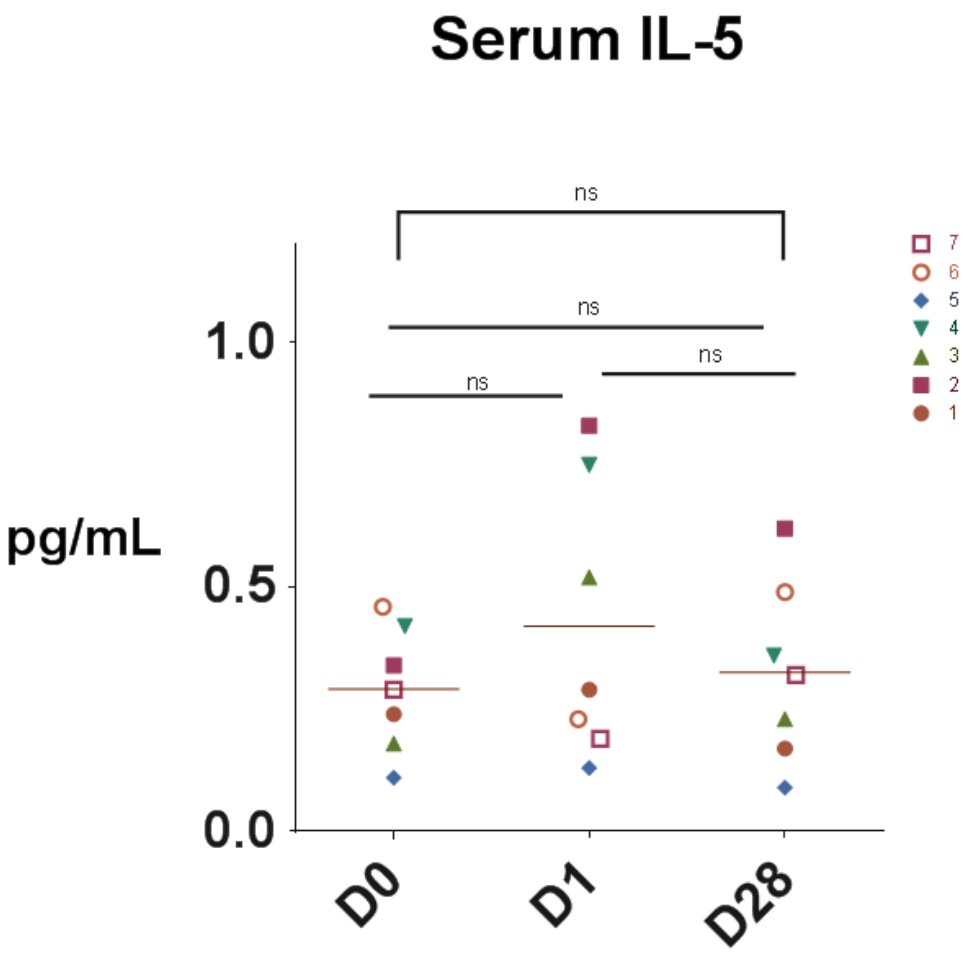

Figure 41: Serum interferon γ level at baseline (D0), day 1 (D1), and day 28 (D28). Each patient is represented with a different colored symbol. As each patient had 3 blood draws, the Friedman's test and Dunn's multiple comparisons tests were used to determine statistical significance. (ns = not significant, * = $p<0.05$)

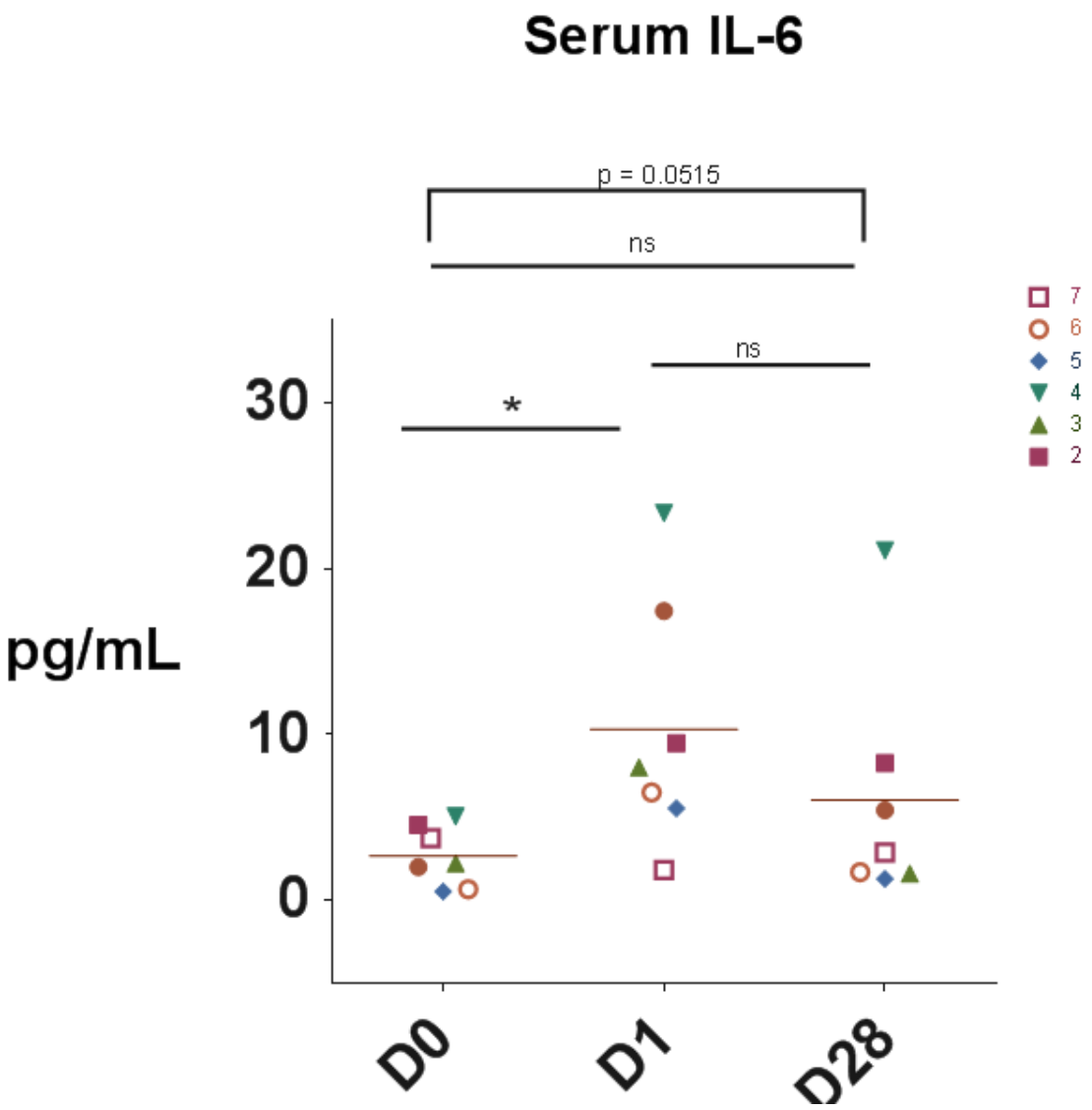

Figure 42: Serum IL-6 level at baseline (D0), day 1 (D1), and day 28 (D28). Each patient is represented with a different colored symbol. As each patient had 3 blood draws, the Friedman's test and Dunn's multiple comparisons tests were used to determine statistical significance. (ns = not significant, * = $p<0.05$)

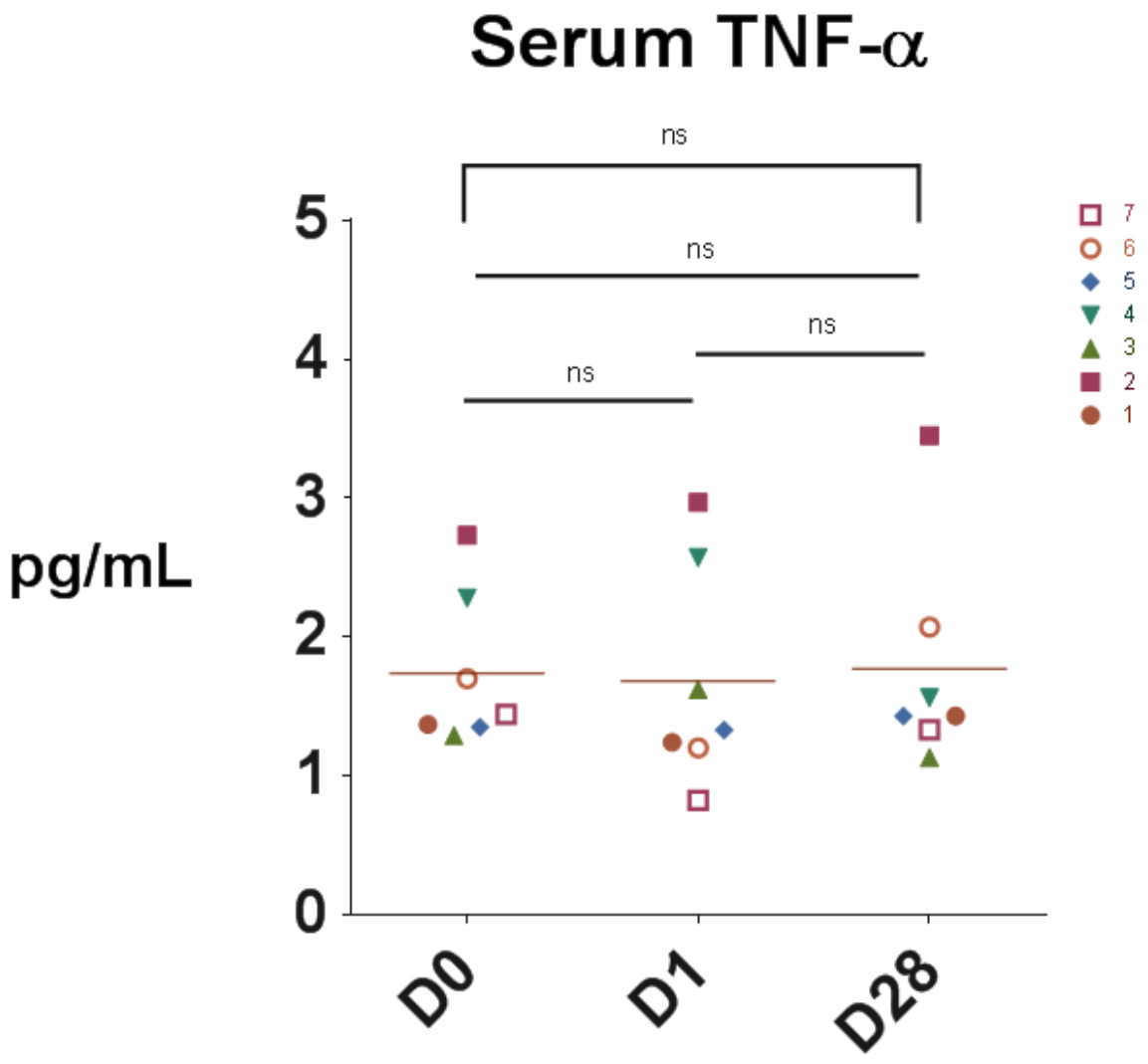

Figure 43: Serum TNF-α level at baseline (D0), day 1 (D1), and day 28 (D28). Each patient is represented with a different colored symbol. As each patient had 3 blood draws, the Friedman's test and Dunn's multiple comparisons tests were used to determine statistical significance. (ns = not significant, * = $p<0.05$)

IV. Discussion

The hypothesis of thermal ablation procedures cause a significant local inflammatory response leading to an immunogenic gene signature that will be confirmed with detectable changes in immune cells identified in tissue with immunohistochemistry and in the peripheral circulation was not established in the studies presented above. The first aim examining a retrospective cohort of patients treated with thermal ablation following nephrectomy compared to nephrectomy alone did appear to find an inflammatory, immunogenic signature. However, finding the inflammatory, immunogenic signature required removal of one sample due to it having significant different properties than the rest and not meeting quality control metrics and our decision to exclude one patient treated with cryoablation leaving only three samples from two patients treated with radiofrequency ablation. As a result, the confidence in these findings is limited despite the BUM modeling and the significance detected by extremely small p-values. Gene signatures have previously been proposed in melanoma implicating the importance of connectivity between the innate and adaptive immune response [58,59] [60].

The upstream molecules found during the Ingenuity analysis are known mediators of inflammation including cytokines, chemokines, toll like receptors, members of the Janus Kinase/Signal Transducer and Activator of Transcription (JAK/Stat) signaling pathway. Triggering Receptor Expressed on Myeloid Cells 1 or TREM1 was found to have significant activation with a p value of (1.73E-09). TREM1 is known to be expressed on neutrophils, monocytes, and platelets [61] [62]. It has been found to be related by Bruton's Tyrosine Kinase (BTK) and Non-T cell activation linker (NTAL) [63]. TREM1 has been described as playing an important role in human sepsis [64] [62] and blunting both toll like receptor 4 and TREM1 has been associated with blunting of the sometimes lethal sepsis response in animal modeling. TREM1

has been described to be an innate receptor for necrotic cell death a mechanism of cell death described in ablation procedures. TREM1 could be further explored in animal models with ablation procedures to understand if blocking TREM1 signaling could augment any protective effect from ablation or disrupt connectivity between innate and adaptive immune signaling.

Gene microarray analysis has exploded in the field of oncology. Given the amount of information generated from a study, generating a clinically meaningful signature that is duplicated by other data sets is challenging. Some of the initial work in gene microarray analysis was carried out by Takahashi et al and published in 2001 [65]. In this work, two distinct signatures were identified that clearly segregated patients into good and poor prognostic categories. In a study by Kosari et al. gene microarray could clearly distinguish normal tissue adjuvant to renal carcinoma, indolent and aggressive biology tumors. The microarray analysis was validated using quantitative reverse transcription-PCR (RT-PCR) [66]. One of the lead candidate genes to discriminate survival was the aptly named gene survivin. In our datasets, survivin was not significant. In 2005, Subramanian proposed using gene expression enrichment analysis to focus on gene sets to help interpret the results of the large amount of data emerging from genomic analysis [67]. Using this approach Maruschke et al. found 16 significantly upregulated or downregulated gene sets that were capable of differentiating high grade from low grade clear cell renal cell carcinomas [68]. More recently, molecular signatures known as ccA and ccB have been proposed and were validated in The Cancer Genome Atlas (TCGA) in clear cell renal cell carcinoma [69 70]. In our analysis, the biologic processes, pathways, and individual genes were all dominated by the immune system. If the inflammation and immunogenicity can be harnessed to prime the immune system prior to additional immune based therapy as has been found in animal

modeling with melanoma and prostate cancer, this could rapidly be brought to clinic and potentially be explored in a wide variety of tumor types.

The second aim of the project was to determine in a retrospective cohort of patients if there is a correlation between the gene signature produced with thermal ablation followed by nephrectomy with changes detected in immunohistochemistry for specific immune cell subsets, comparing to patients treated with nephrectomy alone. Based on our available analysis, we were unable to correlate the findings of our gene signature with differences in immune infiltrate between the two groups of patients studied.

Interpreting the results of the immunohistochemistry retrospectively is challenging. First considering patients who underwent a renal ablation followed later by nephrectomy, there was a wide range in time between the two procedures. Will an ablation procedure have lasting immune impact six years after performed? Will an ablation procedure have a local impact on the immune system 2 months after procedure? These studies are difficult to perform prospectively in this patient population as the purpose of treating with ablative procedures is to provide definitive local control. As a result, patients who receive a partial or radical nephrectomy in this context are viewed as local treatment failure of the RFA or cryoablation. The exception to this role would be patients who have multiple masses and require subsequent surgery for a growing alternative mass as can often be the case in patients with Von Hippel Lindau or other instances in hereditary causes of multiple complex renal masses/cysts. In the case of a solitary renal lesion, cryoablation and RFA are known to have local control rates approaching 90% and have been reported in single series to be greater than 95% in renal tumors less than 3cm [71]. As a result, the studies of our patients may reflect a more aggressive or different local biology than seen in typical series of solitary small renal tumors. Also the impact of immune infiltration may be

significantly different in a patient who has local disease under control versus a patient who has failed previous ablation procedure.

Also adding a layer of complexity is that retrospective data has emerged in regards to the local and systemic immunity being vastly different in the context of higher staged and more aggressive tumor biology. As a result, drawing conclusions from patients with largely T1a or T1b tumors and extrapolating to patients with locally advanced or metastatic disease is likely to be flawed. In 2003, Bromwich et al. noted that patients with increased $CD4^{+}$T cells within their tumor at the time of surgery had worse survival which was found to hold independent prognostic influence on multivariable analysis and was important regardless of tumor grade [72]. Similar findings by Nakano et al, when analyzing 221 patients treated with primary nephrectomy for renal cell carcinoma where both increased $CD4^{+}$ and $CD8^{+}$ T cell infiltrates correlated with shortened survival, more advanced stage and tumor grade [73]. In a study by Cozar et al, looking at both the tumor infiltrating lymphocyte (TIL) population and peripheral blood immune cells in patients with RCC undergoing nephrectomy, increasing stage was associated with diminished TIL presence of NK cells, lower populations of effector memory cells which were characterized as CCR5/CXCR3/$CD4^{+}$ cells, and an increased population of $CD25^{+}$CD4+ cells consistent with a Treg population [74]. In a study of 70 patients with RCC undergoing nephrectomy, 16 patients had matched peripheral blood and TIL. The authors observed high levels of the chemokine receptors CCR5, CXCR3, and CXCR6 on TILS corresponding to chemokines expressed in renal cell tissue. Also observed where higher Treg populations with these chemokine receptors in the TIL population leading to a proposed mechanism of recruitment of these cells into the tumors for immune escape [75].

As increased understanding of important T cell subsets has expanded across research fields, additional studies have found that increased levels of regulatory T cell subsets defined by both flow cytommetry, IHC, and confirmed with functional assays has found a correlation between the presence of T regulatory cells and outcome in patients with renal cell carcinoma [76]. In a large series from the Mayo clinic, the presence of $CD4^{+}CD25^{+}FoxP3^{+}$ tumor infiltrating cells was not associated with poor outcome, but the presence of $CD4^{+}CD25^{+}FoxP3^{-}$ tumor infiltrating cells was associated with poor prognosis [77].

The increased presence of Treg population in TIL population has been associated with worsening survival in patients treated with cytokine based immunotherapy [78,79]. Jensen et al. analyzed the TIL population in patients treated with high dose interleukin-2 treatment and found patients who had significant increases in Treg TIL after IL-2 therapy had worse survival and the only long term survivors observed on study were those who had low baseline Treg population and only a modest rise in Treg population following IL-2 therapy. Griffiths found a higher population of Treg cells in circulation as compared to normal donors and an inferior survival in patients with RCC with elevated levels of Treg cells. [78]

In our analysis of the immunohistochemistry data, limited differences were found in immune cell staining between patients treated with nephrectomy alone or ablation followed by nephrectomy. It is unclear if this is a function of both populations having active tumor at the time of resection, significant lag between ablation and nephrectomy, or lack of power given small sample size. Interestingly, a difference was detected in PD-1 staining in the IM, however this does appear to be influenced by one patient who had significantly higher levels than both control and other treated tumor analyzed.

The third and final aim of the project was to determine in a prospective cohort of patients if thermal ablation produces detectable changes in peripheral blood immune cell subsets and cytokine levels that can be detected over one day, four weeks, and a 6 month timeframe. In a similar fashion as in our retrospective immunohistochemistry studies, the inflammatory gene signature was not confirmed in cytokine or flow cytommetry studies. The only potential exceptions were subtle changes noted in potential T regulatory cell populations and early trends in serum cytokine levels of IL-6 and IL-10.

In the flow cytommetry portion of our study, the most interesting observations occurred within the potential T regulatory (Treg) populations. However, defining the Treg population in this setting is limited and challenging without the additional functional assays. In a seminal work in 1995, Sakaguchi et al. identified CD4 cells expressing the IL-2 receptor alpha-chain (CD25) were crucial in protecting against auto-immunity and in graft rejection in mice [80]. Further work by this group found that depletion of $CD4^{+}CD25^{high}$ lead to tumor rejection in mice [81]. The $CD4^{+}CD25^{high}$ cells population when depleted and transferred into other mice can produce autoimmune disease [82] Work by Baecher-Allen et al. further characterized human $CD4^{+}CD25^{high}$ population of T cells finding they were capable of suppressing other effector T cells, were resistant to activation, but were capable of being activated when plated with anti-CD3 antibody with CD28 cross-linking which resulted in loss of regulatory function. Importantly, when these cells were co-cultured with monoclonal antibodies directed against immune check point inhibitors CTLA-4, PD-1, and PD-L1, the $CD4^{+}CD25^{high}$ continued to have regulatory function [83]. The identification of FoxP3 expression in T regulatory cells was reported by Hori et al in mice and Walker et al. in humans in 2003 [84] [85]. In humans, Walker found that peripheral $CD4^{+}CD25^{-}$ T cells were capable of being induced to express FoxP3, which differed from mice.

Once induced, these cells were capable of suppressing other effector T cells through direct contact, which was not dependent on cytokine. Work by Chen et al. found that in addition to Treg cells produced in the thymus, peripheral $CD4^{+}CD25^{-}$ could be induced to become Treg cells under the influence of transforming growth factor beta (TGF-β) and T cell receptor (TCR) stimulation. In addition FoxP3 could be induced under the influence of TGF-β [86]. Yagi et al. went on to show that human peripheral T cell $CD4^{+}CD25^{-}$ transduced to express FoxP3 went on to up-regulate CTLA-4 and CD25 and exhibited Treg phenotype [87]. Findings by Morgan et al, questioned the expression of FoxP3 as a marker of regulatory T cells only as FoxP3 mRNA could be detected in all T cell clones and stimulated cells expressing FoxP3 were capable of producing interferon gamma and proliferation consistent with effector T cell population [88] . Qiao et al. further identified the role of $CD4^{+}CD25^{+}FoxP3^{+}$ T cells labeled as natural T regulatory cells or nTregs by co-culturing with $CD4^{+}CD25^{-}$ cells with IL-4 and anti-CD3 was capable of inducing a population of cells that were labeled as induced T regulatory cells or iTregs that did not express FoxP3 [89]. Using a RAG 2-/- murine model that has no naturally occurring $CD4^{+}CD25^{+}$ T cells, daily peptide vaccine resulted in a significant population of $CD4^{+}CD25^{+}FoxP3^{+}$ T cells with suppressive function [90].

The accurate identification of a human T regulatory cell is challenging. Part of the limitation revolves around the processing of cells required to identify the intracellular marker FoxP3. Due to the need to permeabilize the cell surface, once stained for FoxP3, functional assays are not possible. The combination of dendritic cell vaccine and low dose interleukin-2 resulted in nearly immediate rise in $CD4^{+}CD25^{high}FoxP3^{+}$ T cells [91] as detected in peripheral blood, which reduced after 8 days but did not return to baseline. In patients with metastatic melanoma and metastatic RCC treated with high dose interleukin 2 therapy, patients who

achieved sustained response had diminished levels of Treg cells detected in peripheral blood following therapy, with those who had progressive disease had the opposite trend [92]. van der Vliet et al. reported high dose IL-2 diminished peripheral dendritic cell subsets, NK cells, while increasing CD4(+)CD25(+) T cells, which included the CD4(+)Foxp3(+) T cell subset [93]. However, interestingly the $CD4^+CD25^+$ T cells were less capable of regulating other T cells as compared to freshly harvested $CD4^+CD25^+$ T cells.

A different marker of Treg cells $CD4^+CD25^+CD117^-$ has been suggested by several groups. However in work done in Dr. Sharma's laboratory, patients treated with anti-CTLA-4 based immune therapy that had cells with the surface markers $CD4^+CD25^+CD117^-$ did not have discriminatory function between T effector and T regulatory cells [94]. In this work, $CD4^+CD25^+Lap^+$ cells were found to accurately identify a subset of T regulatory cells as determined by in vitro functional assays from cells taken from human subjects treated on a clinical trial. Other groups have suggested using FoxP3 promoter methylation status as a way of accurately identifying Treg cells in human studies [95] [96].

In our prospective analysis of circulating serum cytokines, interleukin-6 (IL-6) was the highest at baseline and significantly increased after ablation therapy. Elevated IL-6 levels have been associated with poor outcome in mRCC treated with high dose IL-2 [97]. Compared to healthy controls, Yoshida et al. reported IL-6 levels increase with increasing tumor stage and grade and is significantly elevated in patients with metastatic disease[98]. In addition, TNF-α levels were elevated compared to controls, but not increase in a stage or grade dependence as witnessed with IL-6. In a large multicenter trial evaluating IL-2 and IFN-α, elevated levels of IL-6 were associated with inferior survival [99]. Guida et al. compared serum cytokines and C-reactive protein in healthy controls and patients with mRCC treated with subcutaneous IL-2 both

at baseline and during treatment [100]. C-reactive protein, IL-6, IL-8 were all significantly higher in patients with mRCC compared to healthy controls and greater elevation was associated with poor outcome. Conversely, elevated IL-12 levels were associated with improved outcome. On multivariate analysis, only CRP and IL-12 maintained significance. Using baseline cytokine, circulating angiogenic factors, and the Memorial Sloan Kettering risk grouping, an improved prognostic risk score could be established to predict patients who would survive five years with mRCC [101]. The cytokines included IL-12p40, IL-6, and IL-5.

The changes found in the gene microarray portion of the study serve as a potential fingerprint indicating a locally immunogenic environment created by an ablation procedure. IHC was unable to capture significant differences in immune cell populations, but the retrospective analysis and the cohort of patients selected, progression of tumor after ablation and differing times between procedure and nephrectomy, likely did not serve as a representative patient population to detect such changes. Significant changes were also not noted in peripheral blood immune cell subtypes by flow cytommetry and serum cytokine analysis. However, the time frame of collecting these blood draws one day following the procedure, one month, and six months likely are not the optimal time to analyze for changes in either the innate or adaptive immune response. To have ideally studied this question, an increased patient population would be required. Nephrectomy or biopsy would occur within weeks or short months following the ablation. Timed blood draws at baseline, day1, week 1, week 2, week 4, and then at month 3 and month 6 would be collected in all patients. Unfortunately having patients undergo this degree of blood testing is likely not reasonable in this setting.

The above study was completed to help us analyze changes both within tissue and in the blood of patients treated with ablation in anticipation of an upcoming trial pairing cryoablation

with tremelimumab (anti-CTLA-4 antibody) in patients with metastatic renal cell carcinoma. As the study does not contain a cryoablation only arm, our group wanted to better define changes related to ablation alone to help with interpretation of data from the trial. The use of combination immunotherapy is underway in a variety of malignancies. Ablation procedures may serve as a way to prime the immune system to better pair with immune check point blockade.

V. Conclusions:

Thermal ablation changes the immune microenvironment as detected by gene microarray. These changes could not be confirmed by immunohistochemistry or in peripheral blood studies using flow cytommetry and cytokine analysis. However, small sample sizes, early staged clinical disease, and the potential selection of a subset of patients with aggressive biology could have impacted our findings. Understanding the impact of cryoablation or radiofrequency alone will be important in interpretation of clinical trial information in future studies.

VI. Limitations

The limitations in this analysis are numerous. The tissue collected was performed on a retrospective basis leading to the potential for sample collection bias. Tumor tissue was collected predominately from early stage RCC patients, but several patients who developed metastatic disease were included leading to significant differences in the patient population. Ideally, limiting the patient selection to early stage localized disease would have helped interpretation of results. Also significant differences in time between tissue acquisition and staining occurred, allowing for the potential for batch effects. In the clinical trial of tremelimumab plus cryoablation versus tremelimumab alone, samples will be analyzed rapidly reducing the risk of batch effects. In the gene microarray analysis, out of the five post treatment

samples submitted for analysis, one was deemed a significant outlier and was excluded and one was eventually excluded due to being a different procedure. As a result only three samples remained, of which two were from the same patient potentially biasing the information obtained. Also, differences related to immune cell infiltration and in percentage of stroma versus tumor cells in each sample are not characterized and have the potential to lead to significant differences given such limited samples. In future analysis, having additional control sample biopsies from multiple sites of the same tumor may help control for these differences and lead to more confidence in interpreting the results. In the cytokine studies, significant differences in sample storage time existed. In a study by de Jager et al, storage time leads to cytokine degradation potentially impacting the results of our study [102].

VII. Bibliography

1. Bang HJ LP, Goodrich DJ, Currier BP, Aoun HD, Heilbrun LK, Vaishampayan U, Adam B, Goodman AC.: Percutaneous cryoablation of metastatic renal cell carcinoma for local tumor control: feasibility, outcomes, and estimated cost-effectiveness for palliation. J. Vasc Interv Radiol 23:770-777, 2012

2. Albin RJ SW, Gonder MJ: Prospects for cryo-immunotherapy in cases of metastasizing carcinoma of the prostate. Cryobiology 8:271-279. , 1971

3. Y. S: Cryosurgical treatment of advanced breast cancer and cryoimmunological responses. Skin Cancer 10:19-26., 1995

4. MS S: Cryo-immunology: A review of the literature and proposed mechanisms for stimulatory versus suppressive immune responses. Cryobiology 58:1-11, 2009

5. Gallucci S LM, Matzinger P.: Natural adjuvants: endogenous activators of dendritic cells. Nature Medicine 5:1249-1255, 1999

6. Reiter I KB, Schwamberg G. : Cutting edge: differential effect of apototic versus necrotic tumor cells on macrophage antitumor activities. Journal of Immunology 163:1730-1732, 1999

7. Sauter B AM, Francisco L, Larsson M, Somersan S, Bhardwaj N: Consequences of cell death: exposure to necrotic tumor cells, but not primary tissue cells or apoptotic cells, induces the maturation of immunostimulatory dendritic cells. Journal of Experimental Medicine 191:423-434, 2000

8. P. M: Tolerance, danger and the extended family. Annu Rev Immunol 12:991-1045, 1994

9. Basu S BR, Suto R, Anderson KM, Srivastava PK.: Necrotic but not apoptotic cell death releases heat shock proteins, which deliver a partial maturation signal to dendritic cells and activate the NF-kB pathway. International Immunology 12:1539-1546, 2000

10. Scaffidi P MT, Bianchi ME.: Release of chromatin protein HMGB1 by necrotic cells triggers inflammation. Nature Medicine 418, 2002

11. Shi Y EJ, Rock KL.: Molecular identifcation of a danger signal that alerts the immune system to dying cells. Nature 425:516-521, 2003

12. Scheffer SR NH, Korangy F, Schlote K, Pabst R, Jaffee EM, Manns MP, Greten TF.: Apoptotic, but not necrotic, tumor cell vaccines induce a potent immune response in vivo. Int J Cancer 103:205-211, 2003

13. Kotera Y SK, Mule JJ: Comparative analysis of necrotic and apoptotic tumor cells as a source of antigen(s) in dendritic cell-based immunization. Cancer Research 61:8105-8109, 2001

14. Gamrekelashvili J KC, von Wasielewski R, Hoffmann M, Huster KM, Busch DH, Manns MP, Korangy F, Greten TF.: Necrotic tumor cell death in vivo impairs tumor-specific immune responses. The Journal of Immunology 178:1573-1580, 2007

15. Feng H ZY, Graner MW, Katsanis E.: Stressed apoptotic tumor cells stimulate dendritic cells and induce specific cytotoxic T cells. Blood 100:4108-4115, 2002

16. Strauss AA SS, Crawford RA, Strauss HA: Surgical diathermy of carcinoma of the rectum its clinical end results. JAMA 104:1480-1484, 1935

17. McGahan JP BJ, Tesluk H, Gu WZ, Schneider P, Browning PD.: Hepatic ablation with use of radio-frequency electrocautery in the animal model. . Journal of Vascular Interventional Radiology 3:291-297, 1992

18. Wissnioski TT HJ, Neureiter D, Frieser M, Schaber S, Esslinger B, Voll R, Strobel D, Hahn EG, Schuppan D: Activation of tumor-specific T lymphocytes by radio-frequency ablation of VX2 hepatoma in rabbits. Cancer Research 63:6496-6500, 2003

19. den Brok MH SR, van der Voort R, et al.: In situ tumor ablation creates an antigen source for the generation of antitumor immunity. Cancer Research 64:4024-4029, 2004

20. Dromi SA WM, Herby S, et al. : Radiofrequency ablation induces antigen-presenting cell infiltration and amplification of weak tumor-induced immunity. Radiology 251:58-66, 2009

21. Napoletano C TF, Binnoni M, De Majo A, Coscarella G, Bellati F, Rahimi H, Pauselli S, Pellicciotta I, Burchell JM, Gaspari LA, Ercoli L, Rossi P, Rughetti A.: RFA strongly modulates the immune system and anti-tumor immune responses in metastatic liver patients. International Journal of Oncology 32:481-490, 2008

22. Hansler J WT, Schuppan D, Witte A, Bernatik T, Hahn EG, Strobel D.: Activation and dramatically increased cytolytic activity of tumor specific T lymphocytes after radio-frequency ablation in patients with hepatocellular carcinoma and colorectal liver metastases. World Journal of Gastroenterology 12:3716-3721, 2006

23. Zerbini A PM, Penna A, Pelosi G, Schianchi C, Molinari A, Schivazappa S, Zibera C, Fagnoni FF, Ferrari C, Missale G: Radiofrequency thermal ablation of hepatocellular carcinoma liver nodules can activate and enhance tumor specific T-cell responses. Cancer Research 66:1139-1146, 2006

24. Zerbini A PM, Fagnoni F, Pelosi G, Pizzi MG, Schivazappa S, Laccabue D, Cavallo C, Schianchi C, Ferrari C, Missale G.: Increased immunostimulatory activity conferred to antigen-presenting cells by exposure to antigen extract from hepatocellular carcinoma after radiofrequency ablation. Journal of Immunotherapy 31:271-282, 2008

25. Sidana A CW, Fuchs EJ, Rodriguez R.: Cryoimmunotherapy in urologic oncology. Urology 75:1009-1014, 2010

26. Yantorno C SS, Gonder MJ, Soanes WA.: Studies in cryo-immunology I. The production of antibodies to urogenital tissue in consequence of freezing treatment. Immunology 12:395-410, 1967

27. Shulman S BE, Yantorno C.: Studies in cryo-immunology. II. Tissue specificity of the antibody response and comparison to isoimmunization. . Immunology 14:149-158, 1968

28. Myers RS HW, Ketcham AS.: Tumor-specific transplantation immunity after cryosurgery. Journal of Surgical Oncology 1:241-246, 1969

29. Blackwood CE CI: Response to experimental tumor systems to cryosurgery. Cryobiology 9:508-515, 1972

30. Neel HB KA, Hammond WG.: Experimental evaluation of in situ oncocide for primary tumor therapy: comparison of tumor specific immunity after complete excision, cryonecrosis, and ligation. The Laryngoscope 83:376-387, 1972

31. Bagley DH FR, Marrone JC, Beazley RM.: Lymphocyte mediated cytotoxicity after cryosurgery of a murine sarcoma. Journal of Surgical Research 17, 1974

32. Matsumura K SK, Saji S, Misao A, Kunieda T: Antitumor immunologic reactivity in the relatively early period after cyrosurgery: experimental studies in the rate. Cryobiology 19:263-272, 1982

33. Misao A SK, Saji S, Kunieda T.: Late appearance of resistance to tumor rechallenge following cryosurgery. A study in an experimental mammary tumor of the rate. Cryobiology 18:386-389, 1981

34. Si T GZ, Hao X.: Immunologic response to primary cryoablation of high-risk prostate cancer. Cryobiology 57:66-71, 2008

35. Onishi T OY, Imagawa K, Ohmoto Y, Murata K.: An assessment of the immunological environment based on intratumoral cytokine production in renal cell carcinoma. BJU Int 83:488-492, 1999

36. Ghosh P KK, Cippitelli M, Longo DL, Subleski J, Ye J, Sica A, Young HA, Wiltrout RH, Ochoa AC.: Gradual loss of T-helper 1 populations in spleen of mice during progressive tumor growth. J Natl Cancer Inst 87:1478-1483, 1995

37. Takeuchi T UT, Sasaki Y, Kajiwara T, Li B, Moriyama N, Kawabe K.: Th2-like response and antitumor effect of anti-interleukin-4 mAb in mice bearing renal cell carcinoma. Cancer Immunol Immunother. 43:375-381, 1997

38. Hodi FS MM, Soiffer RJ, Haluska FG, Butler M, Seiden MV, Davis T, Henry-Spires R, MacRae S, Willman A, Padera R, Jaklitsch MT, Shankar S, Chen TC, Korman A, Allison JP, Dranoff G.: Biologic activity of cytotoxic T lymphocyte-associated antigen 4 antibody blockade in previously vaccinated metastatic melanoma and ovarian carcinoma patients. Proc Natl Acad Sci USA 100:4712-4717, 2003

39. Hammers HJ PE, Infante JR, Ernstoff MS, Rini BI, McDermott DF, Razak ARA, Pal SK, Voss MH, Sharma P, Kollmannsberg CK, Heng DYC, Spratlin JL, Shen Y, Kurland JF, Gagnier P, Amin A. : Phase I study of nivolumab in combination with ipilimumab in metastatic renal cell carcinoma (mRCC). . J Clin Oncol 32:suppl; abstr 4504, 2014

40. Wolkchok JD KH, Callahan MK, Postow MA, Rizvi NA, Lesokhin AM, Segal NH, Ariyan CE, Gordon RA, Reed K, Burke MM, Caldwell A, Kronenberg SA, Agunwamba BU, Zhang X, Lowy I, Inzunza HD, Feely W, Horak CE, Hong Q, Korman AJ, Wigginton JM, Gupta A, Sznol M.: Nivolumab plus ipilimumab in advanced melanoma. . N Engl J Med 369:122-133, 2014

41. Topalian SL S, McDermott DF, Kluger HM, Carvajal RD, Sharfman WH, Brahmer JR, Lawrence DP, Atkins MB, Powderly JD, Leming PD, Lipson EJ, Puzanov I, Smith DC, Taube JM, Wigginton JM, Kollia GD, Gupta A, Pardoll DM, Sosman JA, Hodi FS.: Survival, durable tumor remission, and long-term safety in patients with advanced melanoma receiving nivolumab. J Clin Oncol 32:1020-1030, 2014

42. Topalian SL HF, Brahmer JR, Gettinger SN, Smith DC, McDermott DF, Powderly JD, Carvajal RD, Sosman JA, Atkins MB, Leming PD, Spigel DR, Antonia SJ, Horn L, Drake CG, Pardoll DM, Chen L, Sharfman WH, Anders RA, Taube JM, McMiller TL, Xu H, Korman AJ, Jure-Kunkel M, Agrawal S, McDonald D, Kollia GD, Gupta A, Wigginton JM, Sznol M.: Safety, activity, and immune correlates of anti-PD-1 antibody in cancer. N Engl J Med 366:2443-2454, 2012

43. Rizvi NA MJ, Planchard D, Stinchcombe TE, Dy GK, Antonia SJ, Horn L, Lena H, Minenza E, Mennecier B, Otterson GA, Campos LT, Gandara DR, Levy BP, Nair SG, Zalcman G, Wolf J, Souquet PR,

Baldini E, Cappuzzo F, Chouaid C, Dowlati A, Sanborn R, Lopez-Chavez A, Grohe C. : Activity and safety of nivolumab, an anti-PD-1 immune checkpoint inhibitor, for patients with advanced, refractory squamous non-small-cell lung cancer (CheckMate 063): a phase 2, single-arm trial. Lancet Oncol 16:257-265, 2015

44. Weber JS DAS, Minor D, Hodi FS, Gutzmer R, Neyns B, Hoeller C, Khushalani NI, Miller WH, Lao CD, Linette GP, Thomas L, Lorigan P, Grossmann KF, Hassel JC, Maio M, Sznol M, Ascierto PA, Mohr P, Chmielowski B, Bryce A, Svane IM, Grob JJ, Krackhardt AM, Horak C, Lambert A, Yang AS, Larkin J.: Nivolumab versus chemotherapy in patients with advanced melanoma who progressed after anti-CTLA-4 treatment (CheckMate 037): a randomised, controlled, open-label, phase 3 trial. Lancet Oncol 16:375-384, 2015

45. Yang JC HM, Kammula U, Royal R, Sherry RM, Topalian SL, Suri KB, Levy C, Allen T, Mavroukakis S, Lowy I, White DE, Rosenberg SA: Ipilimumab (Anti-CTLA-4 Antibody) causes regression of metastatic renal cell cancer associated with enteritis and hypophysitis. J Immunother 30:825-830, 2007

46. Brahmer JR TS, Chow LQ, Hwu WJ, Topalian SL, Hwu P, Drake CG, Camacho LH, Kauh J, Odunsi K, Pitot HC, Hamid O, Bhatia S, Martins R, Eaton K, Chen S, Salay TM, Alaparthy S, Grosso JF, Korman AJ, Parker SM, Agrawal S, Goldberg SM, Pardoll DM, Gupta A, Wigginton JM: Safety and activity of anti-PD-L1 antibody in patients with advanced cancer. N Engl J Med 366:2455-2465, 2012

47. Carthon BC WJ, Yuan J, Kamat A, Ng Tang DS, Sun J, Ku G, Troncoso P, Logothetis CJ, Allison JP, Sharma P: Preoperative CTLA-4 blockade: tolerability and immune monitoring in the setting of a presurgical clinical trial. Clin Cancer Res 16:2861-2871, 2010

48. Gao J SJ, Ward JF, Rao P, Troncoso P, Araujo JC, Tang DN, Chen H, Thall P, Wen S, Sharma P.: Combination therapy with anti-CTLA-4 plus leuprolide acetate in the pre-surgical setting of patients with regional, high-risk prostate cancer. Abstract 4388 AACR meeting 2012. Cancer Res 72:Supplement 1, 2012

49. Siegel R MJ, Zou Z, Jemel A.: Cancer Statistics, 2014. CA Cancer J Clin 64:9-29, 2014

50. Coppin C PF, Autenrieth M, Kumpf J, Coldman A, Wilt T.: Immunotherapy for advanced renal cell cancer. Cochrane Database of Systematic Reviews:1-89, 2004

51. McDermott DF RM, Clark JI, Flaherty LE, Weiss GR, Logan TF, Kirkwood JM, Gordon MS, Sosman JA, Ernstoff MS, Tretter CPG, Urba WJ, Smith JW, Margolin KA, Mier JW, Gollob JA, Dutcher JP, Atkins MB.: Randomized phase III trial of high-dose interleukin-2 versus subcutaneous interleukin-2 and interferon in patients with metastatic renal cell carcinoma. Journal of Clinical Oncology 23:133-141, 2005

52. Klapper JA DS, Smith FO, Yang JC, Hughes MS, Kammula US, Sherry RM, Royal RE, Steinberg SM, Rosenberg S.: High-dose interleukin-2 for the treatment of metastatic renal cell carcinoma: a retrospective analysis of response and survival in patients treated in the surgery branch at the National Cancer Institute between 1986 and 2006. Cancer 113:293-301, 2008

53. Liakou C KA, Tang DN, Chen H, Sun J, Troncoso P, Logothetis C, Sharma P.: CTLA-4 blockade increases IFN-gamma producing CD4+ICOS(hi) cells to shift the ratio of effector to regulatory T cells in cancer patients. Proc Natl Acad Sci USA 105:14987-14992, 2008

54. Chen H LC, Kamat A, Pettaway C, Ward JF, Tang DN, Sun J, Jungbluth AA, Troncoso P, Logothetis C, Sharma P.: Anti-CTLA-4 therapy results in higher CD4+ICOShi T cell frequency and IFN-gamma levels in both nonmalignant and malignant prostate tissues. Proc Natl Acad Sci USA 106:2729-2734, 2009

55. Chowdhury F WA, Johnson P.: Validation and comparison of two multiplex technologists, Luminex and Mesoscale Discovery, for human cytokine profiling. Journal of Immunological Methods 340:55-64, 2009

56. Kramer A GJ, Pollard J, Tugendreich S.: Causal analysis approaches in Ingenuity Pathway Analysis. Bioinformatics 40:523-530, 2014

57. Pounds S MS: Estimating the occurence of false positives and false negatives in microarray studies by approximating and partitioning the empirical distribution of p-values. Bioinformatics 19:1236-1242, 2003

58. Ulloa-Montoya F LJ, Dizier B, Gruselle O, Spiessens B, Lehmann FF, Suciu S, Kruit WHJ, Eggermont AMM, Vantseenkiste J, Brichard VG.: Predictive gene signature in MAGE-A3 antigen-specific cancer immunotherapy. J Clin Oncol 31:2388-2395, 2013

59. Fuertes MB KA, Kline J, Wood SR, Kranz DM, Murphy KM, Gajewski TF.: Host type I IFN signals are required for antitumor CD8+ T cell responses through CD8{alpha}+ dendritic cells. J Exp Med 208:2005-2016, 2011

60. Gajewski TF FM, Woo SR.: Innate immune sensing of cancer: clues from an identified role for type I IFNs. Cancer Immunol Immunother 61:1343-1347, 2012

61. Bouchon A DJ, Colonna M.: Cutting edge: inflammatory responses can be triggered by TREM-1, a novel receptor expressed on neutrophils and monocytes. . J Immunol 164:4991-4995, 2000

62. Bouchon A FF, Weigand MA, Colonna M.: TREM-1 amplifies inflammation and is a crucial mediator of septic shock. Nature 410:1103-1107, 2001

63. Tessarz AS WS, Zanzinger K, Angeliosva P, Horejsi V, Cerwena A.: Non-T cell activation linker (NTAL) negatively regulates TREM-1/DAP12 induced inflammatory cytokine production in myeloid cells. J Immunol 178:1991-1999, 2007

64. Mezayen RE GM, Seeds MC, McCall CE, Dreskin SC, Nicolls MR.: Endogenous signals released from necrotic cells augment inflammatory responses to bacterial endotoxin. Immunol Lett 111:36-44, 2007

65. Takahashi M RD, Furge KA, Kanayama H, Kagawa S, Haab BB, Teh BT.: Gene expression profiling of clear cell renal cell carcinoma: Gene identification and prognostic classification. Proc Natl Acad Sci 98:9754-9759, 2001

66. Kosari F PA, Kube DM, Lohse CM, Leibovich BC, Blute ML, Cheville JC, Vasmatzis G: Clear cell renal cell carcinoma: gene expression analyses identify a potential signature for tumor aggressiveness. Clin Cancer Res 11:5128-5139, 2005

67. Subramanian A TP, Mootha VK, Mukherjee S, Ebert BL, Gillette MA, Paulovich A, Pomeroy SL, Golub TR, Lander ES, Mesirov JP.: Gene set enrichment analysis: A knowledge-based approach for interpreting genome-wide expression profiles. Proc Natl Acad Sci USA 102:15545-15550, 2005

68. Maruschke M RD, Koczan D, Hakenberg OW, Thiesen HJ: Gene expression analysis in clear cell renal cell carcinoma using gene set enrichment analysis for biostatistical management. BJU Int 108:E29-E35, 2011

69. Brooks SA BA, Parker JS, Fisher JC, Sen O, Kattan MW, Hakimi AA, Hsieh JJ, Choueiri TK, Tamboli P, Maranchie JK, Hinds P, Miller CR, Nielsen ME, Rathmell WK.: ClearCode34: A prognostic risk predictor for localized clear cel renal cell carcinoma. Eur Urol 66:77-84, 2014

70. Network TCGAR: Comprehensive molecular characterization of clear cell renal cell carcinoma. Nature 499:43-49, 2013

71. El Dib R TN, Kapoor A: Cryoablation vs. radiofrequency ablation for the treatment of renal cell carcinoma: a meta-analysis of case series studies. BJU Int 110:510-516, 2012

72. Bromwich EJ MP, Canna K, McMillan DC, McNicol AM, Brown M, Aitchison M.: The relationship between T-lymphocyte infiltration, stage, tumour grade and survival in patients undergoing curative surgery for renal cell carcinoma. Br J Cancer 89:1906-1908, 2003

73. Nakano O SM, Naito Y, Suzuki K, Orikasa S, Aizawa M, Suzuki Y, Shintaku I, Nagura H, Ohtani H: Proliferative activity of intratumoral CD8(+) T-lymphocytes as a prognostic factor in human renal cell carcinoma: clinicopathologic demonstration of antitumor immunity. Cancer Res 61:5132-5136, 2001

74. Cozar JM CJ, Tallada M, Concha A, Cabrera T, Garrido F, Ruiz-Cabello Osuna F: Analysis of NK cells and chemokine receptors in tumor infiltrating CD4 T lymphocytes in human renal carcinomas. Cancer Immunol Immunother 54:858-866, 2005

75. Oldham KA PG, Bhatt RI, Wallace DM, Deshmukh N, Chaudhri S, Adams DH, Lee SP.: T lymphocyte recruitment into renal cell carcinoma tissue: a role for chemokine receptors CXCR3, CXCR6, CCR5, and CCR6. Eur Urol 61:385-394, 2012

76. Liotta F GM, Frosali F, Querci V, Vittori G, Lapini A, Santarlasci V, Serni S, Cosmi L, Maggi L, Angeli R, Mazzinghi B, Romagnani P, Maggi E, Carini M, Romagnani S, Annunziato F.: Frequency of regulatory T cells in peripheral blood and in tumour-infiltrating lymphocytes correlates with poor prognosis in renal cell carcinoma. BJU Int 107:1500-1506, 2011

77. Siddiqui SA FX, Bonne-Annee S, Mercader M, Kuntz SM, Krambeck AE, Sengupta S, Dong H, Cheville JC, Lohse CM, Krco CJ, Webster WS, Leibovich BC, Blute ML, Knutson KL, Kwon ED.: Tumor-infiltrating FoxP3-CD4+CD25+ T cells predict poor survival in renal cell carcinoma. Clin Cancer Res 13:2075-2081, 2007

78. Griffiths RW EE, Gilham DE, Ramani V, Clarke N, Stern PL, Hawkins RE.: Frequency of regulatory T cells in renal cell carcinoma patients and investigation of correlation with survival. Cancer Immunol Immunother 56:1743-1753, 2007

79. Jensen HK DF, Nordsmark M, Marcussen N, von der Maase H: Increased intratumoral FOXP3-positive regulatory immune cells during interleukin-2 treatment in metastatic renal cell carcinoma. Clin Cancer Res 15:1052-1058, 2009

80. Sakaguchi S SN, Asano M, Itoh M, Toda M.: Immunologic self-tolerance maintained by activated T cells expressing IL-2 receptor apha-chains (CD25). Breakdown of a single mechanism of self-tolerance causes various autoimmune diseases. J Immunol 155:1151-1164, 1995

81. Shimuzu J YS, Sakaguchi S.: Induction of tumor immunity by removing CD25+CD4+ T cells: a common basis between tumor immunity and autoimmunity. J Immunol 163:5211-5218, 1999

82. Itoh M TT, Sakaguchi N, Kuniyasu Y, Shimizu J, Otsuka F, Sakaguchi S: Thymus and autoimmunity: production of CD25+CD4+ naturally anergic and suppressive T cells as a key function of the thymus in maintaining immunologic self-tolerance. J Immunol 162:5317-5326, 1999

83. Baecher-Allan C BJ, Freeman GJ, Hafler DA.: $CD4^{+}CD25^{high}$ regulatory cells in human peripheal blood. J Immunol 167:1245-1253, 2001

84. Hori S NT, Sakaguchi S.: Control of regulatory T cell development by the transcription factor FoxP3. Science 299, 2003

85. Walker MR KD, Gersuk VH, Benard A, Van Landeghen M, Buckner JH, Ziegler SF.: Induction of FoxP3 and acquisition of T regulatory activity by stimulated human $CD4^{+}CD25^{-}$ T cells. J Clin Invest 112:1437-1443, 2003

86. Chen W JW, Hardegen N, Lei KJ, Li L, Marinos N, McGrady G, Wahl SM.: Conversion of Peripheral CD4+CD25− Naive T Cells to CD4+CD25+ Regulatory T Cells by TGF-β Induction of Transcription Factor Foxp3. J Exp Med 198:1875-1886, 2003

87. Yagi H NT, Nakamura K, Yamazaki S, Kitawaki T, Hori S, Maeda M, Onodera M, Uchiyama T, Fujii S, Sakaguchi S.: Crucial role of FOXP3 in the development and function of human CD25+CD4+ regulatory T cells. Int Immunol 16:1643-1656, 2004

88. Morgan ME vBJ, Bakker AM, Heemskerk B, Schilham MW, Hartgers FC, Elferink BG, van der Zanden L, de Vries RR, Huizinga TW, Ottenhoff TH, Toes RE.: Expression of FOXP3 mRNA is not confined to CD4+CD25+ T regulatory cells in humans. Hum Immunol 66:13-20, 2005

89. Qiao M TA, Shevach EM.: CD4+ CD25+ [corrected] regulatory T cells render naive CD4+ CD25- T cells anergic and suppressive. Immunology 120:447-455, 2007

90. Dahlberg PE SJ, Timmel A, Seroogy CM.: Daily subcutaneous injections of peptide induce CD4+ CD25+ T regulatory cells. Clin Exp Immunol 149:226-234, 2007

91. Bernsten A BM, thor Straten P, Svane IM.: Increase of circulating CD4+CD25highFoxp3+ regulatory T cells in patients with metastatic renal cell carcinoma during treatment with dendritic cell vaccination and low-dose interleukin-2. J Immunother 33:425-434, 2010

92. Cesana GC DG, Cohen S, Moroziewicz D, Mitcham J, Stoutenburg J, Cheung K, Hesdorffer C, Kim-Schulze S, Kaufman HL.: Characterization of CD4+CD25+ regulatory T cells in patients treated with high-dose interleukin-2 for metastatic melanoma or renal cell carcinoma. J Clin Oncol 24:1169-1177, 2006

93. van der Vliet HJ KH, Yue SC, Uzunparmak B, Seery V, Gavin MA, Rudensky AY, Atkins MB, Balk SP, Exley MA.: Effects of the administration of high dose interleukin-2 on immunoregulatory cell subsets in patients with advanced melanoma and renal cell cancer. Clin Cancer Res 13:2100-2108, 2007

94. Sun J TD, Fu T, Sharma P.: Identification of human regulatory T cells in the setting of T-cell activation and anti-CTLA-4 immunotherapy on the basis of expression of latency-associated peptide. Cancer Discov 2:122-130, 2012

95. Janson PC WM, Marits P, Thörn M, Ohlsson R, Winqvist O: FOXP3 promoter demethylation reveals the committed Treg population in humans. PLoS One 3:e1612, 2008

96. Liu J LA, Illi S, Layland L, Olek S, von Mutius E, Schaub B: T regulatory cells in cord blood--FOXP3 demethylation as reliable quantitative marker. PLoS One 5:e12367, 2010

97. Blay JY NS, Combaret V, Attali S, Goillot E, Merrouche Y, Mercatello A, Ravault A, Tourani JM, Moskovtchenko JF, Phillip T, Favrot M.: Serum level of interleukin 6 as a prognosis factor in metastatic renal cell carcinoma. Cancer Res 52:3317, 1992

98. Yoshida N IS, Narita K, Sugimura K, Wada S, Yasumoto R, Kishimoto T, Nakatani T: Interleukin-6, tumour necrosis factor α and interleukin-1β in patients with renal cell carcinoma. Br J Cancer 86:1396-1400, 2002

99. Negrier S PD, Menetrier-Caux C, Escudier B, Pallardy M, Ravaud A, Douillard JY, Chevreau C, Lasset C, Blay JY: Interleukin-6, interleukin-10, and vascular endothelial growth factor in metastatic renal cell carcinoma: prognostic value of interleukin-6--from the Groupe Francais d'Immunotherapie. J Clin Oncol 22:2371-2378, 2004

100. Guida M CA, Monticelli G, Quaranta M, Colucci G.: Basal cytokines profile in metastatic renal cell carcinoma patients treated with subcutaneous IL-2-based therapy compared with that of healthy donors. J Transl Med 5:51, 2007

101. Montero AJ D-MC, Millikan RE, Liu J, Do KA, Hodges S, Jonasch E, McIntyre BW, Hwu P, Tannir N.: Cytokines and angiogenic factors in patients with metastatic renal cell carcinoma treated with interferon-alpha: association of pretreatment serum levels with survival. Ann Oncol 20:1682-1687, 2009

102. de Jager W BK, Rijkers GT, Prakken BJ, Seyfert-Margolis V.: Prerequisites for cytokine measurements in clinical trials with multiplex immunoassays. BMC Immunol 10:52, 2009

VITA

Matthew T Campbell was born May 14, 1981 to Joseph Benjamin Campbell and Charlotte Freuchtenicht Campbell. After graduating from Homestead High School in Fort Wayne, Indiana he enrolled at DePauw University where he performed his undergraduate work. Matthew graduated with a bachelor in arts from DePauw, majoring in Chemistry and graduated in 2003. Matthew was accepted and enrolled in Indiana University School of Medicine graduating in 2007. After graduation he spent in year performing research in the basic science research laboratory of Kirstan Meldum, M.D. Matthew then completed his internship and residency in Internal Medicine with Indiana University School of Medicine Department of Internal Medicine graduating in 2011. He was selected as a chief resident and served from 2011 to 2012. Matthew then was accepted for a medical oncology fellowship position at University of Texas MD Anderson Cancer Center and began his training in 2012. He is currently serving as the chief fellow for the Medical Oncology/Hematology fellowship and is set to graduate in June of 2015. He began his work in the University of Texas Graduate School of Biomedical Sciences in 2013 under the mentorship of Padmanee Sharma, MD PhD. He is accepted a faculty position at University Texas MD Anderson Cancer Center at the completion of his fellowship and will work as an assistant professor, clinical investigator in the Department of Genitourinary Oncology.